Characterization of Interindividual Variability and Differential Tissue Abundance of UGT2B17: Discovery of a Potential Biomarker and Drug Interaction Prediction

Hae Young Zhang

A dissertation

submitted in partial fulfillment of the

requirements for the degree of

Doctor of Philosophy

University of Washington

2020

Reading Committee:

Kenneth Thummel, Chair

Bhagwat Prasad

Qingcheng Mao

Program Authorized to Offer Degree:

Pharmaceutics

University of Washington

Abstract

Characterization of Interindividual Variability and Differential Tissue Abundance of UGT2B17: Discovery of a Potential Biomarker and Drug Interaction Prediction

Hae Young Zhang

Chair of the Supervisory Committee:
Dr. Kenneth Thummel
Pharmaceutics

UGT2B17 is an androgen- and drug-conjugating enzyme with a remarkably high interindividual variability in its hepatic protein expression. Testosterone is one of its main endogenous substrates, and various clinical associations between UGT2B17 and testosterone-related and other pathophysiological outcomes have been reported, along with associations with drug and xenobiotic disposition. UGT2B17 also exhibits relatively high and variable intestinal abundance, compared to the liver, both in absolute abundance and relative to other UGT isoforms, which brings in concern for first pass metabolism and differential drug-drug interactions. Multiple factors, including a common copy number variation (CNV), sex, age, and certain SNPs, contribute to UGT2B17 tissue abundance variability, but only account for a small portion of that variability. Unexplained interindividual differences in UGT2B17 tissue abundance, along with UGT2B17's unique ontogeny, highlights the need for a phenotypic biomarker to assess in vivo UGT2B17

activity. This dissertation project focuses on characterizing interindividual variability and differential tissue abundance of UGT2B17.

Chapter 2 explores UGT2B17's role in first pass metabolism of testosterone in human in vitro models for the small intestine and liver and explores its role in the disposition of orally administered testosterone. Findings confirm that UGT2B17 drives testosterone glucuronide (TG) formation in liver and intestine, and the higher intestinal abundance may explain oral testosterone's high and variable first pass metabolism and low bioavailability. In Chapter 3, urinary TG normalized with androsterone glucuronide (TG/AG) is identified as a potential urinary biomarker for UGT2B17 and validated in longitudinal urine samples from 63 pediatric subjects. Significant associations between TG/AG and sex, age, and UGT2B17 CNV were found. Chapter 4 investigates regional enzyme abundance of UGT2B17 and non-CYP enzymes in cryopreserved human intestinal mucosa (CHIM), corroborates proteomic findings with activity assays, and proposes enterocyte marker proteins as normalizers to control for intestinal tissue heterogeneity. Non-CYP enzymes that were quantifiable were carboxylesterase 1 (CES1), CES2, UGT1A1, UGT1A3, UGT1A10, UGT2B7, UGT2B17, sulfotransferase 1A1 (SULT1A1), SULT1A3, SULT1B1, and SULT2A1. We also found good enzyme abundance-activity correlations, demonstrating that CHIMs are functionally active with respect to xenobiotic metabolism.

This dissertation improves the understanding of UGT2B17's role in first pass drug metabolism and potential drug-drug interactions. It also establishes a promising phenotypic urinary biomarker for UGT2B17 for further applications in drug development and disease state associations.

TABLE OF CONTENTS

List of Figures v

List of Tables vii

Chapter 1. Introduction 1

1.1 Background 1

1.2 Interindividual variability and differential tissue abundance of UGT2B17 1

1.3 Clinical implications of UGT2B17 interindividual variability 3

1.4 Investigation of intestinal metabolism using in vitro models and quantitative proteomics 9

1.5 Hypothesis and specific aims 10

Chapter 2. Quantitative characterization of UGT2B17 in human liver and intestine and its role in testosterone first-pass metabolism 15

2.1 Introduction 15

2.2 Materials and methods 17

2.2.1 Chemicals and reagents 17

2.2.2 Procurement of human liver and intestinal cells and subcellular fractions 18

2.2.3 Microsome isolation from donor-matched intestinal sections 19

2.2.4 Membrane protein extraction from primary cells and total protein quantification 19

2.2.5 Protein denaturation, reduction, alkylation, enrichment and trypsin digestion 20

2.2.6 Quantification of Surrogate peptides of UGT2B17 and UGT2B15 in subcellular fractions 21

2.2.7 Testosterone glucuronidation assay in subcellular fractions 21
2.2.8 Inhibition of UGT2B17 activity by tyrosine kinase inhibitors in HLM 22
2.2.9 Testosterone metabolism in human hepatocytes and enterocytes..... 23
2.2.10 LC-MS/MS analysis of testosterone metabolites formed in human hepatocytes and enterocytes..... 23
2.2.11 Data analysis 24
2.2.12 Statistical analysis..... 25
2.3 Results..... 26
2.3.1 UGT2B17 and UGT2B15 abundance and correlation with testosterone glucuronidation in human liver and intestinal subcellular fractions 26
2.3.2 Enzyme kinetic parameters for testosterone in HLM 27
2.3.3 Inhibition of UGT2B17 and UGT2B15 by Tyrosine Kinase Inhibitors 27
2.3.4 UGT2B17 and UGT2B15 protein abundance and testosterone metabolism in primary human hepatocytes and enterocytes 27
2.4 Discussion..... 28
Chapter 3. NORMALIZED testosterone glucuronide (TG/AG) as a potential urinary biomarker for highly variable UGT2B17 in children 7 to 18 years 41
3.1 Introduction..... 41
3.2 Methods..... 45
3.2.1 Clinical study details and sample collection..... 45
3.2.2 Urine sample processing..... 45
3.2.3 LC-MS/MS method development, validation, and analysis of urine androgen conjugates 46

3.2.4 UGT2B17 gene copy number determination 47
3.2.5 Statistical analysis 47
3.3 Results 49
3.3.1 Bioanalytical method validation 49
3.3.2 Urinary concentrations of androgen conjugates 49
3.3.3 Association of urinary androgen conjugates with sex, age, and UGT2B17 copy number variation (CNV) 50
3.4 Discussion 51
Chapter 4. Regional proteomic quantification of clinically relevant non-cytochrome P450 enzymes along the human small intestine 60
4.1 Introduction 60
4.2 Methods 63
4.2.1 Materials 63
4.2.2 Protein extraction 64
4.2.3 Protein denaturation, alkylation, enrichment, and digestion 65
4.2.4 Quantification of surrogate peptides of non-CYP DMEs 65
4.2.5 Activity assays 66
4.2.6 Statistical analysis 67
4.3 Results 67
4.3.1 Non-CYP enzyme quantification 67
4.3.2 Relative quantification of non-CYP enzymes using marker proteins 68
4.3.3 Absolute quantification of non-CYP enzymes 68
4.3.4 Comparison of CHIM protein quantification with pooled intestinal S9 fraction 69

4.3.5 Glucuronide formation and sequential metabolism in CHIM model..... 69

4.4 Discussion..... 70

Chapter 5. Conclusions and Future directions..... 90

Bibliography..... 97

LIST OF FIGURES

Figure 1.1. Testosterone glucuronidation. 12
Figure 1.2. Factors affecting interindividual variability in hepatic UGT2B17 content.... 13
Figure 1.3. Relative abundance of UGT isoforms in the liver and intestine 13
Figure 1.4. Typical workflow for targeted quantitative proteomics 14
Figure 2.1. UGT2B protein abundance and testosterone glucuronidation in human liver and intestinal subcellular fractions. 35
Figure 2.2. Testosterone glucuronide formation kinetics and inhibition in HLMs. 37
Figure 2.3. Testosterone metabolism scheme. 38
Figure 2.4. Testosterone metabolism in primary human hepatocytes and enterocytes. ... 39
Figure 2.5. Testosterone metabolism *in vivo* before and after testosterone administration.40
Figure 3.1. Androgen metabolism scheme. 57
Figure 3.2. Representative MS chromatograms. 57
Figure 3.3. TG, AG, and TG/AG with age and CNV, by sex. 58
Figure 3.4. Association of urinary TG/AG levels with age, sex, race, and CNV. 59
Figure 4.1. Relative abundance of enterocyte marker proteins along the intestine. 82
Figure 4.2. Enterocyte marker peptide correlation. 82
Figure 4.3. Sectional comparison of protein-normalized relative abundance of enterocyte marker proteins. 83
Figure 4.4. Relative protein abundance of non-CYP enzymes along the intestine in CHIMs. 84
Figure 4.5. Average relative abundance of non-CYP enzymes along the intestine. 85
Figure 4.6. Absolute protein abundance of non-CYP enzymes along the intestine in CHIMs. 86
Figure 4.7. Average absolute abundance of non-CYP DMEs along the intestine. 87
Figure 4.8. Comparison of protein abundance between pooled GIS9 and CHIM protein extraction. 88
Figure 4.9. CHIM activity in glucuronide formation and UGT2B protein abundance..... 88

Figure 4.10. Sequential metabolism of clopidogrel (CPG) and camptothecin-11 (CPT-11) in CHIMs..... 89

LIST OF TABLES

Table 1.1. Reported clinical implications of UGT2B17 copy number variation (CNV).. 11
Table 2.1. Sample Demographics 33
Table 2.2. Optimized multiple reaction monitoring (MRM) parameters used for quantitative analysis of testosterone metabolites. 33
Table 2.3. Absolute protein abundance and inter-individual variability of UGT2B17 (pmol/mg microsomal protein) in human liver and intestinal microsomes (HLM and HIM)... 34
Table 2.4. Formation rate (pmol/million cells/hour) of testosterone metabolites in human hepatocytes and enterocytes 34
Table 3.1. Sample Demographics 55
Table 3.2. MS parameters for targeted androgen conjugates 55
Table 3.3. Urinary concentrations (ng/mL) of androgen conjugates in children age 7-18 years 56
Table 3.4. Linear regression outputs of β coefficient values 56
Table 4.1. Cryopreserved human intestinal mucosa (CHIM) demographics 73
Table 4.2. LC-MS/MS parameters for analysis of surrogate peptides 74
Table 4.3. LC-MS/MS parameters for analysis of small molecules 79
Table 4.4. Enterocyte marker normalized relative abundance values 81
Table 4.5. Absolute protein abundance values of non-CYP enzymes in the human intestine 81

ACKNOWLEDGEMENTS

I would like to firstly express my sincere gratitude to my advisor, Dr. Bhagwat Prasad. His enthusiasm and dedication inspired me as a researcher, his patience and support helped me grow as a mentor, and his knowledge and guidance developed me as an independent thinker. I wish to express my sincere appreciation to Dr. Kenneth Thummel for his generous contribution as chair of my committee. I am thankful for his expertise, time, and sound advice, which provided much helpful direction in the completion of my thesis project.

To my committee members, Drs. Jashvant Unadkat, Rheem Totah, Qingcheng Mao, and Gail Anderson, I wish to express my deep gratitude for their time, guidance, and encouragement. Each member's thoughtful input helped expand my scientific views and thinking in my research project.

To all the past and present members of the Prasad Lab, I am thankful for your friendship, training, support, and many conversations. I would like to thank the faculty and staff of the Pharmaceutics and Medicinal Chemistry departments, for enabling a positive learning and research environment that is stimulating and collegial. I would like to thank all the academic and industry collaborators who made this interesting research project possible.

Finally, I would like to express my heartfelt appreciation to my friends and family. To my friends: thank you for your encouragement and understanding. To my family, both near and far, thank you for your unwavering love, care, and support. To my husband, Michael, I am most thankful to have journeyed through this time with you.

Chapter 1. INTRODUCTION

1.1 BACKGROUND

Uridine 5'-diphospho-glucuronisyltransferases (UGTs) are conjugating enzymes which utilize uridine 5'-diphospho-glucuronic acid (UDPGA) as a donor to transfer the glucuronic acid moiety to hydrophobic compounds, thus increasing water solubility for subsequent elimination [1]. The UGT2B17 isoform was discovered and characterized in 1996 [2], and shares 95% sequence identity with UGT2B15 and 77% with UGT2B7. With respect to the endogenous role of UGT2B17, C_{19} androgens such as testosterone are its major substrates (Figure 1.1). Interestingly, UGT2B17 is more versatile in its conjugative capacity towards C_{19} steroids with its ability to glucuronidate both the 3-alpha and 17-beta hydroxyl groups with preference towards the 17-beta position. In contrast, UGT2B7 preferentially glucuronidates the 3-alpha position and UGT2B15 specifically the 17-beta position [3]. Mutagenesis studies show that UGT2B17's ability to conjugate 3-alpha position comes from the serine residue at position 121, which is a tyrosine residue for UGT2B15, possibly leading a larger active site [4]. Xenobiotic substrates for UGT2B17 include dietary compounds like coumarins, anthraquinones, flavonoids, and phenolics [5], as well as tobacco carcinogen (R)-NNAL [6], and drugs or active/inactive metabolites such as vorinostat [7], 17-dihydroexemestane [8], and clopidogrel carboxylic acid [9].

1.2 INTERINDIVIDUAL VARIABILITY AND DIFFERENTIAL TISSUE ABUNDANCE OF UGT2B17

UGT2B17 has notably high interindividual variability in protein abundance measured in human liver microsomes (HLMs), up to 3146-fold [1]. Several factors are known to contribute to this variability, including copy number variation (CNV), sex, age, and single nucleotide

polymorphisms (SNPs) [10]. UGT2B17 harbors a commonly occurring CNV and is one of the most frequently deleted genes in humans [11]. This is thought to arise from nonallelic homologous recombination between the two flanking 4.9 kb segmental duplications 119 kb apart [12]. CNV distribution shows a high degree of ethnic variation, with deletion frequencies ranging from 14% in Nigerians to 92% in Japanese [12]. With regard to variation in gene regulation, adult males show a 2.6-fold higher abundance in HLMs compared to females [10]. UGT2B17 also exhibits an interesting ontogeny profile, with age_{50} –the age at which 50% of maximum adult levels are reached—occurring at 13.6 years in males and 10.7 years in females. The ontogenic increase in UGT2B17 expression is more pronounced in males compared to females, as indicated by the Hill coefficient of 14.9 in males and 1.8 in females [10] (Figure 1.2). Additionally, three intronic and one synonymous SNPs have been reported to significantly affect protein expression and activity [10]. Recently, another SNP (rs59678213 G variant) in the promoter region of the gene, a binding site for transcription factor forkhead box protein A1 (FOXA1), has been associated with low protein expression [13]. Multivariate analysis indicated that only 26% of UGT2B17's variability can be explained by CNV, sex, age, and SNPs combined [10], excluding the most recent SNP identified (Figure 1.2).

UGT2B17 and UGT2B15 are uniquely expressed in prostate tissues, in addition to the liver [14], and are considered androgen-inactivating enzymes [15]. In the prostate, UGT2B17 is specifically expressed in proliferating basal cells, where DHT is synthesized, and UGT2B15 in the secretory hormone-target luminal cells [16]. Other extrahepatic tissues with UGT2B17 mRNA expression include kidney, lung, testis, uterus, placenta, mammary gland, adrenal gland, skin [2], tongue, pancreas, brain, and aerodigestive tract [17]. Proteomic assays have confirmed UGT2B17 protein expression in HLMs and human intestinal microsomes (HIMs) [18]. Of note,

proteomics revealed a 2-fold higher intestinal UGT2B17 abundance compared to the liver, constituting 4% of liver and 30% of intestinal UGT isoforms [1]. Conversely, UGT2B7, which is considered the major drug-metabolizing UGT, has >5-fold higher abundance in the liver compared to the intestine, and constitutes 22% and 5% of total UGTs in the liver and intestine, respectively (Figure 1.3). UGT2B15, while abundant in the liver – taking up 12% of all UGT isoforms, is not detected in the intestine [18]. UGT2B17 remains a relatively understudied UGT isoform, possibly due to both its minor presence in the liver as well as its minor known contributions to drug metabolism [19].

1.3 CLINICAL IMPLICATIONS OF UGT2B17 INTERINDIVIDUAL VARIABILITY

UGT2B17 CNV is a well-known major confounding factor in urinary anti-doping tests for athletes [20]. The World Anti-Doping Agency (WADA) uses the urinary ratio of deconjugated T to epitestosterone (T/E ratio) to screen for exogenous testosterone administration. The threshold for declaring testosterone supplementation was set to 6 in 1983 and subsequently lowered to 4 in 2005 [21]. Baseline T/E ratio can differ by over 10-fold between different ethnicities, from 0.15 in Koreans (n=74) to 1.8 in Swedes (n=122) [22], and up to 20-fold between UGT2B17 del/del and ins/ins subjects [23,24]. After 500 mg exogenous T enanthate intramuscular administration, the average T/E ratio increased from 2.3 to 100 for ins/ins, 1.4 to 50.4 in ins/del, and 0.14 to 5.3 in del/del subjects [24]. On the other hand, the UGT2B15 D85Y and UGT2B7 H268Y polymorphisms do not seem to affect basal T/E ratios [24]. WADA now utilizes a Bayesian statistical model of Athlete Biological Passport (ABP), with the T/E ratio included in the urine steroidal module, for more comprehensive longitudinal monitoring of athletes [25].

Given the prevalence of UGT2B17 CNV and its androgen glucuronidating capacity, UGT2B17 CNV has been examined for links with testosterone-related and other pathophysiological outcomes (Table 1.1). Correlations between UGT2B17 and UGT2B15 and prostate cancer risk and progression have been studied. Two recent meta-analyses show a significant association between UGT2B17 CNV and increased prostate cancer risk [26,27]. UGT2B15 D85Y polymorphism (rs1902023) has also been significantly associated with increased prostate cancer risk and progression in several studies [28]. In addition, UGT2B17 CNV has been associated with increased fat mass and decreased insulin sensitivity in elderly men [29] and lower BMI in male Alaska Native people and African Americans [30]. Association with osteoporosis is inconclusive [31–34]. Studies show no association with osteoporosis risk in 1,347 elderly Caucasian women [31] and 203 surgically menopausal Japanese women [32], while a study in 2,379 postmenopausal women showed bone mineral density (BMD) increase comparable to the effect of hormone replacement [33], and a case-control genome-wide CNV analyses in 700 elderly Chinese showed strong association with osteoporotic fractures [34]. Low testosterone levels have been linked to reduced muscle mass, obesity, diabetes mellitus, and decreased bone mineral density [35]. In addition, androgen glucuronides may be involved in the regulation of unconjugated androgens, both in their intracellular concentrations and activities [29]. It has also been reported that UGT2B17 deletion individuals have higher serum testosterone levels [34]. Thus, UGT2B17 deletion with lower body mass index and higher bone mineral density may be related to systemic testosterone levels, which may reflect intracellular or tissue levels, and its subsequent biological activities.

UGT2B17 CNV also show associations with other pathophysiological conditions. For example, UGT2B17 gene deletion has been associated with increased risk for pancreatic cancer

in female Chinese [36], increased breast cancer risk in Iranian women [37], and decreased risk for colorectal cancer in male Caucasian population [38]. One study showed increased risk of lung cancer in Caucasian women [39] while another found no association in Austrian Caucasians [40]. UGT2B17 CNV has shown to be a positive indicator of relapse-free rate in pediatric non-lymphoblastic malignancies [41], and high UGT2B17 expression has been associated with poor prognostic factors for chronic lymphocytic leukemia [42,43]. UGT2B17 CNV has also been reported to act as a minor histocompatibility antigen and linked to occurrence and severity of graft versus host disease [44–46], especially in the intestine [47]. Conflicting results regarding associations may be due to the high degree of UGT2B17 variability. Associations with different cancers may possibly be attributable to UGT2B17's protective role in conjugating various xenobiotics, including potential carcinogens, as a conjugating enzyme.

A sex difference in tissue UGT2B17 protein abundance is not altogether surprising, considering that UGT2B17's main endogenous substrates are androgens. However, this does bring into play differential magnitudes of UGT2B17-related drug disposition or drug-drug interactions (DDIs) for males and females. The dramatically divergent ontogeny curves, again more prominent in males, introduces potential for increased adverse effects and toxicities in pediatric population for medications that are UGT2B17 substrates, as well as potential for lack of efficacy for UGT2B17 substrates for chronic medications, as the child develops.

The higher abundance of UGT2B17 in the intestine compared to the liver becomes relevant with respect to first pass metabolism. Intestinal metabolism is usually thought to be of equal or less importance than the liver, due to lower enzyme content and activity and lower blood flow in the GI tract [48,49]. For UGT2B17 substrates, however, greater intestinal metabolism may occur, resulting in a lower F_g compared to F_h, which can lead to greatly variable

first-pass metabolism with less variable systemic clearance. For example, MK-7246, an antagonist for chemoattractant receptor on T helper cell type 2, was discontinued from drug development due to 25-fold and 82-fold greater area under the curve (AUC) and C_{max} for UGT2B17 gene deletion subjects, respectively [50]. This variability is most likely due to intestinal first pass metabolism (F_g), indicative from parallel terminal elimination slopes and similar times to maximum concentrations. Higher intestinal UGT2B17 abundance, coupled with its high variability, also may augment the clinical significance of first pass metabolism of UGT2B17 substrates such as testosterone. Currently in the US, no oral formulations of testosterone are available, despite increasing use of testosterone replacement therapy, due to significant first pass metabolism [51–53].

High and variable first pass metabolism of UGT2B17 substrates can also lead to highly variable DDIs, due to variability in the fraction metabolized (f_m). Glucuronide conjugates were previously thought to be terminal metabolites, but recently have been found to be anionic substrates and potent mechanism-based inhibitors (MBIs) of CYP2C8 [54]; namely gemfibrozil acyl glucuronide and clopidogrel acyl glucuronide (CAG). Clinical drug interaction studies have shown significant increases in the AUC of pioglitazone and repaglinide (77% to 408%, respectively) after clopidogrel co-administration [55,56]. Both UGT2B7 and UGT2B17 glucuronidate clopidogrel carboxylic acid (CCA) to form CAG [9]. Clopidogrel is an oral anti-platelet agent used to inhibit blood clot formation. Once absorbed, this prodrug requires a 2-step CYP-mediated activation to form its active thiol metabolite, while 85% of the dose circulate as its inactive metabolite CCA [57]. The estimated fractional contribution of UGT2B17 in CAG formation is reported to be 10% in the liver and 84% in the intestine [9]. Possible clinical ramifications regarding CAG-mediated DDI are two-fold. First is the potential for a larger DDI

magnitude in high UGT2B17 expressors, which may result from higher hepatic CAG formation and subsequent CYP2C8 inactivation. Second is the variable formation of CAG during first pass metabolism, especially in the intestine. Highly variable CAG formation, resulting from interindividual variability in intestinal and hepatic UGT2B17 expression, may be of clinical concern, especially with narrow therapeutic index CYP2C8 substrates such as paclitaxel.

The high prevalence and ethnic/racial differences of the UGT2B17 CNV is particularly interesting, compared to other drug-metabolizing enzymes. Common CNVs usually indicate ancestral mutation prior to continental migration, and will be stable within a population, as indicated by Mendelian inheritance and Hardy-Weinberg equilibrium [11]. UGT2B17, along with UGT2B15, seem to be involved in androgen homeostasis; however, there are numerous other enzymes that can contribute to homeostatic balance through alternative metabolic pathways [58]. While UGT2B17 may not be a gene that is essential for life, e.g. deletion does not lead to embryonic or perinatal death, there are indications that both UGT2B15 and UGT2B17 have been under positive selection [59]. UGT2B17's 10-fold higher activity as well as broader substrate spectrum also suggest UGT2B17's impact on steroid homeostasis may be greater than that of UGT2B15 [3,60]. Given its numerous associations with multiple pathophysiological conditions, UGT2B17 may have a significant role in disease state progression [61]. This expands its potential role as a prognostic and susceptibility marker, in addition to implications in drug metabolism and development. Glutathione S-transferase M1 (GSTM1) and GSTT1 also are commonly deleted genes [11]. However, studies have mainly focused on detoxification and onco-protective roles of GSTs; associations with cancer risks seem to be absent or have weak penetrance [62,63]. On the other hand, CYP2D6 gene deletion is not as common, averaging 5%

across populations (0 to 17%); nonetheless, this polymorphism is clinically significant because the enzyme contributes to the metabolic clearance of 25% of currently marketed drugs [64].

The UGT2B17 CNV does not always show a clear gene-dose effect, which can be attributed to the remaining 74% of unexplained variability. A significant portion of UGT2B17 expressors have low tissue abundance of the enzyme and a reduced activity phenotype [10]. The wide range of interindividual variability which cannot be fully elucidated highlights the need for a phenotypic biomarker. The well-established connection between UGT2B17 and testosterone metabolism makes TG an ideal candidate as a starting point. In particular, a specific phenotypic urinary biomarker for UGT2B17 holds promising applications in drug development and disease associations. Urinary biomarkers are generally safer and more economical, as noninvasive measurements can be made without the use of needles or administration of exogenous substrates. Moreover, a urinary UGT2B17 biomarker can be used for prospective phenotypic patient stratification in designing studies for dosing or disease associations. It also allows for early predictions of UGT2B17 inhibition or induction potential, to help guide DDI study design, serving to address false positives from *in vitro* assays. A urinary UGT2B17 biomarker may also aid the accuracy of doping tests by reducing the frequency of false negative results. Potential applications for a UGT2B17 biomarker expand beyond drug development and interactions as a safety, monitoring, and response marker; given UGT2B17's associations with disease and developmental outcomes, a UGT2B17 biomarker also has potential to be a disease susceptibility and prognostic predictive marker [65].

1.4 INVESTIGATION OF INTESTINAL METABOLISM USING IN VITRO MODELS AND QUANTITATIVE PROTEOMICS

Compared to liver metabolism studies, investigation into intestinal metabolism has been limited by historically low activity and unsuccessful reproducibility of available *in vitro* systems. This is in part due to the heterogeneity of intestinal tissues and cell types as well as variation in preparation methodology for subcellular fractions like microsomes and S9 [66]. Measuring F_g, compared to F_a and F_h, is also difficult due to its sequential nature of first-pass metabolism and inherent limitations in the *in vivo* vascular sampling site. In addition, the research focus of intestinal metabolism has been tilted towards phase I enzymes, particularly cytochrome P450s (CYPs), while non-CYP enzymes, such as carboxylesterases (CES), sulfotransferases (SULTs), and UGTs have been relatively understudied [67,68], due to lower contributions to drug clearance [69]. Investigation of UGT2B17-mediated metabolism will require an *in vitro* model that is able to capture sequential metabolism, as UGT2B17 is highly expressed in the intestine and is a phase II conjugating enzyme. Novel systems to assess intestinal metabolism have recently emerged, such as precision cut intestinal slices (PCIS) [70], cryopreserved enterocytes [71], and cryopreserved human intestinal mucosal epithelium (CHIM) [72]. These *in vitro* tools can be applied in *in vitro* to *in vivo* extrapolation (IVIVE) and modeling for prospective prediction of drug disposition and DDIs.

Quantitative proteomics has emerged as a promising tool to fill tissue protein abundance knowledge gap and lead to in better translation and *in vivo* prediction of drug disposition through the generation of accurate scaling factors to be applied in physiologically-based pharmacokinetic (PBPK) modeling [73,74]. Targeted multiple reaction monitoring (MRM)-based proteomics has been widely applied to quantify drug metabolizing enzymes and transporter (DMET) proteins.

Validated protocols for basic work flow – i.e. surrogate peptide selection, sample processing, protein extraction, digestion, LC-MS/MS quantification – have been reported (Figure 1.4). Optimization tools to control for variables that can affect protein quantification have been identified and published, including targeting multiple peptides and associated ions, inclusion of positive controls and internal standards, consideration of matrix effects, and general best analytical practices [75].

This dissertation project aims to characterize the interindividual variability and differential tissue abundance of UGT2B17 and its potential impact on the disposition of exogenous and endogenous substrates. Chapter 2 focuses on investigating the role of UGT2B17 in testosterone first pass metabolism, Chapter 3 describes the identification and validation of a potential urinary UGT2B17 biomarker, and Chapter 4 utilizes quantitative proteomics to examine non-CYP enzyme abundance in intestinal in vitro model CHIMs and test for activity-abundance correlations.

1.5 HYPOTHESIS AND SPECIFIC AIMS

The overarching hypothesis for this dissertation is as follows:

High variability and unique intestinal abundance of UGT2B17 can result in unpredictable pharmacokinetics and drug-drug interactions, and can be prospectively predicted using a phenotypic biomarker and quantitative proteomics which can be applied to physiologically-based pharmacokinetic (PBPK) modeling.

Specific aims of this dissertation research are:

Specific Aim 1: Examine the role of UGT2B17 in testosterone first-pass metabolism

Specific Aim 2: Identify and validate a phenotypic UGT2B17 biomarker, testosterone glucuronide normalized with androsterone glucuronide (TG/AG)

Specific Aim 3: Characterize regional protein abundance of UGT2B17 and other non-CYP enzymes along the small intestine in cryopreserved human intestinal mucosa (CHIM) model using quantitative proteomics, and validate activity in CHIMs

Table 1.1. Reported clinical implications of UGT2B17 copy number variation (CNV)

Clinical condition	Clinical outcomes	Reference(s)
A. Testosterone-disposition related pathophysiological outcomes		
Doping test for athletes	Confounder leading false negatives in *UGT2B17 Del/Del* subjects due to low baseline and undistinguishable changes in deconjugated urinary testosterone to epitestosterone (T/E) ratio after doping	[20,25,76]
Prostate cancer	*UGT2B17 Del/Del* show significant associations with prostate cancer in 2 meta-analyses. - Odds Ratio 1.33 (1.00-1.77) ($p < 0.001$) - Odds Ratio 1.74 (1.14-2.64) ($p < 0.001$)	[26,27]
Body Mass Index (BMI)	*UGT2B17 Del/Del* associated with lower BMI in males in Alaska Natives ($p < 0.001$) and African Americans ($p = 0.01$)	[30]
Fat mass	*UGT2B17 Del/Del* associated with body fat indicators (weight, BMI, total body fat, and trunk fat) ($p <0.05$) in elderly cohort	[29]
Insulin sensitivity	*UGT2B17 Del/Del* associated with serum insulin and Homeostasis model assessment (HOMA) index ($p <0.05$) in elderly cohort	[29]
Osteoporosis	No associations in elderly Caucasian women or Japanese women. *UGT2B17 Del/Del* significantly associated with higher bone mineral density ($p < 0.05$) Individuals with at least one *UGT2B17* gene has increased OR 1.73 (1.22-2.45) for osteoporotic fractures	[31,32] [33] [34]
Puberty	*UGT2B17 Del/Del* significantly associated with delayed pubarche in healthy boys (0.34 years delay per allele, $p = 0.029$)	[77]
B. Other pathophysiological outcomes		
Lung cancer	No association on onset or outcome of lung cancer in Austrian Caucasians *UGT2B17 Del/Del* associated with increased OR 2.0 (1.01-4.0) in women	[40] [39]

Pancreatic cancer	*UGT2B17 Del/Del* associated with increased risk (p = 0.04), more significant in women (p = 0.01)	[36]
Breast cancer	*UGT2B17 Del/Del* associated with increased OR 2.99 (1.94-4.60) for breast cancer	[37]
Colorectal cancer	*UGT2B17 Del/Del* associated with decreased risk of colorectal cancer risk (p = 0.044)	[38]
Non-lymphoblastic malignancy prognosis	Individuals with at least one *UGT2B17* gene has increased hazard ratios 16.1 (1.67-154) for relapse rates	[41]
Chronic lymphocytic leukemia survival	No significant association seen between *UGT2B17 Del/Del* and treatment free or overall survival, but significant associations between levels of UGT2B17 mRNA (low vs high) and treatment free (p < 0.001) and overall survival (p = 0.011)	[42]
C. Xenobiotic disposition		
MK-7246 metabolism	Drug development failure due to variable pharmacokinetics in Phase I study	[50]
Vorinostat metabolism	Patients with *UGT2B17 Del/Del* showed significantly lower mean AUC ratio of vorinostat-O-glucuronide/vorinostat (p = 0.02), trending towards greater adverse events (p = 0.12) and median survival (p = 0.087).	[78]
17-hydroxyexemestane metabolism	Patients with *UGT2B17 Del/Del* associated with higher 17-hydroxyexemestane levels (p = 0.04) and better prognosis (HR = 0.45, 0.2-1.01)	[79]

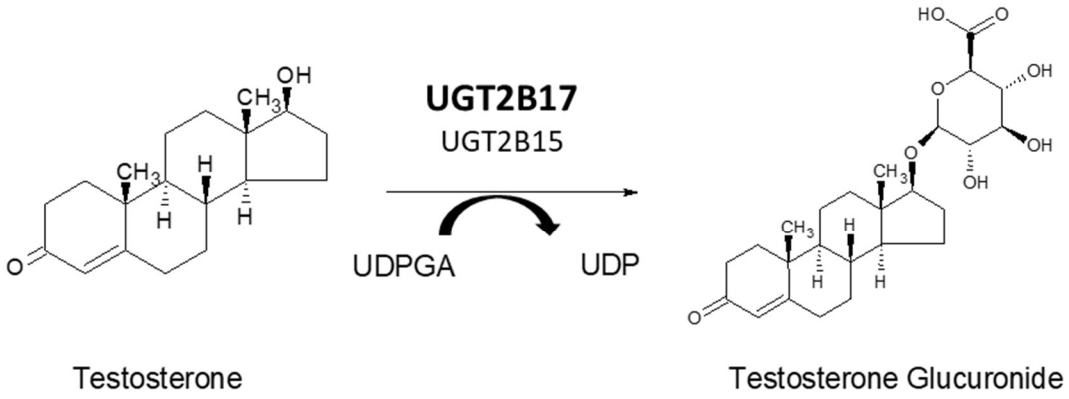

Figure 1.1. Testosterone glucuronidation.

Testosterone is glucuronidated at the 17-beta hydroxy position by both UGT2B17 (major) and UGT2B15 (minor), utilizing UDPGA as a co-factor.

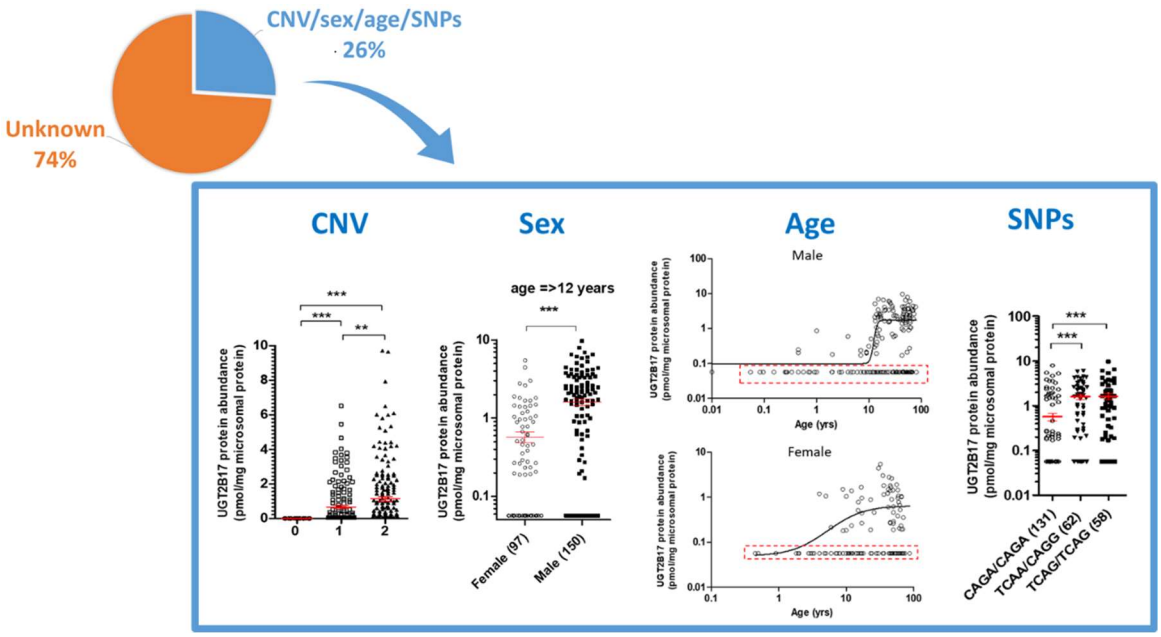

Figure 1.2. Factors affecting interindividual variability in hepatic UGT2B17 content. Multivariate analysis shows only 26% of variability is explained by copy number variation (CNV), sex, age, and single nucleotide polymorphisms (SNPs) combined, leaving 74% of UGT2B17 variability unknown.

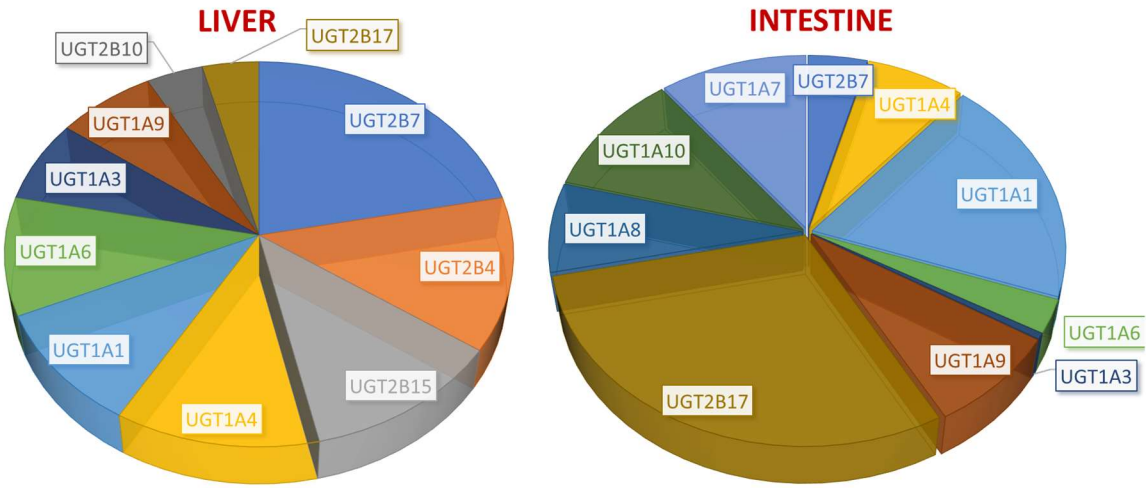

Figure 1.3. Relative abundance of UGT isoforms in the liver and intestine

UGT2B17 is a minor hepatic isoform but a major intestinal isoform, when expressed. The converse is true for UGT2B7, a major drug-metabolizing UGT isoform, as well as UGT2B15, which is undetected in the intestine. Figure 1.3 is reconstructed from [1].

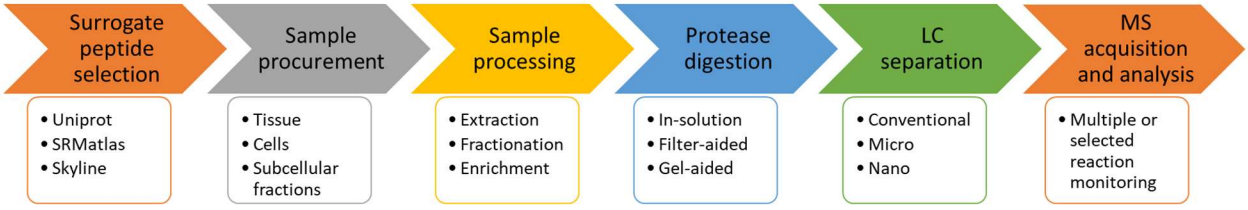

Figure 1.4. Typical workflow for targeted quantitative proteomics

Multiple approaches exist for each step. Figure 1.4 is adapted from [75].

Chapter 2. QUANTITATIVE CHARACTERIZATION OF UGT2B17 IN HUMAN LIVER AND INTESTINE AND ITS ROLE IN TESTOSTERONE FIRST-PASS METABOLISM

(A version of this chapter was published as a research article "Quantitative characterization of UDP-glucuronosyltransferase 2B17 in human liver and intestine and its role in testosterone first-pass metabolism." (2018) Biochemical Pharmacology 156:32-42)

2.1 INTRODUCTION

UGT2B17 is highly variable in its abundance and is one of the most commonly deleted genes in humans, with a higher deletion frequency seen in Asians [12]. Recently, we have shown that, other than copy number variation (CNV), multiple factors contribute to its variability, including sex, age, and single nucleotide polymorphisms [10]. In addition to variable pharmacokinetics (PK) and efficacy or toxicity of drugs (e.g. vorinostat) [78], drug metabolites (e.g., 17-dihydroexemestane) [80], and tobacco carcinogen (NNAL) [81], UGT2B17 variability has been associated with various testosterone-related clinical outcomes [22,24,26,27,29–31,34]. For example, studies show that UGT2B17 deletion individuals have 15% higher serum testosterone levels [34] and up to 90% lower urinary excretion of conjugated plus unconjugated testosterone [22]. UGT2B17 gene deletion is well recognized as a major confounder for anti-doping tests in athletes that can produce false positive and negative results [24], and is also associated with lower body mass index in males in a sex-specific manner [29,30]. Similarly, although controversial [31], a genome-wide CNV study found a strong link between UGT2B17

deletion and lower osteoporosis risk [34]. In addition, recent meta-analyses show increased prostate cancer risk with UGT2B17 gene deletion, amidst conflicting results [26,27].

Testosterone levels in men decline steadily after age thirty, reaching hypogonadal levels in approximately 20% to 50% of men in their 60s and 80s, respectively [82]. Symptomatic hypogonadism is treated with exogenous administration of testosterone, which leads to improvements in fatigue, muscle strength, body mass index, and mood [51]. In 2011 alone, 3.8% of men in their 60s were on testosterone replacement therapy (TRT). TRT is available in the United States (US) in various forms, i.e., transdermal, intramuscular, nasal, buccal, and subdermal. Oral formulations approved in the US are prodrug formulations of alkylated testosterone which, unfortunately, is accompanied by increased risk of hepatotoxicity such as cholestatic jaundice, therefore limiting its use [83,84]. The esterified prodrug, testosterone undecanoate, has been used in Canada [85] and in Europe since 1970s without risk of liver damage [86]. However, it requires co-consumption with a fatty meal due to its lymphatic pathway of absorption and has additional concerns related to elevated dihydrotestosterone (DHT) levels [52,87]. Despite advantages of greater patient adherence and ease of use, oral testosterone formulations have been generally unsuccessful due to significant first-pass metabolism [51–53].

To develop a viable oral testosterone formulation, it is important to characterize factors responsible for its low and variable absolute bioavailability (3.6 ± 2.5 %) [88]. Intravenous testosterone is rapidly eliminated with a half-life ranging from 10 to 100 minutes, with the majority of testosterone excreted as glucuronide conjugates (up to 80%), suggesting extensive involvement of hepatic UGTs [89]. UGT2B17 and UGT2B15 are the major and minor isoforms responsible for TG formation, respectively [15], both of which are expressed in the liver. However, UGT2B17 is also expressed in the intestine [18]. While the collective data

demonstrate the importance of UGT2B17 in testosterone first-pass metabolism, the quantitative role of intestinal and hepatic UGT2B17 has not been elucidated. Therefore, we first examined the abundance and testosterone glucuronidation activity of UGT2B17 and UGT2B15 in adult human liver and intestinal subcellular fractions. These data are important for physiologically-based PK (PBPK) modeling of first-pass metabolism of UGT2B17 substrates.

Testosterone also undergoes metabolism by several other enzymes such as steroid 5-alpha-reductase 2 (SRD5A2), cytochrome P450 3A4 (CYP3A4), 17β-hydroxysteroid dehydrogenase 2 (17βHSD2), and sulfotransferase 2A1 (SULT2A1) [58]. Of note, CYP3A4, 17βHSD2, and SULT2A1 are expressed both in liver and intestine [90–93]. Our recent clinical study confirmed high circulating levels of glucuronides of androsterone, testosterone and etiocholanolone after oral administration of testosterone [60]. However, individual contributions of liver and intestine in formation of these metabolites and their relative significance have not been studied to date.

We therefore investigated quantitative metabolite profiling in human hepatocytes and enterocytes after testosterone incubation. Characterization of UGT2B17 contribution and testosterone glucuronidation in the first-pass organs may lead to improved and more precise oral TRT regimens that may mitigate risks and maximize benefits.

2.2 Materials and methods

2.2.1 *Chemicals and reagents*

Testosterone, alamethicin, UDP-glucuronic acid (UDPGA), magnesium chloride, dibasic and monobasic potassium phosphate were purchased from Sigma-Aldrich (St. Louis, MO). Oxazepam was purchased from Fischer Scientific (Fair Lawn, NJ), and tyrosine kinase inhibitors (TKIs) were kindly provided by Genentech (San Francisco, CA). Testosterone metabolites,

respective conjugates, and standards were purchased from Cerilliant Corporation (Round Rock, TX) and Steraloid (Newport, RI). Bovine serum albumin (BSA) and protein extraction reagents were obtained from Thermo Fisher Scientific (Rockford, IL). Protein quantification chemicals and reagents were obtained as previously reported [94]. Hepatocyte thawing (MCHT50) and incubation (MM250) media were obtained from Lonza (Durham, NC), whereas, enterocytes thawing (CERM) and incubation (HQM) media were from IVAL (Columbia, MD). Synthetic light (with amino acid analysis) and heavy labeled peptides were purchased from New England Peptides (Boston, MA) and Thermo Fisher Scientific (Rockford, IL), respectively.

2.2.2 *Procurement of human liver and intestinal cells and subcellular fractions*

Cryopreserved primary human hepatocytes (n=5) and enterocytes (n=16) were obtained from Lonza (Durham, NC) and IVAL (Columbia, MD), respectively. Pooled human microsomes (HLM), intestinal microsomes (HIM), liver S9 and intestinal S9 fractions were obtained from Xenotech (Kansas City, KS). HLMs (n=26) from individual donors were procured from the University of Washington School of Pharmacy Liver Bank (Seattle, WA); tissue access for this study was exempt from human subjects approval, based on prior UW Institutional Review Board action. Proteomics, activity, and genotyping data were previously published [10]; a subset of adult samples were used for reproduction at differing concentrations of testosterone . Donor-matched intestinal tissue segments (n=6) were procured from Pomeranian Medical University, Szczecin, Poland, and approved by the local Bioethics Committee. Sample demographics are described in Table 2.1.

2.2.3 *Microsome isolation from donor-matched intestinal sections*

Donor-matched HIMs were isolated from different sections of intestine, i.e., duodenum (D), jejunum (J1-J3, three sections), ileum (I), and colon (C), from six individual donors. Tissue samples were disrupted using cell crusher paddles in liquid-nitrogen and HIMs were isolated using protocols from Microsome isolation kit (Abcam, Cambridge, United Kingdom) described elsewhere [95]. Total protein was determined by bicinchoninic acid (BCA) assay using the Pierce BCA Protein Assay Kit (Thermo Fisher Scientific, Rockford, IL) per manufacturer's protocol.

2.2.4 *Membrane protein extraction from primary cells and total protein quantification*

Membrane proteins were extracted from the cells using Mem-PER Plus Membrane Protein Extraction kit protocol (Rockford, IL). Briefly, previously washed and frozen hepatocytes (0.7 to 6 million) and enterocytes (6.7- 37 million) were resuspended with permeabilization buffer (200 or 400 µL), gently mixed, and incubated on a Compact Digital Waving Rotator (Thermo Fisher Scientific, Rockford, IL) for 30 minutes (4°C) at 300 rpm. Permeabilized cells were centrifuged at 16,000 x *g* for 15 minutes (4°C), and resulting supernatant containing cytosolic proteins was removed. Remaining pellet was resuspended with equal volume solubilization buffer, gently mixed, incubated for 60 minutes at 300 rpm (4°C), and centrifuged at 16,000g for 15 minutes (4°C). Resulting supernatant containing membrane proteins was collected and total protein quantification was measured with BCA assay (Thermo Fisher Scientific, Rockford, IL). Remaining solubilized membrane fraction was stored at -80°C for subsequent digestion and LC-MS/MS analysis.

2.2.5 *Protein denaturation, reduction, alkylation, enrichment and trypsin digestion*

Trypsin digestion was performed as previously described [94] for HLM and cell membrane samples. In brief, 10 µL dithiothreitol (250 mM), 30 µL ammonium bicarbonate buffer (100 mM, pH 7.8), 20 µL BSA (0.02 mg/mL), and 10 µL human serum albumin (10 mg/mL) were added to 80 µL samples (≤ 2 mg/mL total protein), followed by heat denaturation and reduction for 10 minutes at 95°C. Upon cooling to room temperature, alkylation of cysteine residues was performed by addition of 20 µL iodoacetamide (500 mM) and incubation in room temperature (in dark) for 30 minutes. Protein enrichment and desalting was done with extraction using chloroform-methanol-water (1:5:4) and resulting pellet washed and resuspended in 60 µL ammonium bicarbonate buffer (50 mM, pH 7.8). Trypsin (0.16 µg/µL) was added for digestion for 16 hours at 300 rpm (37°C). Digestion was quenched on dry ice with addition of 20 µL of heavy peptide internal standard cocktail and 10 µl acetonitrile: water 80:20 (v/v) with 0.5% formic acid. After centrifugation at 4000g for 5 minutes (4°C), resulting supernatant was analyzed by an LC-MS/MS method.

UGT2B17 quantification in donor-matched individual HIMs was performed at a different site (Oswald lab, University of Greifswald, Greifswald, Germany) using a slightly different method. The differences include trypsin digestion by filter-aided sample preparation (FASP) protocol and the use of ProteaseMax (Promega, Madison, WI) as a surfactant as discussed in detail elsewhere [96]. Three quality control HLM samples previously characterized for UGT2B17 abundance using method described above were used as quality controls for FASP protocol to address inter-laboratory technical variability.

2.2.6 *Quantification of Surrogate peptides of UGT2B17 and UGT2B15 in subcellular fractions*

HLM, S9 fractions, and hepatocyte cell membranes were analyzed using a Sciex Triple Quadrupole 6500 system (Sciex, Framingham, MA) coupled to Acquity UPLC System (Waters Technologies, Milford, MA). Chromatographic separation of peptides was achieved on ACQUITY UPLC HSS T3 1.8 μm, C_{18} 100A; 100 × 2.1 mm (Waters, Milford, MA) column. Skyline and Analyst 1.6.2 software were used to process acquired LC-MS/MS data. Detailed LC-MS/MS parameters have been previously published [10]. To address technical variability, we used heavy peptide internal standard as well as BSA for exogenous protein standard for all samples except enterocytes due to preexistence of BSA.

For donor-matched HIMs and three quality control samples digested using FASP protocol, LC-MS/MS analysis was performed using Kinetex C18 reverse phase column (100 x 2.1 mm, Phenomenex, Torrance, CA) and AB Sciex QTRAP 5500 system (Sciex, Framingham, MA). Data analysis was done using MultiQuant 3.0.2 software (Sciex, Framingham, MA). As individual HIM samples were quantified using FASP protocol, three HLM samples representing deletion, mid and high UGT2B17 abundance were used as quality controls and calibrators to address any technical variability.

2.2.7 *Testosterone glucuronidation assay in subcellular fractions*

Testosterone glucuronidation assay was performed with individual and pooled microsomes and S9 fractions, except donor-matched HIMs due to limited sample quantity. Assays were performed in triplicates with 10 μg of protein in 5 mM $MgCl_2$ and 100 mM potassium phosphate buffer (pH 7.4), 0.01% BSA, and 0.1 mg/mL of alamethicin in 100 μL final volume with testosterone (50 nM to 5 μM). After 15 minutes of pretreatment on ice, reactions

were initiated by addition of 2.5 mM UDP-glucuronic acid (UDPGA), incubated for 30 minutes (37°C) at 300 rpm, and terminated using 200 µL of ice-cold acetonitrile containing deuterated TG or rosuvastatin as internal standard. Samples were centrifuged at 10,000g for 5 minutes (4°C). TG (Table 2.2) and rosuvastatin (*m/z* 482.1→258.2; DP 70; CE 40) were quantified in supernatant by LC-MS/MS.

Enzyme kinetic parameters (Vmax and Km) were determined for UGT2B17 using three HLMs with high, mid, or null UGT2B17 abundance (9.7, 2.3, and 0.06 pmol/mg microsomal protein, respectively) with comparable UGT2B15 abundance (27, 20, and 34 pmol/mg microsomal protein, respectively). Assays were performed in triplicates with varying testosterone concentrations (0.05, 0.25, 0.5, 2.5, 5, 10, 15, 25 µM) and closely followed the protocol for the testosterone glucuronidation assay.

2.2.8 *Inhibition of UGT2B17 activity by tyrosine kinase inhibitors in HLM*

UGT2B17 inhibition assays were performed on two HLMs expressing high and below limit of detection (LOD) UGT2B17 abundance (9.7 and 0.06 pmol/mg microsomal protein) with comparable UGT2B15 abundance (27 and 24 pmol/mg microsomal protein). Inhibition assays were performed in triplicates and followed the testosterone glucuronidation assay. One and 25 µM of various TKIs (gefitinib, lapatinib, pazopanib, sorafenib, sunitinib, sirolimus, temsirolimus, dasatinib, nilotinib, and imatinib) were preincubated for 5 minutes at 37°C prior to reaction initiation with UDPGA with 5 µM testosterone to screen for UGT2B17 specificity. The most potent and selective UGT2B17 inhibitor imatinib was further assayed for IC_{50} determination with varying imatinib concentrations (0.01, 0.02, 0.05, 0.1, 0.5, 1, 10, 50, and 100 µM). UGT2B17 activity was measured with TG formation with 1 µM testosterone. Oxazepam

was used as a probe substrate for UGT2B15 activity by measuring oxazepam glucuronide formation (*m/z* 463.3→287.1, 269.1; DP 70; CE 20) with 10 µM oxazepam.

2.2.9 *Testosterone metabolism in human hepatocytes and enterocytes*

Hepatocytes (n=5) were thawed for 90 to 120 seconds in a 37°C waterbath, resuspended in 15 mL of MCHT50, and centrifuged at 100g for 8 minutes at room temperature. Cell count was performed using Nexcelom Bioscience Cellometer Auto T4 (Lawrence, MA), followed by a second centrifugation at 100g for 1 minute. Cells were then resuspended in MM250 at 1 million cells per mL concentration and preincubated for 10 minutes at 37°C. Reactions were initiated by adding 500 µL of hepatocyte suspension to 500 µL pre-warmed MM250 containing 100 µM Testosterone in 12-well plates. The final 1 mL mixture in each well contained 0.5 million cells in 50 µM Testosterone, which was incubated for 60 minutes (37°C) at 100 rpm. Total organic solvent (v/v) did not exceed 0.1%. The incubation was terminated by addition of 2 mL ice-cold acetonitrile containing internal standards. Cells were mechanically lysed by vortex mixing and centrifugation at 3000g for 10 minutes (4°C). The supernatant was immediately stored at -80°C prior to analysis by LC-MS/MS. Characterization of enterocyte activity (n=16) followed a similar protocol using CERM and HQM as thawing and incubation media, respectively, and were seeded to yield a final 100 µL mixture in 96-well plate containing up to 150,000 cells in 50 µM Testosterone, followed by a 120-minute incubation (37°C) at 100 rpm.

2.2.10 *LC-MS/MS analysis of testosterone metabolites formed in human hepatocytes and enterocytes*

Testosterone and its metabolites (Table 2.2) were measured by LC-MS/MS using the same system as protein quantification. Quantified metabolites include testosterone glucuronide

(TG), 5α-dihydrotestosterone (DHT), DHT glucuronide (DHTG), androsterone (A), androsterone glucuronide (AG), androstenedione (AED), 6-hydroxy testosterone (6OHT), etiocholanolone (E), and etiocholanolone glucuronide (EG). LC conditions were set at 0.3 mL/min flow rate and 5 µL injection volume with mobile phase A: water with 0.1% formic acid and B: acetonitrile with 0.1% formic acid. The gradient program was: 85% A (0-2.5 min), 85-60% (2.5-8.5 min), 60-50% (8.5-12.8 min), 50-2% (12.8-13 min), 2-85% (13-15 min). Whenever available, deuterated internal standards were used. Lower limit of quantification (LLOQ) was established, with limit of detection (LOD) set as one-third of LLOQ values. Multiple reaction monitoring (MRM) parameters used to quantify testosterone metabolites are shown in Table 2.2.

2.2.11 *Data analysis*

The fractional contribution (f_m) of UGT2B17 to total metabolic activity was calculated using Equation 2.1 through 2.3. We assumed, based on prior published work, that the activity measured by TG formation was mediated only by UGT2B17 and UGT2B15. Thus all TG formation was via UGT2B15 in homozygous UGT2B17 gene deletion samples (UGT2B17 del-del). A normalized average UGT2B15 activity was calculated as the average activity in the sample divided by the average UGT2B15 protein expression (Equation 2.1). We then obtained individual UGT2B15 activity by multiplying average UGT2B15 activity with individual UGT2B15 protein abundance. This value was subtracted from total individual activity ($CL_{total\ obs}$) to acquire individual UGT2B17 activity ($CL_{UGT2B17}$) (Equation 2.2). Individual UGT2B15 and UGT2B17 f_m are the respective individual activities divided by total individual TG formation (Equation 2.3). Negative estimates of UGT2B17 activity were adjusted to zero. Calculations were performed using Microsoft Excel (Redmond, WA).

$$\text{Avg } CL_{UGT2B15} = \frac{\text{Mean } CL_{UGT2B15}(\text{UGT2B17 del}-\text{del})}{\text{Mean } [E]_{UGT2B15}\ (\text{UGT2B17 del}-\text{del})} \quad (2.1)$$

$$CL_{UGT2B17} = CL_{\text{total obs}} - \text{Avg}CL_{UGT2B15} * [E]_{UGT2B15} \quad (2.2)$$

$$f_{m,UGT2B17} = \ CL_{UGT2B17}/CL_{\text{total obs}} \quad (2.3)$$

Enzyme kinetic parameters (K_m and V_{max}) were obtained by fitting the Michaelis-Menten equation to the activity data using GraphPad Prism version 5.03 for Windows (La Jolla, CA) (Equation 2.4), where Y is testosterone glucuronidation rate (pmol/mg protein/min) and X is testosterone concentration (μM).

$$Y = \frac{V_{max} * X}{(K_m + X)} \quad (2.4)$$

IC_{50} values were calculated using the following nonlinear regression model (Equation 2.5), where Y is relative glucuronidation activity (% TG formation) and X is inhibitor concentration (μM). IC_{50} values were obtained using GraphPad Prism version 5.03 for Windows (La Jolla, CA).

$$Y = \frac{100}{(1+\frac{X}{IC_{50}})} \quad (2.5)$$

2.2.12 *Statistical analysis*

UGT2B217 protein abundance between HLM and HIM (excluding colon) was compared using Mann-Whitney test. UGT2B17 protein abundance-TG formation correlation and corresponding p-values were obtained using Spearman's correlation. Statistical analyses were performed with GraphPad Prism version 5.03 for Windows (La Jolla, CA).

2.3 RESULTS

2.3.1 *UGT2B17 and UGT2B15 abundance and correlation with testosterone glucuronidation in human liver and intestinal subcellular fractions*

Protein abundance in adult HLMs (n=26) showed high inter-individual variability for UGT2B17 (>160-fold) with 46% (n=12) falling below LLOQ, which included 23% confirmed gene deletions (n=6) (Table 2.3). UGT2B15 protein abundance was much less variable (4-fold) (Figure 2.1A). High variability in UGT2B17 was also observed in HIMs (>492-fold), with a trend for increasing abundance when comparing distal to proximal gastrointestinal (GI) segments (Figure 2.1C). Average UGT2B17 protein abundance in the HIM (excluding colon) was significantly higher (4.4-fold) than HLM (p=0.016). UGT2B15 was not detectable in donor-matched HIMs and pooled fractions, in agreement with published literature [18,96,97]. . UGT2B17 protein abundance in individual HLM showed a strong correlation with testosterone glucuronidation activity (r^2= 0.77, p<0.001) (Figure 2.1E), confirming its major role in TG formation. UGT2B15 showed a significant correlation with TG formation only in samples with UGT2B17 level below LLOQ (r^2=0.65, p=0.02) (Figure 2.1F), consistent with our previous findings [10]. In addition, UGT2B17 abundance and TG formation was higher in pooled subcellular fractions from intestine compared to liver (Figure 2.1F). Estimated fractional contribution for UGT2B17 ($f_{m,UGT2B17}$) and UGT2B15 ($f_{m,UGT2B15}$) ranged from 0 to 0.91, and 0.09 to 1, respectively, depending on UGT2B17 variability (Figure 2.1B). For example, $f_{m,UGT2B17}$ was 0.74 or higher in samples with UGT2B17 abundance >1 pmol/mg microsomal protein, whereas, $f_{m,UGT2B15}$ was 0.85 or higher in samples that were below LLOQ for UGT2B17.

2.3.2 *Enzyme kinetic parameters for testosterone in HLM*

Calculated K_m (μM) and V_{max} (pmol/mg protein/min) for high, mid, and null UGT2B17-expressing HLMs were 13.5, 4.0, and 8.1 μM, and 5.96, 1.44, and 0.295 nmol/mg protein/min, respectively (Figure 2.2A). High and mid UGT2B17-expressing HLMs had a 4-fold difference in absolute UGT2B17 protein abundance (9.6 and 2.3 pmol/mg protein, respectively) with a corresponding 4-fold difference in calculated V_{max}. Noticeable substrate depletion was observed for high UGT2B17 expressing HLM at low- and mid-range testosterone concentration, perhaps leading to variability observed in K_m values.

2.3.3 *Inhibition of UGT2B17 and UGT2B15 by Tyrosine Kinase Inhibitors*

Among the 10 TKIs screened for UGT2B17 inhibition, imatinib was the most potent and selective inhibitor of UGT2B17 (Figure 2.2D). IC_{50} values for imatinib using testosterone as a substrate was 0.31 μM for high-UGT2B17 expressing HLM and 69 μM for low-UGT2B17 expressing HLM (Figure 2.2B), with the lower value being in agreement with published literature for recombinant UGT2B17 [98]. When oxazepam was used as a probe substrate for UGT2B15, imatinib IC_{50} values in high- and low-UGT2B17 expressing HLM were similar, with mean values of 54 μM and 79 μM, respectively (Figure 2.2C).

2.3.4 *UGT2B17 and UGT2B15 protein abundance and testosterone metabolism in primary human hepatocytes and enterocytes*

In hepatocytes, protein abundance (mean ± SD, pmol/mg membrane protein) for UGT2B17 and UGT2B15 were 0.4 ± 0.4 and 6.5 ± 4.3, respectively. In enterocytes, UGT2B17 protein abundance (mean ± SD, fmol/million cells) was 11.8 ± 12.6 and UGT2B15 was not detected.

Structures of quantified testosterone metabolites with corresponding enzymes in a simplified metabolism scheme are shown in Figure 2.3A, with respective metabolite formation rates of each metabolite listed in Table 2.4. A representative chromatogram of a hepatocyte incubation showing chromatographic and MS/MS separation is shown in Figure 2.3B. The three most abundant metabolites were AED, TG, and 6OHT for both hepatocytes and enterocytes, whereas, DHT, DHTG, A, and AG combined constituted less than 4% (hepatocytes) and 1% (enterocytes), and E and EG were below LLOQ (Figures 2.4A, 2.4C). TG was the second major metabolite measured, at two-fold or higher abundance levels compared to other metabolites except AED. TG formation rate (mean ± SD, pmol/million cells/hour) was higher in hepatocytes (4836 ± 2460) compared to enterocytes (437 ± 433). Correlation between relative UGT2B17 protein abundance and TG formation was significant in enterocytes (r^2=0.69, p=0.003). However, the correlation was not significant in hepatocytes, perhaps due to smaller sample size and confounding contribution from UGT2B15 (Figures 2.4B, 2.4D). UGT2B15 also showed nonsignificant correlation with TG formation in hepatocytes and was not detected in enterocytes.

2.4 DISCUSSION

To the best of our knowledge, this is the first study to demonstrate the regional distribution of UGT2B17 in paired intestinal microsomes. It is also the first to apply a primary enterocyte model to study testosterone metabolomics and UGT activity in enterocytes in comparison with hepatocytes. Here we also propose a facile method of f_m estimation for UGT2B17 substrates in HLMs using gene deletion samples when two or more UGT isoforms are involved in glucuronidation.

UGT2B17 protein abundance in subcellular fractions revealed two findings with notable implications. First, UGT2B17 showed 4.4-fold higher abundance in intestine compared to liver,

in agreement with published literature reporting two-fold higher levels of UGT2B17 in intestine [18]. The same article reports UGT2B17 constituting 3% of total UGT isoforms in the liver but 59% in the intestine, in contrast to UGT2B15 which has high relative hepatic expression of 12% but was undetected in intestine, similar to our findings. Again in contrast to UGT2B17, UGT2B7, which is considered to be a major drug-metabolizing UGT isoform [1], constitutes 22% and 4% of total UGT isoforms in the liver and intestine, respectively [18]. This unique pattern of expression of UGT2B17 augments the clinical significance of first pass metabolism for orally administered UGT2B17 substrates. Bioavailability (F) is a product of fraction absorbed (F_a), fraction escaping intestinal metabolism (F_g), and fraction escaping hepatic metabolism (F_h). While CYP3A4, the most prominent enzyme involved in first pass metabolism, was found to be in equal or higher abundance in the intestine compared to the liver, other drug metabolizing enzymes, such as CYP2D6, CYP2C9, and CYP2C19, have shown equal or lower levels in the intestine compared to the liver—nonetheless, CYP3A4 remains the major drug metabolizing CYP isoform in both organs [48,49,90]. However, for UGT2B17 substrates, significantly greater intestinal metabolism may occur relative to other UGTs, resulting in lower F_g than F_h, leading to a highly variable first-pass effect with less variable systemic clearance. An example of this is MK-7246, which was discontinued from development due to unexpected PK variability. This was later attributed to UGT2B17, showing a 25-fold higher area under the curve in subjects with UGT2B17 gene deletion [50]. Secondly, UGT2B17 showed a trend for increased abundance down the GI tract, from duodenum to colon. This indicates that the site of absorption may impact the extent of UGT2B17-mediated GI metabolism (F_g), which can potentially contribute to significant variability in systemic drug exposure due to factors affecting GI motility and transit time. This may be exploited for enhancing oral biovailability. It also brings into play the

likelihood of variability in drug disposition by affecting the extent of enterohepatic recycling. In contrast, UGT2B15 showed relatively consistent expression in the liver and was undetected in pooled intestinal subcellular fractions and cells. This supports the absence of UGT2B15 in intestinal tissues, where literature reports detection of UGT2B15 mRNA and inconsistency at protein levels [18,97,99].

Considering the higher expression of UGT2B17 in HIM, it is reasonable to expect more TG formation in enterocytes compared to hepatocytes. However, enterocytes showed an overall 10-fold lower activity compared to hepatocytes, despite a metabolome profile that was similar to that of hepatocytes. This is possibly due to lower soluble protein content of enterocytes and loss of activity during cryopreservation of enterocytes. There have been two published studies reporting cryopreserved enterocyte activities [71,100] and further characterization would be beneficial.

Our method for estimating fractional metabolic contributions is applicable to other polymorphic enzymes such as CYP2D6. The wide range of $f_{m,UGT2B17}$ from 0 to 0.91 shows variable DDI potentials for UGT2B17-specific substrates, which is highlighted by imatinib as a potent UGT2B17-specific inhibitor. Imatinib IC_{50} value of 0.3 μM, combined with calculated maximum unbound hepatic input concentration of 0.7 μM [98], can lead to double the exposure of a UGT2B17-specific substrate. However, the magnitude of imatinib inhibition will vary widely depending on UGT2B17 protein abundance levels thus $f_{m,UGT2B17}$. For the subset of high UGT2B17-expressors, potential DDIs become particularly concerning, where UGT2B17 inhibition will lead to dramatic increase in systemic exposure of its substrate. However, identification of these high-expressors cannot easily be done, as genotype, age, sex, and SNP combined accounts for only 29% of UGT2B17 variability [10]. Thus, identifying a phenotypic

biomarker or probe drug for UGT2B17 would be beneficial in identifying these individuals at high risk for DDI.

Androstenedione (AED), rather than TG, as the dominant metabolite in both hepatocytes and enterocytes was a surprising, albeit reasonable finding. 17 β-HSD2 mediates AED formation from testosterone, while 17β-HSD1,17β-HSD3, and 17β-HSD5 convert AED to testosterone [91]. 17β-HSD2 has high expression in GI and liver, while 17β-HSD1 and 17β-HSD3 are sex tissue-specific, and 17β-HSD5 is ubiquitously expressed [101,102]. AED is one of the main adrenal hormones in circulation along with DHEA as an inactive adrenal precursor. Considering AED as an androgen reservoir pool explains preferential AED formation over elimination via the glucuronidation pathway at supra-physiological testosterone concentrations tested, which would likely have saturated UGT2B17 and UGT2B15, given their reported K_m values of 10 and 6.5 μM, respectively [103,104]. This metabolite ratio may change at physiological testosterone concentrations, which are well below their K_m values.

Figure 2.5 shows the average plasma metabolite profile in seven healthy adult men at baseline (Figure 2.5A), following an 800mg oral testosterone administration up to 24 hours after chemical castration with acyline (Figure 2.5B), and the fold-difference from baseline (Figure 2.5C) [60]. TG had the most significant increase in percentage and absolute concentration (10-fold and 280-fold, respectively), compared to the next highest increase seen in DHTG and EG (both about 1.5-fold and 40-fold, respectively). This indicates the important role of glucuronidation in exogenous testosterone elimination, which may have been attenuated by AED formation in the cell systems.

There are several limitations of this study, a major limitation being small sample sizes. In addition, while we could detect most of the testosterone metabolites, we were unable to quantify

all known and intermediate metabolites, such as testosterone sulfate, androstenedione, estradiol, or potential metabolites that have not yet been reported, such as 6OHT glucuronide, which has an additional potential glucuronidation site at 6β-hydroxy position after CYP3A oxidation. Having this information would present a more comprehensive picture of testosterone metabolism. In addition, the *in vitro* enterocyte cell system that was used has not been extensively validated, although exhibited metabolic activity [71]. Moreover, restrictions in experimental incubation times may produce an incomplete picture of *in vivo* metabolism that encompass sequential reactions.

In summary, we characterized UGT2B17 abundance and catalytic activity in first-pass effect organs, where its role in drug metabolism remains understudied and underappreciated. For example, while one study showed UGT2B17 to be one of the main isoforms responsible for clopidogrel acyl glucuronide (CAG) formation [9], another study did not include this isoform and hence concluded that UGT2B7 forms CAG [105]. In addition, TRT has recently come under scrutiny due to reports of possible increased cardiovascular events, and the risks and benefits of TRT still remain contentious among practitioners [82,106–108]. As TRT use continues to increase, elucidation of the testosterone elimination pathways is crucial for individualized dosing and optimizing treatment with TRT. Our data on UGT2B17 abundance will be applicable in building a PBPK model for first-pass metabolism for UGT2B17 substrates including testosterone. An extensive body of research literature on testosterone biosynthesis pathways exists, but data on exogenous testosterone metabolism and elimination pathways are still lacking. This report addresses some of that knowledge gap.

Table 2.1. Sample Demographics

	Sex	n	Age range (mean, years)	Ethnicity[a]
Human liver microsomes	Male	14	21-61 (44)	13 C, 1 A
	Female	12	45-70 (57)	12 C
Human intestinal microsomes	Male	5	22-59 (37)	5 C
	Female	1	62	
Human hepatocytes	Male	3	18-55 (33)	3 C
	Female	2	45-54 (50)	2 C
Human enterocytes	Male	8	32-60 (49)	7 C, 1 H
	Female	5	48-54 (53)	5 C
	Unknown	3	Unknown	3 Unknown

[a] Caucasian, C; Asian, A; Hispanic, H

Table 2.2. Optimized multiple reaction monitoring (MRM) parameters used for quantitative analysis of testosterone metabolites.

Metabolite/internal standard	Precursor ion (m/z)	Daughter Ion(s) (m/z)	DP (V)	CE (eV)	LLOQ[a] (ng/mL)
6β-Hydroxytestosterone	305.3	269.1, 121, 109	90	30, 21, 30	1 [0]; 0.5 [0]
6β-Hydroxytestosterone-d3	308.3	272.2, 290.2	80	30	
Androstenedione	287.2	109.1, 97.1	80	30	50 [0]; 50 [0]
Androsterone	291.2	255.1	60	25	10 [2]; 5 [8]
	273.1	255.1, 147	60	15, 20	
Androsterone glucuronide	449.1	255.2	70	25	5 [1]; 5 [11]
	484.3	255.2, 273.2	70	35	
Androsterone-d2	275.2	275.1, 147.1	80	5, 30	
Androsterone glucuronide-d4	453.2	259.2, 277.4	80	30, 22	
	488.3	259.3	80	30	
5α-Dihydrotestosterone	291.1	255.4, 159.1	70	22, 28	5 [0]; 1 [1]
	273.1	255.4	70	22	
5α-Dihydrotestosterone glucuronide	467.3	255.2	70	35	5 [0]; 1 [7]
	484.3	273.2	70	35	
5α-Dihydrotestosterone-d3	294.3	91, 258.2	70	69, 25	
5α-Dihydrotestosterone glucuronide-d3	470.2	294.2, 276.2, 159.2	80	30	
Etiocholanolone	273.2	255.1, 147	80	25	5 [5]; 1 [16]
	291.1	255.1	80	30	
Etiocholanolone glucuronide	484.3	273.2, 255.2	70	35	0.5 [2]; 5 [16]
	467.3	255.2	70	35	
Testosterone	289.1	109.1, 97.1	80	30	
Testosterone glucuronide	465.2	289.2, 271.2, 109.1	70	25, 30, 35	0.5 [0]; 0.5 [0]
Testosterone-d3	292.2	109.1, 97.1	80	30	
Testosterone glucuronide-d3	468.2	292.2, 274.2, 256.2	70	25, 30, 35	

[a] Lower limit of quantification (LLOQ) in hepatocytes; enterocytes. Value in brackets indicates number of samples below LLOQ, which were assigned limit of detection (LOD) as one-third of LLOQ values.

Table 2.3. Absolute protein abundance and inter-individual variability of UGT2B17 (pmol/mg microsomal protein) in human liver and intestinal microsomes (HLM and HIM).

	Mean ± SD (Range)[a]	Fold difference[b]
HLM (n=26)	1.7 ± 2.7 (0.06-9.7)	161
HIM-Average Small Intestine (n=6)	7.6 ± 6.6 (0.06-19.2)	319
HIM-Duodenum (n=6)	6.0 ± 8.2 (0.06-22.0)	366
HIM-Jejunum (n=6)	6.8 ± 6.0 (0.06-20.8)	346
HIM-Ileum (n=6)	10.8 ± 10.8 (0.06-28.7)	479
HIM-Colon (n=6)	16.2 ± 11.4 (0.06-29.5)	492

[a] For reference, UGT2B15 abundance was 30.9±8.8 (11.8-44.7) in HLMs with 3.8-fold difference. UGT2B15 was not detected in pooled intestinal subcellular fractions and in donor-matched HIM.

[b] fold difference from LOD (0.06 pmol/mg microsomal proteins).

Table 2.4. Formation rate (pmol/million cells/hour) of testosterone metabolites in human hepatocytes and enterocytes

Cell type	Parameter	AED[a]	TG[a]	6OHT[a]	DHT[a]	DHTG[a]	A[a]	AG[a]	E[a]	EG[a]
Hepatocytes[b]	Mean ± SD	16154 ± 10314	4836 ± 2460	2684 ± 1527	479 ± 393	115 ± 76	95.6 ± 113	214 ± 333	<2.8[c]	<3.5[c]
	Median	13179	5515	3044	389	102	63	93	N/A	2
	Relative level (%)	66	20	11	2	0.5	0.4	0.9	0.01	0.01
	Relative to TG (fold difference)	3.3	1	0.6	0.1	0.02	0.02	0.04	0.001	0.001
Enterocytes[b]	Mean ± SD	5743 ± 3035	437 ± 433	220 ± 128	25 ± 10	2.7 ± 4.1	15 ± 31	7.6 ± 15	<0.33[c]	<0.96[c]
	Median	5450	430	199	24	1	7	4	N/A	N/A
	Relative level (%)	89	6.8	3.4	0.4	0.04	0.2	0.1	0.01	0.04
	Relative to TG (fold difference)	13	1	0.5	0.06	0.006	0.03	0.02	0.001	0.002

[a] Androstenedione, AED; testosterone glucuronide, TG; 6-hydroxy testosterone, 6OHT; dihydrotestosterone, DHT; DHT glucuronide, DHTG; androsterone, A; A glucuronide, AG; etiocholanolone, E; E glucuronide, EG.

[b] Cryopreserved primary human hepatocyte and enterocyte suspensions were incubated in 50 μM testosterone for 60 and 120 minutes, respectively

[c] LOD = limit of detection

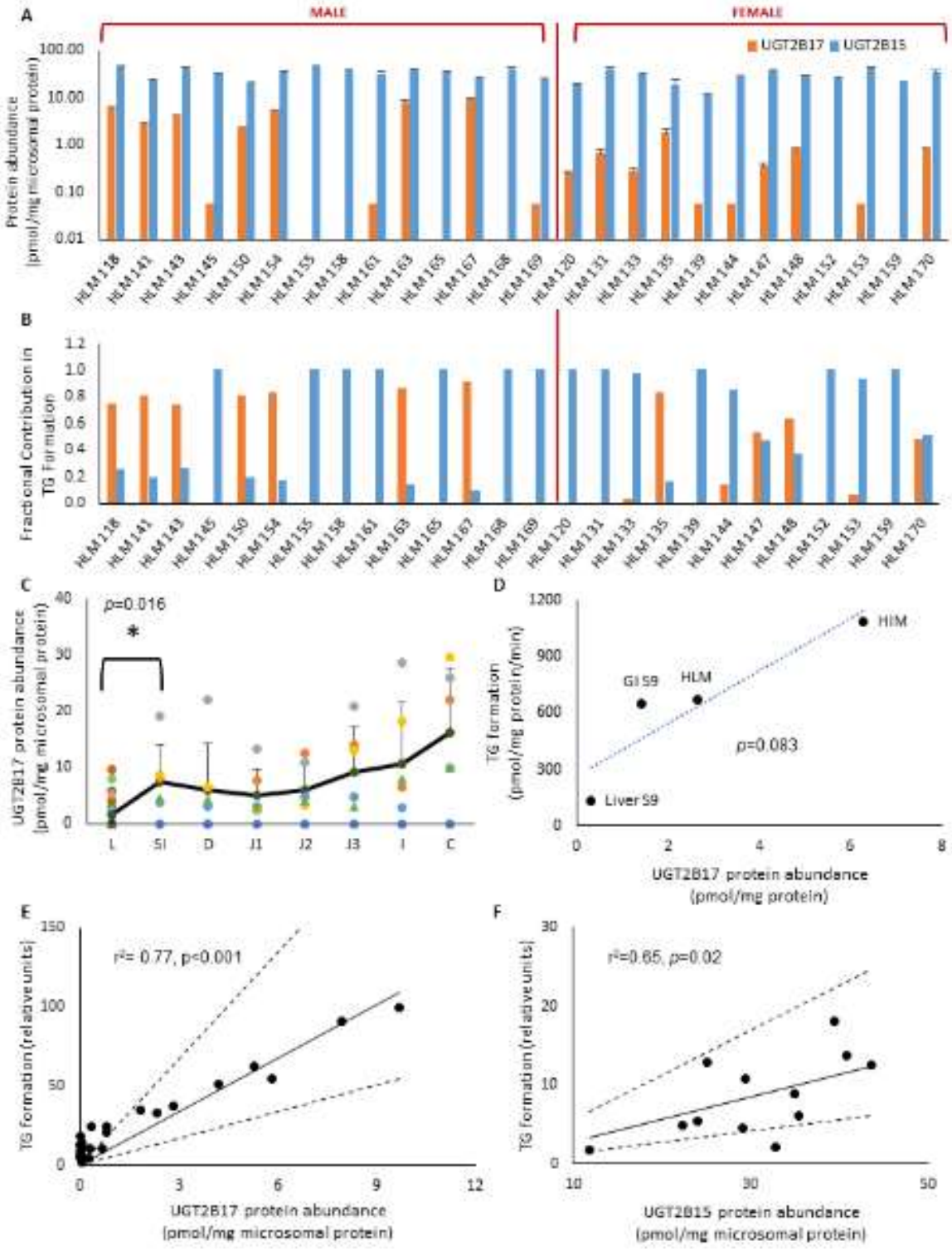

Figure 2.1. UGT2B protein abundance and testosterone glucuronidation in human liver and intestinal subcellular fractions.

Figure 2.1 A shows UGT2B17 and UGT2B15 protein abundance in HLM (n=26). 21% (n=6) HLM were confirmed UGT2B17 gene deletions (HLM 152, 155, 158, 159, 165, 168). Figure 2.1 B depicts Estimated fractional contribution of UGT2B17 and UGT2B15 in testosterone glucuronidation in HLM (n=26). Figure 2.1 C shows UGT2B17 protein abundance (pmol/mg microsomal protein) in human liver microsomes (L, n=26) and donor-matched human intestinal microsomes (n=6) shown as average small intestine (SI), duodenum (D), jejunum (J1, J2, J3), ileum (I), and colon (C). Black solid line shows average values for each group. Average UGT2B17 values for L and SI showed statistically significant difference (p=0.016). 46% of HLM (n=12) and 21% of HIM (n=1) were below lower limit of quantification (LLOQ). Figure 2.1 D shows correlation between testosterone glucuronide (TG) formation (pmol/ min/ mg microsomal protein) and UGT2B17 abundance (pmol/mg protein) in human liver and intestinal microsome and S9 fractions; figure 2.1 E and F show correlations between relative testosterone glucuronidation activity in adult HLM and (E) UGT2B17 abundance (n=26) and (F) UGT2B15 abundance in UGT2B17-LLOQ samples (n=12). Solid and dashed lines depict expected and two-fold range values for perfect correlation, respectively.

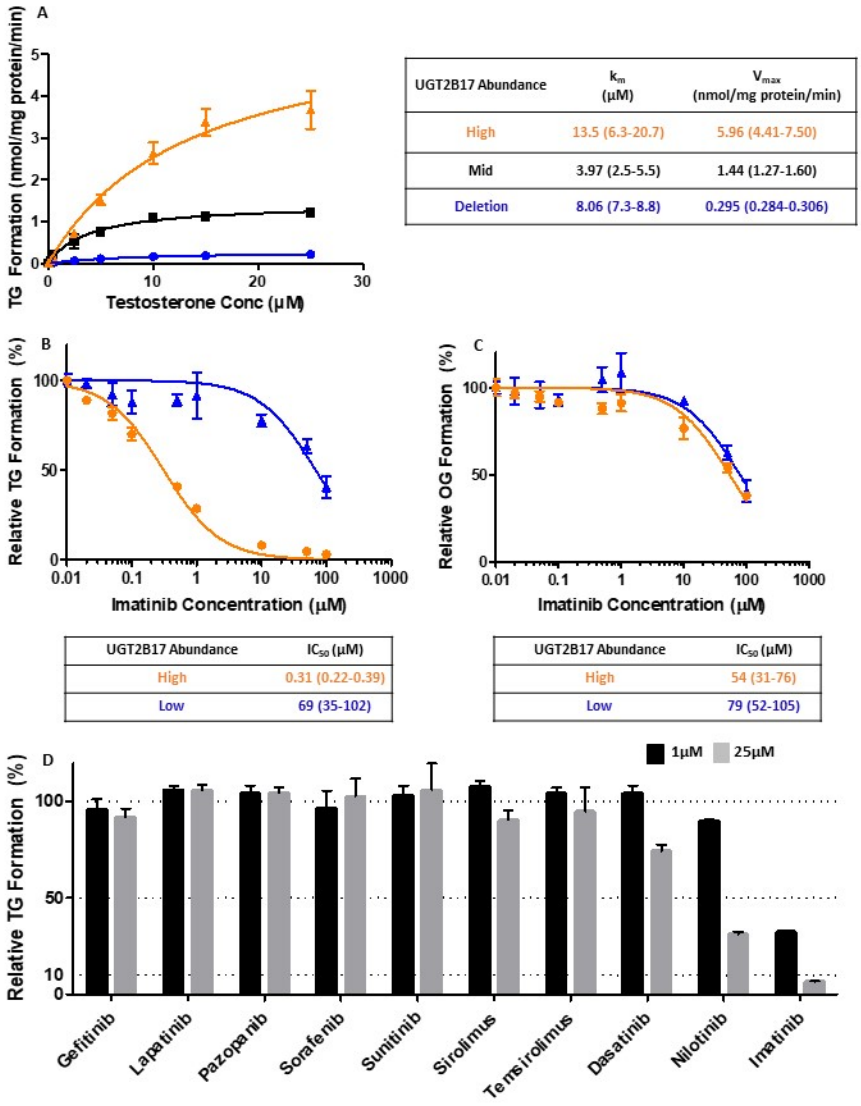

Figure 2.2. Testosterone glucuronide formation kinetics and inhibition in HLMs.

Figure 2.2 A shows the Michaelis-Menten plot of testosterone glucuronide (TG) formation in high (orange), mid (black), and null (blue) UGT2B17-expressing HLMs. Inhibition of imatinib in high (orange) and low (blue) UGT2B17-expressing HLMs is shown with testosterone (B) and oxazepam (C) as probe substrates for UGT2B17 and UGT2B15, respectively. Percent TG formation in high UGT2B17-expressing HLM inhibited by various tyrosine kinase inhibitors at 1 μM and 25 μM is shown in D.

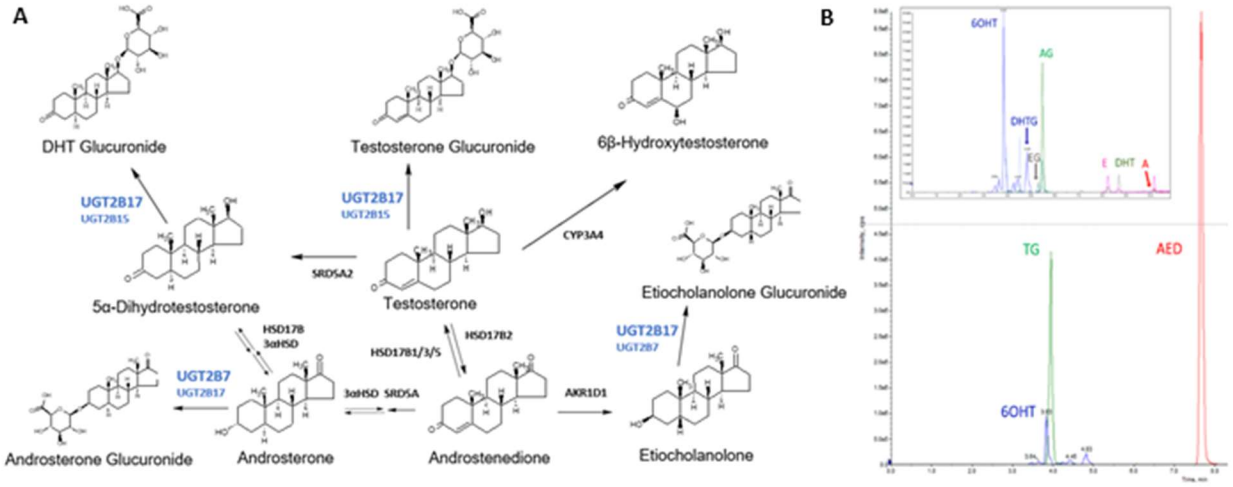

Figure 2.3. Testosterone metabolism scheme.

Figure 2.3 A shows a simplified testosterone metabolic pathway with respective structures and enzymes, while B shows a representative LC-MS/MS chromatogram of quantified metabolites from hepatocyte.

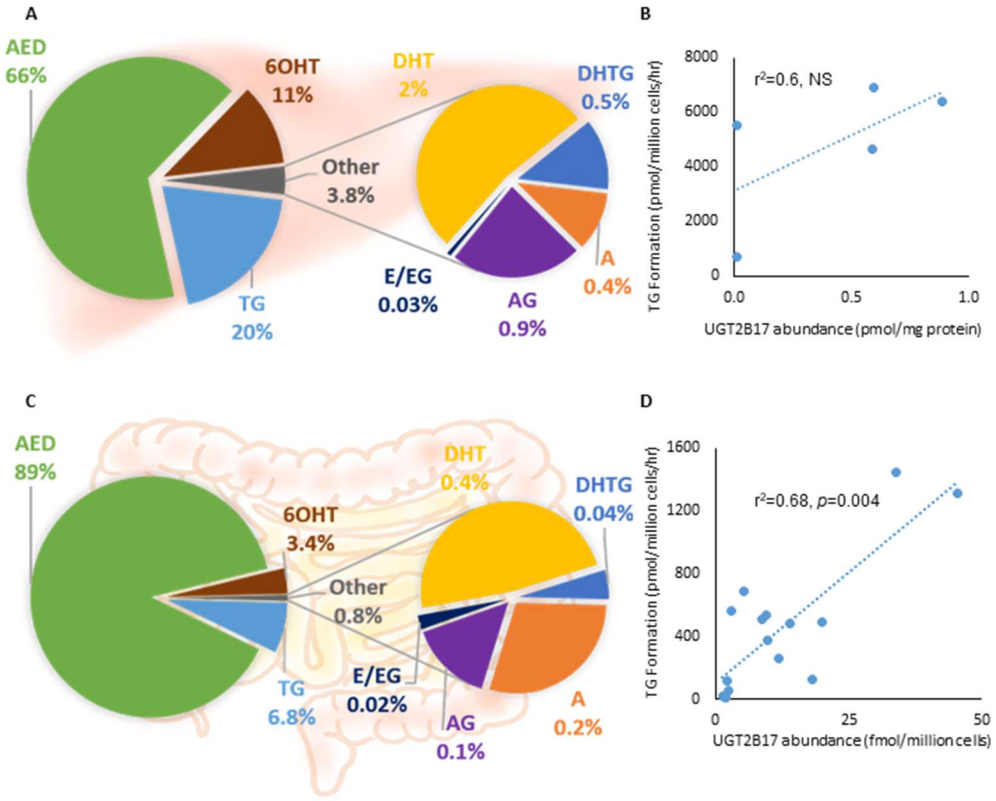

Figure 2.4. Testosterone metabolism in primary human hepatocytes and enterocytes.

Figure 2.4 A and C show percent of quantified testosterone metabolites in hepatocytes (n=5) and enterocytes (n=16), respectively, after incubation in 50 µM testosterone for 60 and 120 minutes, while Figure 2.4 B and D show UGT2B17 abundance vs. TG formation correlation in hepatocytes and enterocytes, respectively.

TG: testosterone glucuronide, DHT: dihydrotestosterone, DHTG: DHT glucuronide, A: androsterone, AG: androsterone glucuronide, AED: androstenedione, 6OHT: 6-hydroxy testosterone, E: etiocholanolone, EG: etiocholanolone glucuronide, NS: non-significant

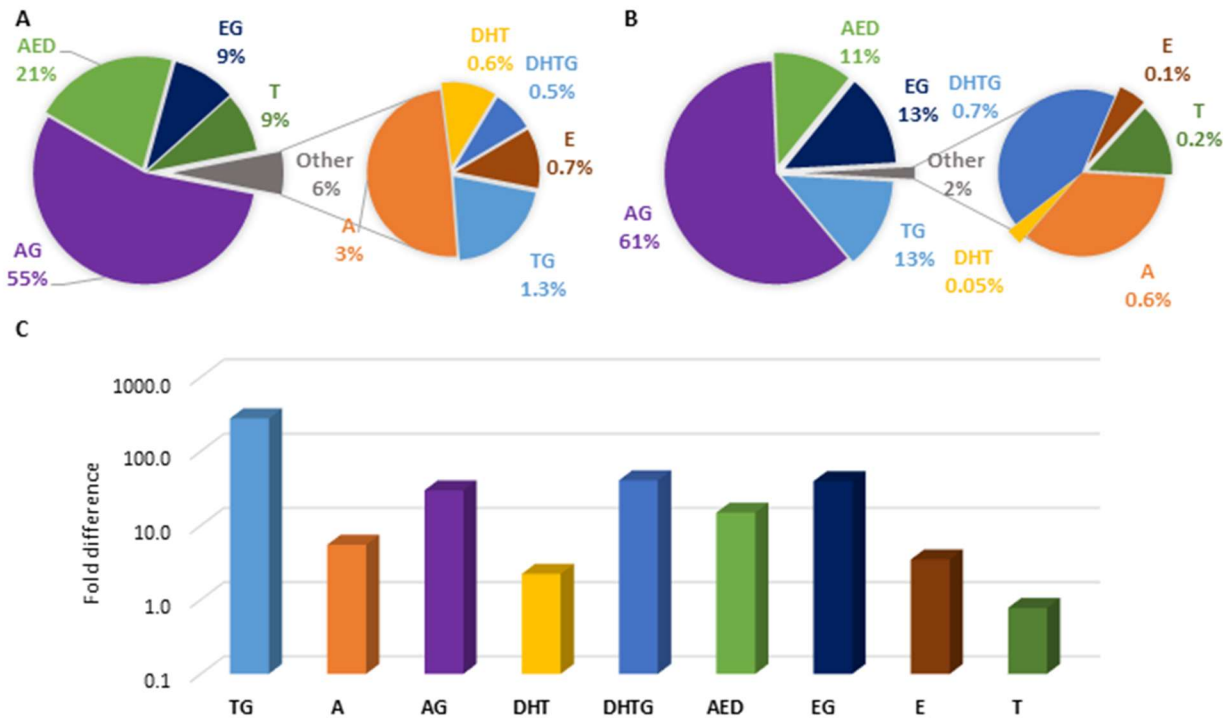

Figure 2.5. Testosterone metabolism *in vivo* before and after testosterone administration.

Figure 2.5 A and B show the metabolite composition in plasma at baseline and after oral administration of 800 mg testosterone (T), respectively, as average of all time-points (up to 24 hours) in seven healthy adult males after chemical castration with acyline. Figure 2.5 C shows the fold-change in absolute concentrations after 800mg T compared to baseline in log scale. Abbreviations are defined under Figure 2.4.

Chapter 3. NORMALIZED TESTOSTERONE GLUCURONIDE (TG/AG) AS A POTENTIAL URINARY BIOMARKER FOR HIGHLY VARIABLE UGT2B17 IN CHILDREN 7 TO 18 YEARS

(A version of this chapter was accepted by Clinical Pharmacology and Therapeutics on December 18th, 2019)

3.1 INTRODUCTION

UDP-glucuronosyltransferase 2B17 (UGT2B17) is a highly variable androgen- and drug-metabolizing enzyme, showing over a 3000-fold variability in hepatic protein expression [1]. It is one of the most commonly deleted genes in the human genome with the frequency of the gene deletion event ranging from 16% in Caucasians up to 96% in Asians [12]. However, even among expressers carrying two copies of the *UGT2B17* gene, greater than 160-fold variability in tissue expression has been reported [109], suggesting that copy number variation (CNV) is not the only determinant of interindividual variability. Indeed, factors such as age, sex, and single nucleotide polymorphisms (SNPs) also affect UGT2B17 tissue expression and activity. Still, only 26% of the variability can be explained by all these factors combined [10].

UGT2B17 also exhibits a unique developmental trajectory. UGT2B17 is minimally expressed in children under 9 years of age (0.11 ± 0.02 pmol/mg protein) but increases approximately 10-fold throughout adolescence to adulthood (1.31 ± 0.15 pmol/mg protein) in its hepatic protein expression. The increase is much more prominent in males, compared to females, and adult males have on average 2.6-fold higher levels compared to females (1.75 ± 0.20 vs. 0.65 ± 0.18 pmol/mg protein, respectively) [110]. Major endogenous substrates for UGT2B17 are C_{19}

steroids, such as testosterone, androsterone, and etiocholanolone [111,112], and UGT2B17, when present, drives testosterone glucuronide (TG) formation, leading to highly variable TG formation [109].

High variability in UGT2B17 expression has been associated with several important *in vivo* outcomes. UGT2B17 gene deletion is associated with increased risk of prostate cancer, albeit with some conflicting results [26,27]. Other testosterone-related outcomes, such as lower body mass index (BMI) and higher fat mass [29,30], decreased osteoporotic fractures and increased bone mineral density [33,34] are also associated with UGT2B17 deletion. However, again, other studies report conflicting results [31,32], possibly due to the high interindividual variability in UGT2B17-mediated testosterone metabolism. In addition, UGT2B17 genotype is a well-known confounder in antidoping tests for athletes, where the urinary testosterone to epitestosterone ratio (T/E ratio) is measured after deconjugation with β-glucuronidase [24,25].

UGT2B17 expression variability has led to unexpected pharmacokinetic (PK) outcomes resulting in drug development failures. For example, an antagonist of chemoattractant receptor-homologous molecule expressed on T-helper type 2 cells (CRTH2), MK-7246, failed its first-in-human study due to unexpected PK variability, and UGT2B17 was retrospectively identified as the primary source of variability, with 25-fold higher systemic exposure in subjects with two gene copies compared to those homozygous for a gene deletion event [50]. Similarly, unpredictable high variability in the metabolism of PT2385, an inhibitor of hypoxia-inducible factor-2α, led to discontinuation of its development program [113]. UGT2B17 variability also affects drug disposition in currently utilized therapeutics. For example, 17-hydroexemestane, the major active metabolite of the oral antineoplastic drug exemestane, showed significantly higher exposure in patients homozygous for *UGT2B17* deletion, compared to those with 2 copies,

presumably due to reduced glucuronidation [114]. Additionally, metabolism of the oral antineoplastic agent vorinostat is significantly affected by UGT2B17 CNV, which is reflected by trends in higher adverse events and longer median progression-free survival for patients with no *UGT2B17* copies compared to those with at least 1 copy of the gene [78].

Despite these *in vivo* reports, UGT2B17 receives limited attention from regulatory agencies and pharmaceutical industries, compared to other UGTs, possibly due to the small number of clinically approved compounds primarily metabolized by UGT2B17, along with its minor presence in commonly used *in vitro* models such as pooled liver microsomes. However, UGT2B17 can play a significant role in drug metabolism and drug-drug interactions (DDIs) in high UGT2B17 expressers (e.g., individuals with 100-fold higher abundance compared to low expressers). Furthermore, intestinal UGT2B17 expression is on average 4-fold higher than that in the liver [109], and UGT2B17 is the major UGT isoform expressed in the intestine, with a 3- and 7-fold higher expression than UGT1A1 and UGT2B7, respectively [18]. High and variable intestinal expression of UGT2B17 may significantly affect drug bioavailability [50]. Effects of genetic variability also have the potential to be compounded in children due to a steep increase in UGT2B17 expression during development, especially for chronic medications, where dose adjustment may be warranted to address the rapidly changing UGT2B17 expression.

An endogenous phenotypic biomarker may be of considerable value to predict UGT2B17 activity *in vivo*, considering the potential role of UGT2B17 in xenobiotic and endobiotic disposition, its association with pathophysiological outcomes, and high interindividual and age-related variability. Specific and sensitive endogenous biomarkers offer advantages in drug development by reducing unnecessary and costly DDI trials and avoiding late-stage

discontinuations [115], and improving patient safety by its less invasive nature, as recognized by United States Food and Drug Administration (FDA) [65].

Urinary TG is strongly associated with UGT2B17 activity in children and adults [22,116], but TG alone as a biomarker is confounded by differing levels of endogenous testosterone synthesis. Although testosterone (T) would be the ideal normalizer, it is undetectable in urine. Thus, we propose androsterone glucuronide (AG) as a normalizer for TG. AG normalization should control for the interindividual variability in endogenous testosterone production. Androsterone is an inactive androgen, is reported to represent peripheral androgen metabolism, and its conjugated metabolite AG is abundant in urine and blood [58]. AG formation is primarily mediated by UGT2B7, which has substantially less variability and ontogeny after 2-years of age [73], with negligible contribution from UGT2B17 (Figure 3.1) [60]. Total (conjugated and deconjugated) urinary epitestosterone is a commonly used normalizer found in the T/E ratio for anti-doping tests. Such tests aim to identify exogenous testosterone administration. However, epitestosterone does not address the fluctuations in endogenous testosterone production, as it is regulated by a separate pathway [58]. Epitestosterone also exhibits poorer sensitivity due to lower urinary levels and is susceptible to the effects of other polymorphisms, menstrual cycles, and drugs [117,118]. Genetic polymorphisms, allosteric regulation and reversible metabolism of sulfotransferase catalyzed reactions limit the potential for normalization with sulfate conjugates of androgens [119].

In this study, we investigated TG normalized by androsterone glucuronide (TG/AG) as a potential noninvasive urinary biomarker for UGT2B17 activity by testing its association with age, sex, and CNV state, using longitudinal pediatric urine samples and targeted metabolomics by LC-MS/MS. Targeted analyses of ten other androgen conjugates were also assayed. In

addition, we performed exploratory analysis to investigate associations of race and sexual maturity rating (SMR) with urinary TG/AG levels.

3.2 METHODS

3.2.1 *Clinical study details and sample collection*

Pediatric urine samples were obtained from a previous longitudinal phenotyping study conducted at Children's Mercy Hospital, Kansas City, MO, USA [120]. Samples were collected during seven visits, over a three-year period, with subject ages ranging from 7 to 18 years old. Urine samples were obtained in the morning prior to exogenous biomarker dosing and were previously unthawed from -80ºC storage. Sample demographics are shown in Table 3.1.

3.2.2 *Urine sample processing*

Solid phase extraction (SPE) was performed using Oasis® hydrophilic-lipophilic balanced (HLB) 1 mL cartridges with 30 mg sorbent (Waters Technologies, Milford, MA). Distilled water (300 µL) containing internal standards (IS) was added to 300 µL aliquot of urine and vortexed. HLB cartridges were conditioned with methanol and equilibrated with distilled water. Samples were loaded and passed through, followed by wash with 2% formic acid in 5% methanol in water. Elution was performed with 5% ammonia in methanol, the solvent removed by evaporation under a nitrogen stream, and the residue reconstituted with 100 µL of 1:1 methanol: water. Processed samples were stored in -80ºC prior to LC-MS/MS analysis. Quality controls and pooled samples were included in each batch processing, to control for technical and instrumental variabilities.

3.2.3 *LC-MS/MS method development, validation, and analysis of urine androgen conjugates*

Glucuronide (G) and sulfate (S) conjugates for 6 androgens were analyzed: testosterone (T), androsterone (A), etiocholanolone (Etio), epitestosterone (EpiT), epiandrosterone (EpiA), and dehydroepiandrosterone (DHEA). LC-MS/MS analysis was performed using a Sciex Triple Quadrupole 6500 system (Sciex, Framingham, MA) coupled with Acquity UPLC System (Waters Technologies, Milford, MA). An ACQUITY UPLC HSS T3 1.8 µm, C18 100A; 100 x 2.1 mm (Waters Technologies, Milford, MA) column was used to achieve chromatographic separation of conjugates, as shown in Figure 3.2. LC conditions had a flow rate of 0.3 mL/min with 5 µL injection volume. Mobile phases A1 and A2 were 0.1% formic acid in water and 10 mM ammonium acetate in water with 0.1% acetic acid and B1 and B2 were 0.1% formic acid in acetonitrile and 0.1% acetic acid in acetonitrile. A1 and B1 were used for quantification of glucuronides and A2 and B2 for sulfates. Gradient programs were set as follows: 75% A1 (0-1 min), 75-60% (1-6 min), 60-58% (8-9 min), 58 to 50% (9-10 min), 50-10% (10-12 min), 10-75% (13-13.1 min), 75% (13.1-15 min) for glucuronides, and 74% A2 (0-1 min), 74-71% (1-6 min), 71-63% (6-12 min), 63-5% (12-12.5 min), 5-73% (13-13.1 min), 73% (13.1-15 min) for sulfates. Positive and negative ESI modes were used for glucuronides and sulfates, respectively; other MS parameters are shown in Table 3.2. Acquired data was processed using Skyline daily software (University of Washington, Seattle, WA). Lower limit of quantifications (LLOQ) were established, and the lower limit of detection (LOD) was set as one-third of the LLOQ (Table 3.2). Samples that were below limit of quantification (BLOQ) were assigned LOD values and included for statistical analysis. The US FDA guidance for bioanalytical method validation was followed (https://www.fda.gov/files/drugs/published/Bioanalytical-Method-Validation-Guidance-for-Industry.pdf).

3.2.4 *UGT2B17 gene copy number determination*

CNV analysis was performed at Children's Mercy Hospital (Kansas City, MO); the method is described in detail, elsewhere [121]. In brief, quantitative multiplex PCR amplification (MPA) was performed, fragments separated on an ABI 3730 instrument, and subsequently analyzed with GeneMapper v5 (both Thermo Fischer, Waltham, MA). UGT2B17 copy number was determined by normalizing against UGT2B15 which is not known to undergo copy number variation.

3.2.5 *Statistical analysis*

Statistical analysis was performed using GraphPad Prism 5.03 (La Jolla, CA) and R (version 3.5.1). Linear correlation tests between CNV and subject demographic variables were performed using data from the first clinic visit. Similarly, correlations of age, sex, and CNV with other androgen conjugates were examined.

TG/AG was log-transformed to ensure normality. To assess the association of log (TG/AG) with age and sex, we used a linear spline model with a generalized estimating equation for population inference, after exclusion of CNV=0 subjects (Equation 3.1). Age splines were set at 11 and 14 years, the average male ages for onset of SMR stages 2 and 4, respectively, to account for disproportionate increases in reported urinary androgens between SMR 2 and 4 [122]. Age spline settings were also consistent with exploratory LOWESS curve fitting.

$$E\left[\log\left(\frac{TG}{AG}\right)\middle|sex_i, age_{ij}\right] = \beta_0 + \beta_1 sex_i + \beta_2 age_{ij} + \beta_3\left(age_{ij} - 11\right)^+ + \beta_4\left(age_{ij} - 14\right)^+ + \beta_5 sex_i \times age_{ij} + \beta_6 sex_i \times \left(age_{ij} - 11\right)^+ + \beta_7 sex_i \times \left(age_{ij} - 14\right)^+ \quad (3.1)$$

The β coefficient indicates the rate of change in log (TG/AG) for the following variable, and *i* is the index for each subject, while *j* is the index for each time point. The (+) sign sets the

lower boundary as zero, allowing age spline formation based on the distance to the knots (e.g. 11 and 14 years).

We examined the association of log (TG/AG) with CNV and age separately in males and females, after observation of significant trend differences in sex and age. The linear spline model was applied, and CNV was treated as a continuous variable to incorporate increasing trend of TG/AG with increasing copy number (Equation 3.2).

$$E\left[\log\left(\frac{TG}{AG}\right)\middle|CNV_i, age_{ij}\right] = \beta_0 + \beta_1 CNV_i + \beta_2 age_{ij} + \beta_3\left(age_{ij} - 11\right)^+ + \beta_4\left(age_{ij} - 14\right)^+ + \beta_5 CNV_i \times age_{ij} + \beta_6 CNV_i \times \left(age_{ij} - 11\right)^+ + \beta_7 CNV_i \times \left(age_{ij} - 14\right)^+ \quad (3.2)$$

The association of log (TG/AG) with race (i.e., African American and Caucasian) was explored using equation 3.3:

$$E\left[\log\left(\frac{TG}{AG}\right)\middle|race_i, age_{ij}\right] = \beta_0 + \beta_1 race_i + \beta_2 age_{ij} + \beta_3\left(age_{ij} - 11\right)^+ + \beta_4\left(age_{ij} - 14\right)^+ + \beta_5 race_i \times age_{ij} + \beta_6 race_i \times \left(age_{ij} - 11\right)^+ + \beta_7 race_i \times \left(age_{ij} - 14\right)^+ \quad (3.3)$$

Given the physiological as well as statistical correlation between age and SMR, we also looked at association with SMR (Equation 3.4), with splines set at stages 2 and 4, reflecting the average age splines from Equation 3.2.

$$E\left[\log\left(\frac{TG}{AG}\right)\middle|CNV_i, SMR_{ij}\right] = \beta_0 + \beta_1 CNV_i + \beta_2 SMR_{ij} + \beta_3\left(SMR_{ij} - 2\right)^+ + \beta_4\left(SMR_{ij} - 4\right)^+ + \beta_5 CNV_i \times SMR_{ij} + \beta_6 CNV_i \times \left(SMR_{ij} - 2\right)^+ + \beta_7 CNV_i \times \left(SMR_{ij} - 4\right)^+ \quad (3.4)$$

Fitted model outputs for β coefficients were tested against the null hypothesis of β =0 (no association) and considered significant at $p < 0.05$. There was no correction for multiple comparisons, given the exploratory nature of the study.

3.3 RESULTS

3.3.1 *Bioanalytical method validation*

We developed a sensitive and specific LC-MS/MS-based method to analyze both glucuronide (G) and sulfate (S) conjugates for six androgens: testosterone (T), epitestosterone (EpiT), androsterone (A), epiandrosterone (EpiA), etiocholanolone (Etio), and dehydroepiandrosterone (DHEA). Sensitivity was established with an acceptable LLOQ, specificity was confirmed, and accuracy and precision across different runs were within 20% for both for TG and around 30% and 15%, for AG, respectively. Different measures of variability and stability testing were performed, including interday variability, intraday variability, and inter-analyst variability, as well as freeze-thaw stability, benchtop stability, 1-year long-term stability, and autosampler stability. Interday, intraday and inter-analyst variability (%CV) was 14.1% and 6.9% for TG, and 16.4% and 7.8% for AG, respectively. Freeze-thaw, benchtop, long-term and autosampler stability (% difference) was 1.3%, 3.4%, 8.9%, and 0.4% for TG, and 7.7%, 11.7%, 4.6%, and 4.1% for AG, respectively. Most other conjugates were acceptable, CV within 20%; EtioG was readily detected but not quantifiable due to IS normalization issues. Recovery for TG was 111% and AG was 55%.

3.3.2 *Urinary concentrations of androgen conjugates*

Androgen conjugates were quantified in urine samples (n=439) collected for 63 subjects from 7 visits over 3 years (Table 3.1). Average urinary concentrations and standard deviation for quantified androgen conjugates in male and female age groups (<11, 11-14, and >14 years) are shown in Table 3.3, with DHEAG and EpiAG mostly below the limit of quantification, and EtioG not quantified as explained above. TG and EpiTG concentrations increased with age, and

the percentage of samples with TG and EpiTG concentrations below the lower limit of quantitation decreased from 29-48% and 71-94% for males and females under 11 years of age, respectively, to 0-17% and 4-9% in the >14 years age group. T and EpiT sulfate levels were comparatively much lower than glucuronides—TS was undetectable in 50% and 89% of samples, compared to 20% and 21% for TG, for male and females, respectively.

3.3.3 *Association of urinary androgen conjugates with sex, age, and UGT2B17 copy number variation (CNV)*

Average age for males (n=39, 62%) was 12.4 years and for females (n=24, 38%) was 11.7 years. CNV distributions were as follows (n, average age in years): for males, CNV0 (n=6, 11.8 years), CNV1 (n=17, 12.3 years), CNV2 (n=16, 12.6 years), and for females, CNV0 (n=4, 11.6 years), CNV1 (n=9, 12.1 years), CNV2 (n=11, 11.4 years) (Table 3.1). CNV showed no association with sex, age, body mass index (BMI), or sexual maturity rating (SMR), but was significantly associated with race, i.e. Caucasian Americans (CA) and African Americans (AA) with AA as the reference group (p=0.0015). Simple correlation analyses showed significant associations with age but not with sex for most metabolites. Androgen metabolites, except EtioS (p=0.0405), showed no significant associations with *UGT2B17* CNV (data not shown).

TG, AG, and TG/AG in males and females with age and by CNV is shown in Figure 3.3. Age-related increase in TG was more prominent in males compared to females, while the increase in AG was similar in both sexes (Figure 3.3A and 3.3B). Visual association with CNV was seen with urine TG but not AG (Figure 3.3D and 3.3E). TG/AG normalization resulted in greater spread of the data (Figure 3.3C). Visual associations with CNV were still present when grouped by SMR stages i.e., SMR 1 and SMR 4/5, which controls for the influence of sexual maturation and increasing androgen synthesis (Figure 3.3F and 3.3G).

TG/AG associations with age, sex, race, and CNV were all significant (p<0.001) (Table 3.4). Fitted linear spline model for log (TG/AG) with age for male and female is shown in Figure 3.4A. Figure 3.4B shows the fitted model by race (CA and AA). The significant difference between the two races in this analysis is likely due to different CNV frequencies in CA and AA as a confounder. Earlier correlation analysis showed significant association between CNV and race (Table 3.1), thus genetic differences in CNV frequency may manifest as racial differences. It has been reported that the *UGT2B17* deletion allele is five times more frequent in Caucasians (11%) than African Americans (2%) [59]. Fitted models for log (TG/AG) by CNV with age in male and females are shown in Figures 3.4C and 3.4D, respectively. Log (TG/AG) was also associated with SMR (p<0.001).

3.4 DISCUSSION

We quantified a panel of androgen conjugates in longitudinal collection of pediatric urine samples, with a comprehensive analysis of association between TG/AG with multiple variables including genotype and SMR. Urinary concentrations of androgen conjugates were in agreement with available reported ranges [58,116,122]. The observed association of urinary TG with *UGT2B17* CNV has also been reported, and supports the 20- to 50-fold difference seen between CNV=2 and CNV=0 [22,123]. EtioS association with *UGT2B17* CNV that was observed has also previously been reported [124]. Interestingly, while we showed TG/AG showed significant association with SMR, urinary testosterone to epitestosterone ratio (T/E) is reported to be invariant between SMR stages [122]. Consistent with our hypothesis, TG/AG showed significant associations with age, sex, and CNV state, with a steeper increase in males compared to females, which also visually matches UGT2B17 ontogeny profile in hepatic protein abundance from a separate dataset [110].

Once validated as a UGT2B17 biomarker, TG/AG has potential utilization for better predictions of drug disposition variability, DDI risk, and enhanced study design in children and adults. For example, measurement of urinary TG/AG levels of subjects in Phase I clinical trials could predict if an investigational drug is a likely inhibitor of UGT2B17. This application is important, as UGT2B17 inhibition is not routinely tested during early drug development. TG/AG may also be used for *in vivo* predictions of the variable UGT2B17 activity and its contribution to drug clearance. In addition, acyl glucuronide metabolites such as gemfibrozil glucuronide and clopidogrel acyl glucuronide, (CAG) have recently gained attention as potent cytochrome P450 2C8 inhibitors that lead to clinically significant DDIs [125]. UGT2B17's contribution to CAG formation is estimated to be on average around 10% and UGT2B7 as a major contributor [9]. However, in high UGT2B17 expressers, CAG formation can substantially increase, and the subsequent increased risk of a DDI may be screened using TG/AG. Stratification of DDI study subjects as null, mid, and high UGT2B17 expressers rather than CNV=0, CNV=1, CNV=2, should provide more robust and reliable results.

Given UGT2B17's role in androgen metabolism, the TG/AG biomarker may also elucidate the role of UGT2B17 in pubertal development. The *UGT2B17* deletion allele is associated with delayed puberty in a study of 668 healthy boys, with 0.34 years delay in pubarche onset per deletion allele, but no differences in circulating testosterone or DHEAS [77]. This suggests that UGT2B17 may play an important part in androgen intracrinology, where regulation of androgen activation and metabolism occur within the cell, with minimal release of active androgens into systemic blood circulation. UGT2B17 may also play a part in disease susceptibility, such as development of polycystic ovary syndrome (PCOS), where ethnic

differences have also been observed [126]. TG/AG may also aid in controlling for UGT2B17 confounding for better robustness of antidoping tests.

The association between the *UGT2B17* deletion allele and cancer is very intriguing due to bidirectional associations with cancer risk versus cancer progression. Absence of *UGT2B17* gene (CNV=0) seems to increase the risk of cancer for prostate [26,27], breast, pancreatic [36], and lung [39] cancer, but decrease the risk of colorectal cancer [38]. On the other hand, overexpression of UGT2B17 protein has been linked to biochemical recurrence of prostate cancer [127], expedited progression to castration-resistant prostate cancer [128], and poorer prognosis in chronic lymphocytic leukemia due to inactivation of protective prostaglandin E_2 [129]. While presence of the *UGT2B17* gene may be onco-protective, its seemingly deleterious role in cancer progression suggests a separate function that is under differential regulation. Unfortunately, much is still unknown regarding UGT2B17 regulation, in both normal physiology as well as abnormal tissue proliferation. It is unknown if overexpression in tumors is related to higher baseline expression levels of UGT2B17. Conflicting findings from CNV-based association testing may partly be due to the variability in UGT2B17. A biomarker (TG/AG) could potentially allow for baseline stratification based on UGT2B17 expression levels without solely relying on CNV state, possibly yielding more conclusive results.

Limitations of the study include the small sample size of 63 subjects and the relatively short follow-up period of 3 years. Both these factors may partially explain the relatively flat TG/AG trend with age seen in females, although conclusive associations could still be drawn. Study demographics had no Asians to allow further exploration of race; however, we did see ethnic differences between Caucasians and African Americans, which is likely attributable to differences in CNV frequency. In addition, lower levels of TG excretion in *UGT2B17* deletion

individuals and women poses problems in TG detectability, and instrumental sensitivity is an area for improvement. Low levels of DHEAG and EpiAG and incomplete quantification of EtioG are other limitations. There are potential limitations of TG/AG as a biomarker, such as disease states that offset endogenous production. Numerous enzymes are involved in steroidogenesis and pubertal development [58], and steroid- or steroidal enzyme- related disorders, such as precocious puberty or hyperandrogenism, may alter TG or AG levels, rendering TG/AG unreliable for UGT2B17 estimation. Nonetheless, TG/AG shows potential as a promising UGT2B17 biomarker in healthy children and adults.

In conclusion, urinary TG/AG was associated with age, sex, and *UGT2B17* CNV. TG/AG is a promising biomarker to characterize the highly variable UGT2B17 activity in children 7 to 18 years old. Clinical studies using UGT2B17 probe substrates are needed for validation of TG/AG as an endogenous UGT2B17 biomarker. Once validated, TG/AG has potential applications in non-invasive *in vivo* assessment of UGT2B17 activity for prediction of interindividual variability, DDIs, as well as disease-state associations.

Table 3.1. Sample Demographics

		Overall[1]	CNV=0		CNV=1		CNV=2		CNV correlation
			Male	Female	Male	Female	Male	Female	*p* value
Sex (%)		39 M (62) 24 F (38)	6 (10)	4 (6)	17 (27)	9 (14)	16 (25)	11 (17)	0.85
Age (years)		12 ± 2.5	11.8 ± 2.9	11.6 ± 3.0	12.3 ± 2.1	12.1 ± 2.2	12.6 ± 2.2	11.4 ± 2.2	0.72
BMI[2] (kg/m2)		20.8 ± 4.8	20.7 ± 3.1	19.8 ± 0.9	19.6 ± 3.6	23.8 ± 7.2	21.2 ± 6.3	22.9 ± 5.0	0.93
Ethnicity[3] (%)	AA	28 (44)	1 (2)		5 (8)	5 (8)	10 (16)	7 (11)	ref
	CA	28 (44)	5 (8)	4 (6)	9 (14)	2 (3)	4 (6)	4 (6)	0.0015**
	AA/NH	1 (2)			1 (2)				0.41
	CA/AA	4 (6)			2 (3)		2 (3)		0.84
	CA/NH	2 (3)				2 (3)			0.25
SMR[4] (%)	1	125 (28)	14 (3)	7 (2)	49 (11)	10 (2)	28 (6)	17 (4)	ref
	2	87 (20)	10 (2)	7 (2)	24 (5)	14 (3)	23 (5)	9 (2)	0.68
	3	61 (14)	4 (1)	2 (0.5)	10 (2)	8 (2)	21 (5)	16 (4)	0.37
	4	79 (18)	6 (1)	6 (1)	18 (4)	11 (3)	18 (4)	20 (5)	0.48
	5	87 (20)	8 (2)	6 (1)	17 (4)	20 (5)	22 (5)	14 (3)	0.69

[1]63 subjects were followed over 7 visits with total 439 urine samples analyzed
[2]BMI: Body mass index; [3]CA: Caucasian American, AA: African American, NH: Non-Hispanic; [4]SMR: Sexual maturity rating

Table 3.2. MS parameters for targeted androgen conjugates

Metabolite	Precursor ion (m/z)	Product Ion(s) (m/z)	DP (V)	CE (eV)	LLOQ[#] (ng/mL)
GLUCURONIDES					
Androsterone glucuronide (AG)	449.1	255	70	25	2
Androsterone glucuronide-d4*	453.1	259	70	25	-
Etiocholanolone glucuronide (EtioG)	484.3	273, 255	70	35	1
Testosterone glucuronide (TG)	465.2	289, 271, 253, 109, 97	70	25, 30, 35, 40, 35	0.5
Testosterone glucuronide-d3*	468.2	292, 274, 256, 109, 97	70	25, 30, 35, 40, 35	-
DHEA[+] glucuronide (DHEAG)	465.2	289, 271, 253, 109, 97	70	25, 30, 35, 35, 35	25
Epitestosterone glucuronide (EpiTG)	482.2	253, 271, 252	50	25, 30, 37	1.5
Epiandrosterone glucuronide (EpiAG)	449.1	273, 255	70	25, 30	7.5
SULFATES					
Androsterone sulfate (AS)	369.2	97, 80	-155	-78, -130	2.5
Androsterone sulfate-d4*	373.2	97, 80	-155	-78, -130	-
Etiocholanolone sulfate (EtioS)	369.2	97, 80	-150	-90, -118	5
Etiocholanolone sulfate-d5*	374.2	97, 80	-150	-90, -118	-
Testosterone sulfate (TS)	367.2	351, 97, 80	-165	-54, -84, -120	2.5
Testosterone sulfate-d3*	370.2	354, 97, 80	-165	-54, -84, -120	-
DHEA[+] sulfate (DHEAS)	367.2	97, 80	-120	-72, -114	3
DHEA[+] sulfate-d5*	372.2	97, 80	-120	-72, -114	-
Epitestosterone sulfate (EpiTS)	367.2	97, 80	-140	-80, -124	0.5
Epitestosterone sulfate-d3*	370.2	97, 80	-140	-80, -124	-
Epiandrosterone sulfate (EpiAS)	369.2	97, 80	-125	-88, -116	3

* deuterated internal standard, + dehydroepiandrosterone, # lower limit of quantification

Table 3.3. Urinary concentrations (ng/mL) of androgen conjugates in children age 7-18 years

	< 11 years		11-14 years		>14 years	
	Male (n=85)	Female (n=70)	Male (n=113)	Female (n=62)	Male (n=74)	Female (n=35)
GLUCURONIDES[1]						
TG	1.8 ± 2.2 (48)	3.3 ± 3.8 (29)	20 ± 31 (12)	6.6 ± 5.7 (15)	75 ± 69 (0)	9.8 ± 9.7 (17)
AG	1216 ± 894	1273 ± 883	3016 ± 2306	3450 ± 2281	6826 ± 3468	4924 ± 2482
EtioG[2]	Detected[2]					
DHEAG[3]	BLOQ[3]					
EpiTG	0.4 ± 1.4 (94)	1.2 ± 2.1 (71)	5.5 ± 9.6 (44)	5.1 ± 4.8 (11)	22 ± 25 (4)	9.7 ± 8.1 (9)
SULFATES[1]						
TS	0.32 ± 0.27 (87)	0.27 ± 0.11 (96)	0.89 ± 1.81 (51)	0.36 ± 0.33 (82)	4.18 ± 9.41(7)	0.34 ± 0.27 (89)
AS	296 ± 327	156 ± 164	461 ± 439	356 ± 502	613 ± 497	534 ± 451
EtioS	106 ± 104	93 ± 85	112 ± 124	190 ± 174	114 ± 119	282 ± 263
DHEAS	199 ± 361	67 ± 109	430 ± 851	550 ± 2307	694 ± 1402	1668 ± 4154
EpiTS	2.9 ± 1.8 (5)	2.0 ± 1.5 (10)	6.4 ± 5.3 (2)	3.4 ± 2.8 (13)	18 ± 12 (0)	4.7 ± 3.4 (3)
EpiAS	44 ± 59	17 ± 19	73 ± 89	55 ± 111	98 ± 95	97 ± 104

[1] mean ± SD (%BLOQ, otherwise all detected)
[2] Absolute quantification not performed due to problems with normalization
[3] Below limit of quantification (BLOQ) were assigned lower limit of detection (LOD) calculated as LLOQ/3

Table 3.4. Linear regression outputs of β coefficient values

	Age and sex	Age and CNV (Male)	Age and CNV (Female)	Age and Race	CNV and SMR (Male)	CNV and SMR (Female)	Significance[#]
β_0	-6.69	-8.36	-9.96	-6.21	-8.32	-8.71	***
β_1	1.25	1.07	1.65	-2.41	0.92	0.93	***
β_2	0.06	-0.04	0.13	-0.01	-0.18	0.05	***
β_3	-0.12	0.78	-0.33	0.33	1.41	-0.41	***
β_4	0.00	-0.61	0.08	-0.34	-1.26	0.62	***
β_5	-0.20	0.03	-0.01	0.15	0.32	0.43	***
β_6	1.06	-0.10	0.06	-0.14	-0.59	-0.38	***
β_7	-0.73	0.05	0.08	0.15	0.33	-0.08	***

Statistically significant for all β coefficient values for H_0: β=0

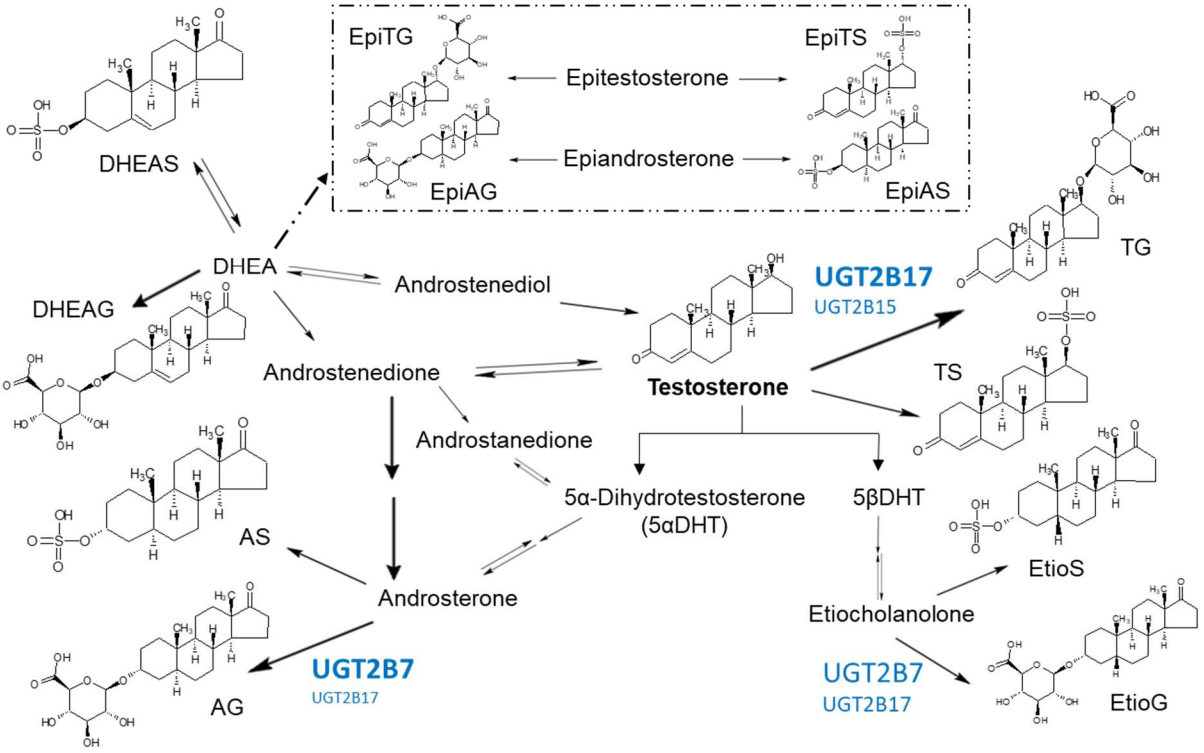

Figure 3.1. Androgen metabolism scheme.

A simplified androgen metabolism scheme is shown [14,130], with relative UGT contribution in glucuronidation depicted in blue. Dashed arrow and box indicate a separately regulated metabolic pathway for epitestosterone and epiandrosterone that is not fully understood.

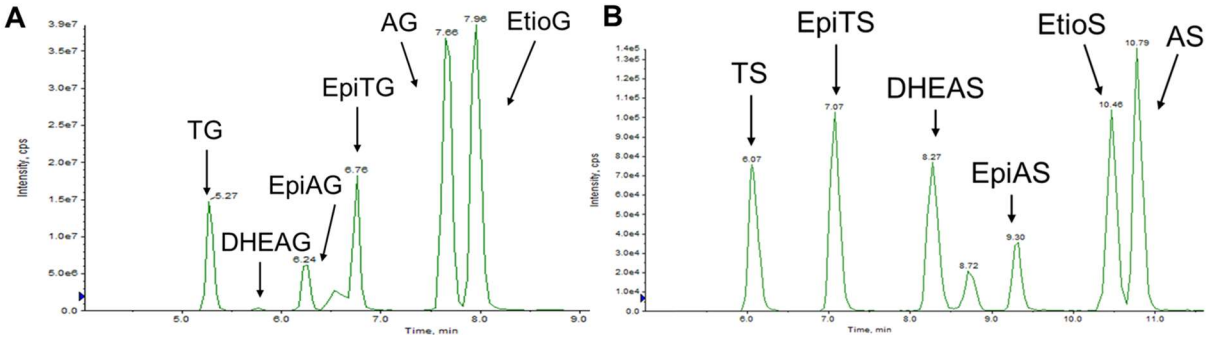

Figure 3.2. Representative MS chromatograms.

Chromatographic separation of androgen glucuronides (A) and sulfates (B). T: testosterone, A: androsterone, Etio: etiocholanolone, EpiT: epitestosterone, EpiA: epiandrosterone, DHEA: dehydroepiandrosterone, –G: glucuronide, –S: sulfate.

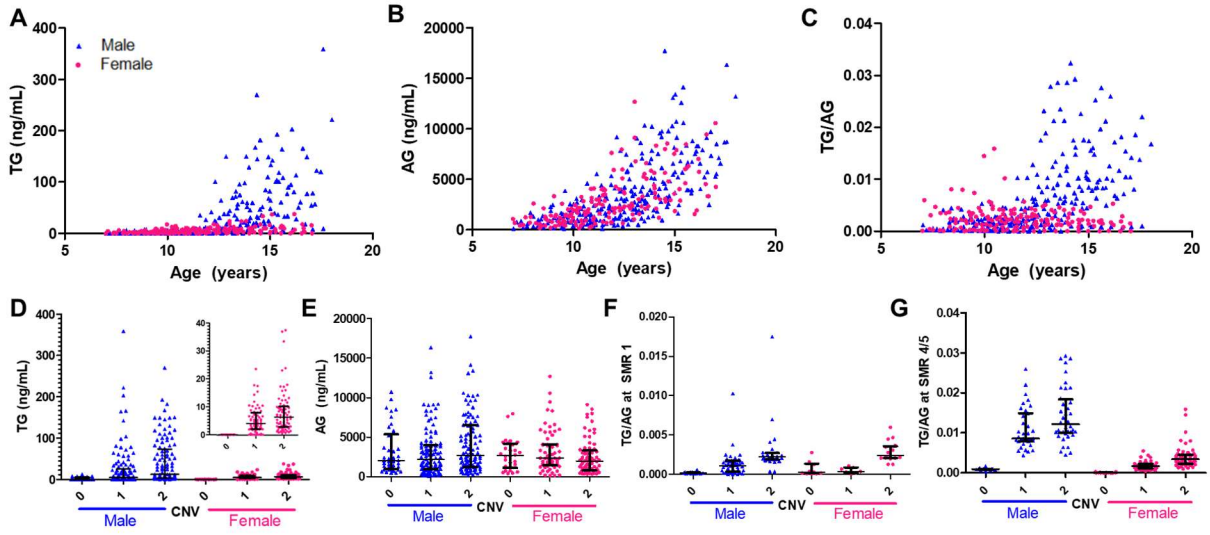

Figure 3.3. TG, AG, and TG/AG with age and CNV, by sex.

Testosterone glucuronide (TG), androsterone glucuronide (AG), and TG/AG with age is shown in Figure 3.3 A, B, and C, and TG and AG with copy number variation (CNV) is shown in D and E, respectively. TG/AG with CNV is separated by sexual maturity rating (SMR) at stage 1 (F) and stages 4 and 5 (G), to remove the influence of sexual maturation. Males are depicted in blue triangles and females in pink circles; line and bars show median and interquartile ranges.

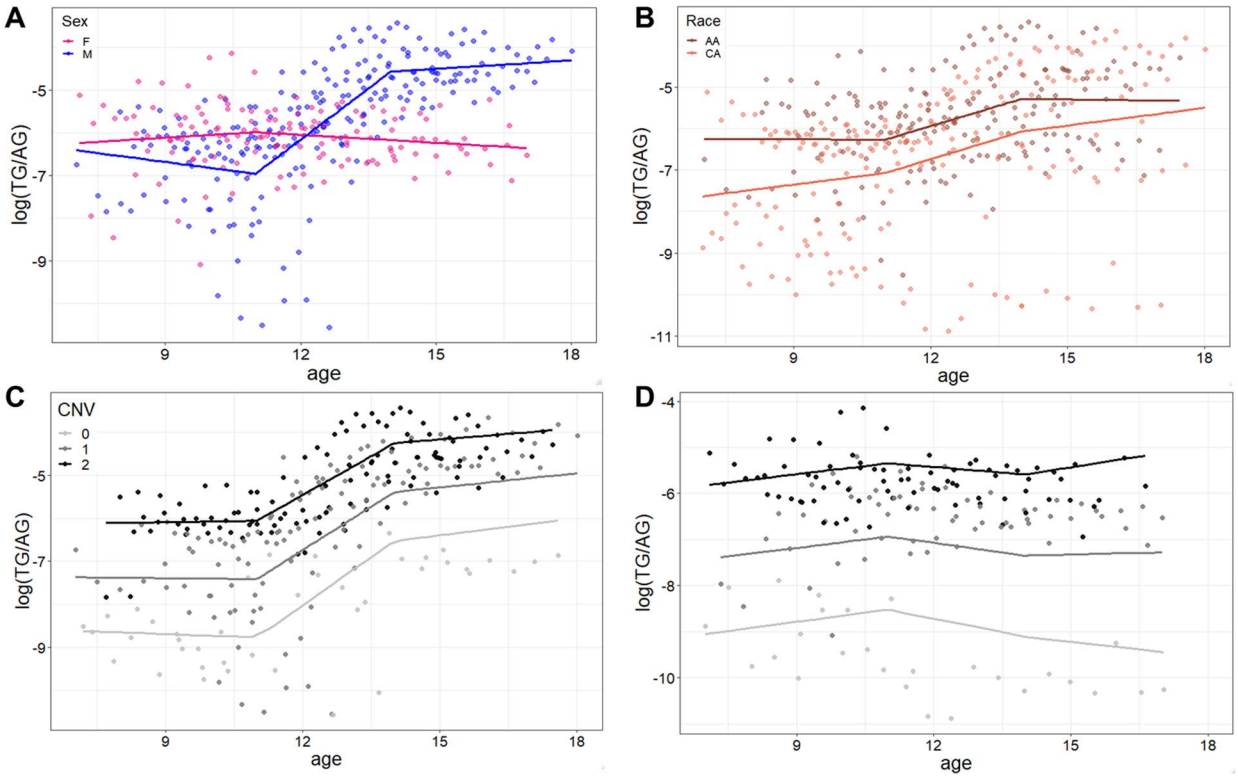

Figure 3.4. Association of urinary TG/AG levels with age, sex, race, and CNV.

Figure 3.4A shows the model-fitted log (TG/AG) with age splines set at 11 and 14 years, with males in blue and females in pink. Log (TG/AG) association with race is shown in Figure 3.4B, with African Americans (AA) in dark brown and Caucasian Americans (CA) in light brown. Log (TG/AG) association with copy number variation (CNV=0 in light grey, CNV=1 in dark grey, CNV=2 in black) is shown for males and females in Figure 3.4C and D, respectively.

Chapter 4. REGIONAL PROTEOMIC QUANTIFICATION OF CLINICALLY RELEVANT NON-CYTOCHROME P450 ENZYMES ALONG THE HUMAN SMALL INTESTINE

(A version of this chapter is under preparation to be submitted to Drug Metabolism and Disposition in December 2019)

4.1 INTRODUCTION

Oral intake is the most common route of drug administration due to its convenience and cost-effectiveness [131]. Incomplete and variable bioavailability (F) arise from oral administration, as drugs pass through barriers in absorption (F_a), intestinal metabolism (F_g), and hepatic metabolism (F_h) before reaching systemic circulation [90]. Absorption and subsequent intestinal and hepatic first-pass metabolism are sequential events with multiplicative effects that can significantly reduce drug exposure. Historically, intestinal metabolism was considered mostly insignificant compared to the liver [90]; however, significant intestinal contribution of cytochrome P450 3A4 (CYP3A4) has been demonstrated for drugs such as cyclosporine [132] and midazolam [133]. Further, clinically significant food-drug interactions with CYP3A4 involving furanocoumarins from grapefruit juice has been shown *in vivo*, resulting in labeling changes for several medications [134].

A major limitation in investigating intestinal metabolism is the lack of reproducibility in available *in vitro* systems [135,136]. This is in contrast to well-established *in vitro* tools available for hepatic metabolism, from subcellular fractions such as microsomes to human hepatocytes, which are considered as gold standard [72]. Preparation techniques differ widely for intestinal

isolation and fractionation of microsomes, leading to inconsistent quality of preparations which may impact scaling factors [66,137]. Commonly used colon cancer Caco2 cell lines, while useful for studying absorption, have low baseline expression of drug metabolizing enzymes (DMEs), limiting its use in intestinal metabolism assessment [138]. Exploration of other cell lines (LS180, T84) and fetal human small intestinal epithelial cells (fSIECs) have failed to replicate intestinal metabolism [139]. Human precision cut intestinal slices (PCIS), while most biologically representative, do not offer long-term viability or preservation for widespread and reproducible use [70]. Primary human enterocytes show promising activity [71], but isolation may also be more sensitive to the methodology employed, due to the heterogeneous nature of the small intestine compared to the liver [66,72]. Intestinal 3D organoid cultures have shown to be useful for investigating disease states, but its utility in drug development is limited by lack of quantitative applications such as inability to form monolayer or tight junction development. Knowledge deficits in enzyme abundance and resulting lack of scaling factors are the major limitations of *in vitro* tools, which are further hampered in preclinical animal models due to inter-species differences [135].

Physiologically based pharmacokinetic (PBPK) modeling has been proposed as an important tool to address the complexities of intestinal metabolism, but lack of information on enzyme abundance and scaling factors are cited as major deficits in application of *in vitro* methods [135]. Indeed, PBPK modeling is now recognized by regulatory agencies as a useful tool to combine system-specific physiology and drug-specific properties to help guide labeling decisions for certain conditions or populations [140,141]. It is important to note that successful modeling requires high-quality data [66,135,136]. In a recent effort to assess PBPK applications of orally administered drugs, large discrepancies were noted between measured and simulated profiles,

with an indication that knowledge gaps are present in intestinal physiological system [142–144]. Quantitative proteomics in different tissues allows for generation of scaling factors to be applied in mechanistic modeling approaches and lessen the knowledge gap [74]. While intestinal abundance of CYPs are fairly well known, studies in non-cytochrome P450 drug metabolizing enzymes (non-CYP DMEs) including UDP-glucuronosyltransferases (UGTs) are relatively lacking in general [67]. In addition, despite being a major intestinal isoform when expressed, UGT2B17 is a further understudied isoform harboring a common gene deletion and high interindividual variability [109].

We used cryopreserved human intestinal mucosal epithelium (CHIM) as a surrogate model for proteomic quantification of intestinal tissues. CHIM is a novel *in vitro* tool for evaluation of intestinal metabolism, and is prepared using collagenase digestion to separate the mucosal epithelium, followed by gentle homogenization and cryopreservation [72]. Minimal processing of CHIMs aims to retain the heterogeneous nature of the intestinal mucosa, thus allowing a more physiologically representative experimental system [72]. Proteomic characterization of such heterogenous tissue is necessary to generate scaling factors for *in-vitro* to *in-vivo* extrapolations (IVIVE) for further translation and application of CHIM model [145].

Heterogeneity of intestine necessitates additional considerations for proteomic characterization. In particular, incorporation of marker proteins which are specific for mature enterocytes is needed for a more accurate scaling. CHIM lots are provided with total protein content (mg protein/mL) rather than number of cells (million cells/mL), avoiding enterocyte isolation which can impact viability and activity. Thus, it is important to utilize marker proteins to assess lot-to-lot technical variability of mature enterocytes. Several specific markers for enterocytes have been reported. Villin-1 (VIL1) is an actin-binding protein that is a major structural constituent of

enterocyte brush borders and microvilli establishment, with high levels found in differentiated cells [146]. Sucrase isomaltase (SI) is reported to be a specific marker for intestinal epithelial cells [147]. Intestinal fatty-acid binding protein (FABP2) is a cytosolic protein that is specific for mature enterocytes [148].

Here, we report a proteomic characterization of non-CYP enzymes along the human small intestine in CHIMs using LC-MS/MS quantitative proteomics with stable isotope labeled (SIL) peptides. The following 17 enzymes were examined: aldehyde oxidase (AO), carboxylesterase 1 (CES1), CES2, UGT1A1, UGT1A3, UGT1A4, UGT1A6, UGT1A8, UGT1A10, UGT2B4, UGT2B7, UGT2B17, sulfotransferase 1A1 (SULT1A1), SULT1A3, SULT1B1, SULT2A1. We compared the non-CYP abundance in CHIM with commercially available pooled intestinal S9 fraction and also validated our proteomic findings with activity assays using CHIMs. We investigated testosterone glucuronidation as a UGT2B17-specific reaction, and UGT2B-mediated clopidogrel acyl glucuronide (CAG) formation using clopidogrel carboxylic acid (CCA) as a substrate and imatinib as a UGT2B17-specific inhibitor. Additionally, we qualitatively examined sequential metabolism using clopidogrel (CPG) and camptothecin-11 (CPT-11) as substrates for CES1 and CES2, respectively, with subsequent glucuronidations mediated by UGT2Bs and UGT1A1, respectively.

4.2 METHODS

4.2.1 *Materials*

Stable isotope labeled (SIL) peptides and synthetic unlabeled peptides were purchased from Thermo Fisher Scientific (Rockford, IL) and New England Peptides (Boston, MA), respectively. Ammonium bicarbonate (ABC, 98% purity), bovine serum albumin (BSA), dithiotreitol (DTT), iodoacetamide (IAA), trypsin protease (MS grade), testosterone, and CPT-11 were obtained from

Thermo Fisher Scientific (Rockford, IL). Clopidogrel, clopidogrel carboxylic acid, and clopidogrel acyl glucuronide were ordered from Toronto Research Chemicals (North York, Ontario), and testosterone glucuronide-d3 from Cerilliant Corporation (Round Rock, TX). Human serum albumin (HSA) was acquired from Calbiochem (Billerica, MA). Mem-Per Plus Membrane Protein Extraction kit, Pierce bicinchoninic acid (BCA) protein assay kit, optima MS-grade acetonitrile, chloroform, methanol, and formic acid were purchased from Fischer Scientific (Fair Lawn, NJ). Pooled GIS9 fractions were purchased from Xenotech (Kansas City, KS). CHIM samples, cryopreserved enterocyte recovery media (CERM®), and hepatocyte/ enterocyte incubation media (HQM) were purchased from In Vitro ADMET Laboratories, Inc (Columbia, MD). Sample demographics for CHIM are shown in Table 4.1.

4.2.2 *Protein extraction*

Protein extraction was performed using the Mem-PER Plus Membrane Protein Extraction kit (Thermo Fisher Scientific, Rockford, IL), closely following a previously published protocol [109]. CHIM samples were thawed in 37 ℃ waterbath for 90 to 120 seconds, then resuspend in Mem-PER kit cell wash solution or recovery media (CERM), followed by centrifugation at 300 xg for 5 minutes or 100 xg for 10 minutes at room temperature, respectively, and supernatant removal. This wash process was performed twice with cell wash solution. Samples washed with CERM underwent an additional resuspension in hepatocyte/enterocyte incubation media (HQM) and centrifugation at 300 xg for 5 minutes at 4 ℃. CHIMs were then resuspended in 110 to 500 µL of permeabilization buffer and placed on an Eppendorf ThermoMixer® (Hauppauge, NY) at 300 rpm for 30 minutes at 4 ℃. Permeabilized cells were then centrifuged at 16,000 xg for 15 minutes at 4 ℃, and resulting supernatant containing cytosolic proteins were collected. Remaining pellets were resuspended in 110 to 500 µL of solubilization buffer, sonicated for 30

seconds, and incubated at 300 rpm for 60 minutes at 4 ℃. Total protein concentrations were measured from protein extraction aliquots using Pierce BCA protein assay, according to manufacturer's protocol (Thermo Fisher Scientific, Rockford, IL). Aliquots with protein concentrations higher than 2 mg/mL were standardized for protein digestion to 2 mg/mL and 0.5 mg/mL for membrane and cytosolic proteins, respectively. All samples were stored in -80 ℃ until further analysis.

4.2.3 *Protein denaturation, alkylation, enrichment, and digestion*

Trypsin digestion followed previously described procedures [73]. Extracted protein aliquots were mixed with ABC buffer (100 mM, pH 7.8), DTT (250 mM), BSA (0.02 mg/mL), and HSA (10 mg/mL), then denatured for 10 minutes at 95 ℃. Upon cooling, IAA (500 mM) was added for alkylation followed by dark incubation at room temperature for 30 minutes. Protein enrichment and desalting was done with chloroform-methanol-water (1:5:4) with vacuum extraction, pellet wash with methanol, drying, and resuspension with ABC buffer (50 mM, pH 7.8). Digestion was initiated with trypsin (0.16 µg/µL) addition at 300 rpm for 16 hours at 37 ℃, and stopped with addition of ice-cold acetonitrile: water 80:20 (v/v) with 0.5% formic acid and SIL internal standard cocktail. A minimum of five positive quality controls (QCs) and three pooled GI S9 fractions were included in each batch of processing to control for technical and instrumental variability.

4.2.4 *Quantification of surrogate peptides of non-CYP DMEs*

Processed samples were analyzed using Acquity UPLC system (Waters, Milford, MA) coupled to Sciex Triple Quadrupole 6500 system (Sciex, Framingham, MA). ACQUITY UPLS HSS T3 1.8 µm, C_{18} 100 A; 100 x 2.1 mm column (Waters, Milford, MA) was used to achieve

chromatographic peptide separation using previously established protocols [73]. Skyline software (University of Washington, Seattle, WA) was used to process acquired data. Detailed LC-MS/MS parameters specific to this study can be found in Table 4.2.

Both absolute and relative quantifications were performed. Absolute abundance data are presented as pmol protein/mg membrane protein, whereas relative abundance was calculated as area ratio normalized with average area ratio of villin-1 and sucrase isomaltase. Relative quantification was done to address technical variability associated with CHIM preparations and the multicellular nature of intestinal tissue. Relative quantification was performed for eleven DMEs and all marker proteins: CES1, CES2, UGT1A1, UGT1A3, UGT1A10, UGT2B7, UGT2B17, SULT1A1, SULT1A3, SULT1B1, SULT2A1, and VIL1, SI, and FABP2. Absolute quantification was performed utilizing a positive quality control (PQC) sample as a calibrator from our previous studies for all proteins listed above except SULT1A3, SULT1B1, and marker proteins [75].

4.2.5 *Activity assays*

CHIM samples were thawed in 37°C water bath for up to 120 seconds. Samples were then resuspended in CERM, centrifuged at 100 xg for 10 minutes at room temperature, followed by supernatant removal; this process was repeated with HQM. CHIM samples were then reconstituted with HQM to protein concentration of 0.5 mg/mL. 50 µL of CHIM suspension was added to 96-plate wells with 50 µL of HQM containing double the final concentration of substrates for a final reaction volume of 100 µL. Final substrate concentrations for testosterone, clopidogrel carboxylic acid (CCA), clopidogrel (CPG), and camptothecin-11 (CPT-11) were 5 µM, 100 µM, 40 µM, and 20 µM, respectively. Upon addition of CHIM suspension and gentle mixing, plates were incubated for 30 to 60 minutes at 37°C and quenched with ice-cold

acetonitrile containing internal standard testosterone glucuronide-d3. Plates were centrifuged at 300 xg for 5 minutes at 4 °C, and 50 µL aliquots were transferred to corresponding LC-MS/MS compatible plates and stored in -80 °C until analysis. Detailed LC gradient conditions and multiple reaction monitoring (MRM) parameters are described in Table 4.3. Activity assays were performed based on protein content (mg protein/mL), and correlation was examined with absolute protein quantification (pmol/mg protein).

4.2.6 *Statistical analysis*

Statistical analysis was performed using Microsoft Excel (Redmond, WA) and GraphPad Prism version 5.03 for Windows (La Jolla, CA). Sectional comparisons (duodenum, jejunum, and ileum) were evaluated using nonparametric Kruskal-Wallis test, followed by Dunn's multiple comparison test. Segmented CHIM lots (6023, 6037, 6038) were grouped into duodenum (A), jejunum (B-H), and ileum (I and J). Protein abundance-activity correlations were examined using the Spearman rank test. *P* values less than 0.05 were considered significant.

4.3 RESULTS

4.3.1 *Non-CYP enzyme quantification*

CES and UGTs were quantified in protein extracted CHIM membrane fractions, and SULTs were quantified in CHIM cytosolic fractions. Among the 17 proteins investigated, six proteins (i.e, AO, UGT1A4, UGT1A6, UGT1A8, UGT2B4, and SULT1E1) were undetectable. UGT1A8, which is considered an intestinal UGT isoform, could not be detected due to lower sensitivity in LC-MS/MS for its surrogate peptide.

4.3.2 *Relative quantification of non-CYP enzymes using marker proteins*

Relative quantification for membrane enzymes was performed by normalization with average sucrase isomaltase (SI) and villin-1 (VIL1), and for cytosolic enzymes with intestinal fatty acid binding protein (FABP2). Protein concentration normalized relative regional distributions of VIL1, SI, FABP2, and their average values are shown in Figure 4.1. There was a strong correlation between SI and VIL1 relative abundance, as well as significant correlation between SI and VIL1 average and FABP2 as a cytosolic enterocyte marker, but no correlation with pan-UGT1A peptide as seen in Figure 4.2. VIL1 and SI also showed significantly lower abundance in duodenum, while FABP2 trended the same but remained nonsignificant (Figure 4.3). Relative quantifications for each enzyme are graphically shown in Figure 4.4, compiled average values normalized to duodenum for all enzymes are shown in Figure 4.5, and numerical values are reported in Table 4.4. Relative abundance generally seemed to trend higher in duodenum compared to jejunum and further decreasing in ileum, which is likely due to the lower abundance of normalizing marker proteins. Segmented proteomic analyses across multiple sections (n=10) indicate interindividual variability may be greater than inter-regional variability, indicated by the degree of non-overlap between subjects.

4.3.3 *Absolute quantification of non-CYP enzymes*

Absolute quantifications are reported from membrane fractions (pmol/mg membrane protein) for CES and UGTs and from cytosolic fractions (pmol/mg cytosolic protein) for SULTs. Table 4.5 shows the average values, and graphical representation for each enzyme and compiled average values are presented in Figure 4.6 and 4.7, respectively. Absolute quantification showed higher variability and fluctuations between lots compared to relative quantification, possibly an indicator of technical variability. Absolute quantifications for cytosolic fractions in seven lots of

CHIMs were excluded due to low and unreliable total protein content (lots 6017, 6018, 6023-I, 6037-E, 6037-G, 6037-H, 6038-H).

4.3.4 *Comparison of CHIM protein quantification with pooled intestinal S9 fraction*

CHIM membrane and cytosolic protein fractions for non-CYP enzymes and various marker proteins were compared with pooled (n=15) GIS9 fraction from Xenotech (Figure 4.8). CES and UGTs were undetectable in cytosolic fractions, while majority of SULTs were present in cytosolic fractions, consistent with FABP2 recovery. SI as a brush border enzyme was enriched in the membrane fraction, while cytoskeletal protein VIL1 was present in both fractions, but also with a strong significant correlation with SI (Figure 4.2). Calnexin and pan-UGT1A conserved peptide as marker proteins for ER membrane showed enrichment in the membrane fraction. These data indicate that the DME protein abundance is not compromised in the CHIM samples.

4.3.5 *Glucuronide formation and sequential metabolism in CHIM model*

To validate the integrity of CHIM model as a physiological surrogate of intestinal tissue, non-CYP functional activity assays were performed using four substrates, i.e., testosterone, CCA, CPG and CPT-11. Testosterone glucuronide (TG) formation in the intestine is solely mediated by UGT2B17, while clopidogrel acyl glucuronide (CAG) formation from CCA is mainly by UGT2B7 and UGT2B17, with minor contributions from UGT1A3 and UGT1A9 [9]. UGT2B17 CHIM protein abundance showed robust correlation with TG formation (r^2= 0.97, p =0.0004). CAG formation rate showed significant correlation with UGT2B17 abundance (r^2= 0.86, p =0.011) but not with UGT2B7 abundance (r^2= 0.33, ns) as shown in Figure 4.9. Correlation between CAG formation and UGT2B17 abundance became non-significant with imatinib co-

incubation as a UGT2B17-specific inhibitor. UGT1A3 and UGT1A10 abundance showed no significant correlation with CAG formation.

Sequential metabolism of CES-mediated hydrolysis and UGT-mediated glucuronidations were examined using relative metabolite to parent ratios (M/P ratios) and absolute protein abundance (Figure 4.10). M/P ratios for CES-mediated hydrolysis showed visual activity-abundance correlation for CPG and CPT-11, with the exception of C6015 with CPG. Secondary M/P ratios for glucuronides also showed visual correlation with UGT2B17 abundance for CCA to CAG, while SN38 to SN38-G closely following parent M/P ratios.

4.4 DISCUSSION

Limitations exist in available *in vitro* tools for assessing intestinal metabolism for accurate estimation, and knowledge gaps in intestinal physiology also limit reliable extrapolation. These limitations stem from the multifaceted nature of the intestine, which acts as a physical and biochemical protective barrier as well as an absorptive organ, comprising of a heterogeneous mixture of cell types, majority being mature enterocytes with a short life cycle [149]. Varying technical methods employed in isolation or preparation of intestine have resulted in inconsistent and irreproducible results, with each *in vitro* model having its own advantages and limitations [150]. Quantitative proteomic reports on regional distribution of intestinal enzymes are lacking, and non-CYP enzymes are further understudied. Quantitative proteomics can be utilized to assess technical variabilities due to different preparation methods as well as biological variabilities due to multiple cell types. Here, we utilized quantitative proteomics to investigate regional intestinal enzyme abundance, and enterocyte marker proteins as a normalizer to address technical variability.

Proteomic characterization was performed in two ways. Absolute quantification (pmol/mg protein) was done in membrane or cytosolic fractions of CHIM protein extractions, and relative quantification was done using enterocyte marker proteins. Although no head-to-head comparison is available for absolute quantification, values seem comparably in agreement to published results: slightly lower compared to intestinal microsomes [151,152] and significantly higher than tissue abundance [96]. Absolute quantification will allow extrapolation of in vitro clearance to overall intestinal metabolism.

Relative quantification using marker normalization was performed to control for technical variabilities including lot to lot variation. Relative normalization resulted in a smoother curve compared to absolute quantification, suggesting that technical variability can significantly affect quantification. Marker proteins such as VIL1, SI, or FABP2 for mature enterocytes may be further applied in IVIVE to generate accurate scaling factors. Given the complex anatomy and physiology of the intestine, it would be beneficial to better characterize marker proteins for mature enterocytes as well as for subcellular fractions to provide accurate physiological knowledge on enzyme abundance. The necessity for marker protein incorporation spans across all *in vitro* tools, and becomes more important as *in vitro* developments better reflect the multicellular complexity of the intestine, such as organoids. Relative normalization also showed higher enzyme abundance in duodenum compared to jejunum, which is contrary to reports of jejunum having higher enzyme contents [96]. This is likely due to lower normalizer marker abundance, i.e., villin-1 and sucrase isomaltase, which may be due to lower microvilli and brush border content per gram of tissue in duodenum. While utilization of marker proteins is beneficial, this highlights the importance of accurate physiological knowledge in characterization of marker proteins.

Activity assays examined UGT2B-mediated glucuronidation and CES and UGT-mediated sequential metabolism. UGT2B17, while a minor hepatic isoform, is a major isoform in the intestine, and the converse is true for UGT2B7, which is considered the major drug-metabolizing isoform [18,69,153]. Accordingly, clopidogrel acyl glucuronide (CAG) formation is reported to be mediated by UGT2B7 mainly in the liver (50 to 60%) but only 12% in the intestine. UGT2B17's contribution is around 10% in the liver, and increases to 87% in the intestine [9]. Intestinal contribution of UGT2B17 is reproduced in CHIMs in the strong correlation between CAG formation and UGT2B17 protein abundance. This also highlights the importance in consideration of UGT2B17 in intestinal and first-pass metabolism, where the fraction metabolized may vary widely. In CHIMs, a 5-fold increase in UGT2B17 protein abundance resulted in a 55-fold increase in CAG formation rate (data not shown). Sequential metabolisms were also qualitatively examined. In particular, CES1 and UGT2B mediated clopidogrel metabolism showed an outlier with high CES1 but low CCA/CPG ratio. A possible explanation may be transporter effects; P-glycoprotein (P-gp, *MDR1*) has been shown to influence clopidogrel absorption up to 9-fold *in vitro*, and clinical associations of lower maximum concentration and exposure for clopidogrel and its active metabolite have been reported with *MDR1 C3435T* genotype [154].

Some limitations of this study include incomplete protein extraction for cytosolic proteins, resulting in cytosolic proteins being detected in membrane fractions. This may be due to the differential brush border composition of enterocytes with tight junctions and residual mucus layers, leading to reduced surfactant activity and protein extraction. While we still saw enrichment of cytosolic proteins, further optimization may be beneficial. In addition, only qualitative activity assessments were made for sequential metabolisms of clopidogrel and CPT-

11. Protein concentrations used in activity assays were also relatively low at 0.25 mg/mL; although activity was still detected, higher CHIM protein concentrations may yield higher activity.

In conclusion, absolute and relative non-CYP proteomic quantification was performed along the human small intestine using CHIM model, using stable isotope labeled peptides and enterocyte marker proteins. Activity assays validate the proteomic quantifications and also indicate the potential impact of UGT2B17 on intestinal first pass metabolism as the major intestinal UGT isoform that is highly variable.

Table 4.1. Cryopreserved human intestinal mucosa (CHIM) demographics

Donor ID	**Age (yr)**	**Sex**	**Race**	**Available intestinal sections**
6023	49	F	Caucasian	A-B, D-J (n=9)
6037	59	F	Pacific Islander	A-J (n=10)
6038	38	M	Caucasian	A-J (n=10)
6001/03/05 (1)	20	M	Caucasian	Duodenum, Jejunum, Ileum
6008/07/06 (2)	20	M	Caucasian	Duodenum, Jejunum, Ileum
6012/ 11 (3)	36	F	Asian	Duodenum, Jejunum
6015/ 10/ 16 (4)	59	M	Caucasian	Duodenum, Jejunum, Ileum
6018/ 17/ 19 (5)	57	F	Caucasian	Duodenum, Jejunum, Ileum
HE3061/64/48 (6)	59	M	Hispanic	Duodenum, Jejunum, Ileum

Table 4.2. LC-MS/MS parameters for analysis of surrogate peptides

LC gradient program			
Acquity UPLC® HSS T3 C_{18} column (2.1 × 100 mm, 1.8 µm)			
Time (min)	**Flow rate (ml/min)**	**Water with 0.1% formic acid, %**	**Acetonitrile with 0.1% formic acid, %**
0	0.3	97	3
4	0.3	97	3
8	0.3	87	13
18	0.3	70	30
21.5	0.3	65	35
22	0.3	20	80
22.9	0.3	20	80
23	0.3	97	3
26	0.3	97	3

MS Parameters						
Protein	**Peptide sequence**	**Peptide type***	**Parent ion (*m/z*)**	**Product ion (*m/z*)**	**CE (eV)**	**DP (V)**
AOX	GLHGPLTLNSPLTPE**K**	Light	837.5	1366.8	42	92.2
			837.5	1309.7	42	92.2
			837.5	373.2	42	92.2
		Heavy	841.5	1374.8	42	92.2
			841.5	1317.8	42	92.2
			841.5	381.2	42	92.2
	LILNEVSLLGSAPGG**K**	Light	784.5	886.5	37.1	88.3
			784.5	573.3	37.1	88.3
			784.5	358.2	37.1	88.3
		Heavy	788.5	894.5	37.1	88.3
			788.5	581.3	37.1	88.3
			788.5	366.2	37.1	88.3
CES1	AGQLLSELFTN**R**	Light	674.9	866.4	33.2	80.3
			674.9	257.1	33.2	80.3
			674.9	370.2	33.2	80.3
		Heavy	679.9	876.4	33.2	80.3
			679.9	257.1	33.2	80.3
			679.9	370.2	33.2	80.3
CES2	ADHGDELPFVF**R**	Light	701.8	1079.6	39	82.3
			701.8	665.4	39	82.3
			701.8	322.2	39	82.3
		Heavy	706.8	1089.6	39	82.3
			706.8	675.4	39	82.3
			706.8	332.2	39	82.3
	FTEEEEQLS**R**	Light	634.3	1019.5	31.7	77.4

			634.3	890.4	31.7	77.4
			634.3	761.4	31.7	77.4
		Heavy	639.3	1029.5	31.7	77.4
			639.3	900.4	31.7	77.4
			639.3	771.4	31.7	77.4
UGT1A1	DGAFYTL**K**	Light	457.7	671.4	25.3	64.5
			457.7	260.2	25.3	64.5
			457.7	244.1	25.3	64.5
		Heavy	461.7	679.4	25.3	64.5
			461.7	268.2	25.3	64.5
			461.7	244.1	25.3	64.5
	ESFVSLGHNVFENDSFLQ**R**	Light	742.4	1155.5	31	85.2
			742.4	879.4	31	85.2
			742.4	650.4	31	85.2
		Heavy	745.7	1165.6	31	85.2
			745.7	889.4	31	85.2
			745.7	660.4	31	85.2
UGT1A3	YLSIPTVFFL**R**	Light	678.4	1079.6	33.3	80.6
			678.4	879.5	33.3	80.6
			678.4	277.2	33.3	80.6
		Heavy	683.4	1089.6	33.3	80.6
			683.4	889.5	33.3	80.6
			683.4	277.2	33.3	80.6
UGT1A4	FFTLTAYAVPWTQ**K**	Light	836.9	992.5	32	92.1
			836.9	758.4	32	92.1
			836.9	659.4	32	92.1
		Heavy	840.9	1000.5	32	92.1
			840.9	766.4	32	92.1
			840.9	667.4	32	92.1
	VTLGYTQGFFETEHLL**K**	Light	661.7	1016.5	33.6	79.4
			661.7	892.0	33.6	79.4
			661.7	835.4	33.6	79.4
		Heavy	664.4	1024.6	33.6	79.4
			664.4	896.0	33.6	79.4
			664.4	839.4	33.6	79.4
UGT1A6	DIVEVLSD**R**	Light	523.3	718.4	27.7	69.3
			523.3	589.3	27.7	69.3
			523.3	490.3	27.7	69.3
		Heavy	528.3	728.4	27.7	69.3
			528.3	599.3	27.7	69.3
			528.3	500.3	27.7	69.3
	SFLTAPQTEY**R**	Light	656.8	965.5	27.5	79
			656.8	864.4	27.5	79

			656.8	793.4	27.5	79
		Heavy	661.8	975.5	27.5	79
			661.8	874.4	27.5	79
			661.8	803.4	27.5	79
UGT1A8	GIAC[CAM]HYLEEGA QC[CAM]PAPLSYVP**R**	Light	830.1	999.6	35.7	81.6
			830.1	500.3	35.7	81.6
			830.1	745.3	35.7	81.6
		Heavy	833.4	1009.6	35.7	81.6
			833.4	505.3	35.7	81.6
			833.4	745.3	35.7	81.6
UGT1A10	TYSTSYTLEDQN**R**	Light	789.4	1313.6	37.3	88.7
			789.4	1038.5	37.3	88.7
			789.4	875.4	37.3	88.7
		Heavy	794.4	1323.6	37.3	88.7
			794.4	1048.5	37.3	88.7
			794.4	885.4	37.3	88.7
UGT2B4	ADIWLI**R**	Light	443.8	700.5	24.8	63.5
			443.8	587.4	24.8	63.5
			443.8	401.3	24.8	63.5
		Heavy	448.8	710.5	24.8	63.5
			448.8	597.4	24.8	63.5
			448.8	411.3	24.8	63.5
	FSPGYAIE**K**	Light	506.3	777.4	27.1	68
			506.3	680.4	27.1	68
			506.3	235.1	27.1	68
		Heavy	510.3	785.4	27.1	68
			510.3	688.4	27.1	68
			510.3	235.1	27.1	68
UGT2B7	IEIYPTSLT**K**	Light	582.8	922.5	29.8	73.6
			582.8	809.4	29.8	73.6
			582.8	646.4	29.8	73.6
		Heavy	586.8	930.5	29.8	73.6
			586.8	817.5	29.8	73.6
			586.8	654.4	29.8	73.6
	TILDELIQ**R**	Light	550.8	886.5	28.7	71.3
			550.8	773.4	28.7	71.3
			550.8	658.4	28.7	71.3
		Heavy	555.8	896.5	28.7	71.3
			555.8	783.4	28.7	71.3
			555.8	668.4	28.7	71.3
UGT2B15	NYLEDSLL**K**	Light	547.8	817.5	28.6	71.1
			547.8	704.4	28.6	71.1

			547.8	278.1	28.6	71.1
		Heavy	551.8	825.5	28.6	71.1
			551.8	712.4	28.6	71.1
			551.8	278.1	28.6	71.1
	SVINDPVY**K**	Light	517.8	848.5	27.7	69.4
			517.8	735.4	27.7	69.4
			517.8	424.7	27.7	69.4
		Heavy	521.8	856.5	27.7	69.4
			521.8	743.4	27.7	69.4
			521.8	428.7	27.7	69.4
UGT2B17	FSVGYTVE**K**	Light	515.3	882.5	27.4	68.7
			515.3	795.4	27.4	68.7
			515.3	696.4	27.4	68.7
		Heavy	519.3	890.5	27.4	68.7
			519.3	803.4	27.4	68.7
			519.3	704.4	27.4	68.7
	SVINDPIY**K**	Light	524.8	862.5	27.7	69.4
			524.8	749.4	27.7	69.4
			524.8	431.7	27.7	69.4
		Heavy	528.8	870.5	27.7	69.4
			528.8	757.4	27.7	69.4
			528.8	435.7	27.7	69.4
SULT1A1	VHPEPGTWDSFLE**K**	Light	547.9	738.4	27.4	71.1
			547.9	623.3	27.4	71.1
			547.9	237.1	27.4	71.1
		Heavy	550.6	746.4	27.4	71.1
			550.6	631.4	27.4	71.1
			550.6	237.1	27.4	71.1
SULT1A3	AHPEPGTWDSFLE**K**	Light	538.6	738.4	26.9	70.4
			538.6	623.3	26.9	70.4
			538.6	209.1	26.9	70.4
		Heavy	541.3	746.4	26.9	70.4
			541.3	631.4	26.9	70.4
			541.3	209.1	26.9	70.4
	NYFTVAQNE**K**	Light	607.3	936.5	30.7	75.4
			607.3	789.4	30.7	75.4
			607.3	278.1	30.7	75.4
		Heavy	611.3	944.5	30.7	75.4
			611.3	797.4	30.7	75.4
			611.3	278.1	30.7	75.4
SULT1E1	NHFTVALNE**K**	Light	391.5	574.3	18.9	59.7
			391.5	503.3	18.9	59.7
			391.5	500.2	18.9	59.7

		Heavy	394.2	582.3	18.9	59.7
			394.2	511.3	18.9	59.7
			394.2	500.2	18.9	59.7
SULT2A1	TLEPEELNLIL**K**	Light	706.4	1068.6	34.3	82.6
			706.4	344.2	34.3	82.6
		Heavy	710.4	1076.6	34.3	82.6
			710.4	344.2	34.3	82.6
CALNEXIN	GLVLMS**R**	Light	388.2	506.3	22.8	59.4
			388.2	393.2	22.8	59.4
		Heavy	393.2	516.3	22.8	59.4
			393.2	403.2	22.8	59.4
	IPDPEAVKPDDWDEDAPA**K**	Light	703.3	891.9	35.9	82.4
			703.3	326.2	35.9	82.4
		Heavy	706.0	895.9	35.9	82.4
			706.0	326.2	35.9	82.4
CALRETICULIN	EQFLDGDGWTS**R**	Light	705.8	893.4	34.3	82.6
			705.8	778.3	34.3	82.6
		Heavy	710.8	903.4	34.3	82.6
			710.8	788.4	34.3	82.6
	FVLSSG**K**	Light	369.2	491.3	22.1	58
			369.2	247.1	22.1	58
		Heavy	373.2	499.3	22.1	58
			373.2	247.1	22.1	58
PAN-UGT1A[#]	IPQTVLW**R**	Light	506.8	802.5	27.1	68.1
			506.8	674.4	27.1	68.1
			506.8	450.3	27.1	68.1
		Heavy	511.8	812.5	27.1	68.1
			511.8	684.4	27.1	68.1
			511.8	455.3	27.1	68.1
SI	ILGLTDSVTEV**R**	Light	651.9	1076.6	25.3	68.6
			651.9	906.5	25.3	68.6
		Heavy	656.9	1086.6	25.3	68.6
			656.9	916.5	25.3	68.6
VIL1	GSLNITTPGLQIW**R**	Light	519.3	474.3	18.8	59
			519.3	435.3	18.8	59
		Heavy	522.6	484.3	18.8	59
			522.6	440.3	18.8	59
	EVQGNESEAF**R**	Light	633.3	909.4	24.7	67.3
			633.3	609.3	24.7	67.3
		Heavy	638.3	919.4	24.7	67.3
			638.3	619.3	24.7	67.3
FABP2	LTITQEGN**K**	Light	502.27	789.41	19.9	57.7

	502.27	676.33	19.9	57.7
Heavy	506.28	797.42	19.9	57.7
	506.28	684.34	19.9	57.7

* Heavy indicates stable isotope labeled (SIL) peptides labeled at lysine (**K**) and arginine (**R**) with $^{13}C_6$ and $^{15}N_2$
# Pan-UGT1A peptide is conserved in all UGT1A isoforms in humans

Table 4.3. LC-MS/MS parameters for analysis of small molecules

Clopidogrel, Clopidogrel Carboxylic Acid, and Testosterone Assays			
LC gradient program			
Acquity UPLC® HSS T3 C_{18} column (2.1 × 100 mm, 1.8 μm)			
Time (min)	**Flow rate (ml/min)**	**Water with 0.1% formic acid, %**	**Acetonitrile with 0.1% formic acid, %**
0	0.3	85	15
1	0.3	85	15
2.5	0.3	60	40
8.5	0.3	50	50
12	0.3	2	98
12.8	0.3	2	98
13	0.3	85	15
15	0.3	85	15

MS Parameters				
Compound# or Internal Standard*	**Parent ion (*m/z*)**	**Product ion (*m/z*)**	**DP (V)**	**CE (eV)**
Clopidogrel (CPG)	322	155	80	35
Clopidogrel (CPG)	322	212	80	35
Clopidogrel Carboxylic Acid (CCA)	308.13	197.8	76	28
Clopidogrel Carboxylic Acid (CCA)	308.13	151.9	76	38
Clopidogrel Carboxylic Acid (CCA)	308.13	168.8	76	42
Clopidogrel Carboxylic Acid (CCA)	308.13	124.9	76	56
Clopidogrel Acyl Glucuronide (CAG)	484.3	197.8	76	28
Clopidogrel Acyl Glucuronide (CAG)	484.3	151.9	76	42
Clopidogrel Acyl Glucuronide (CAG)	484.3	168.8	76	47
Clopidogrel Acyl Glucuronide (CAG)	484.3	308.13	76	35
Testosterone	289.1	109.1	80	30
Testosterone	289.1	97.1	80	30
Testosterone-d3	292.2	109.1	80	30
Testosterone-d3	292.2	97.1	80	30
Testosterone Glucuronide	465.24	289.21	70	25
Testosterone Glucuronide	465.24	271.21	70	30
Testosterone Glucuronide	465.24	253.21	70	35
Testosterone Glucuronide	465.24	109.1	70	35
Testosterone Glucuronide	465.24	97.1	70	35
Testosterone Glucuronide-d3	468.24	292.2	70	25
Testosterone Glucuronide-d3	468.24	274.2	70	30

Testosterone Glucuronide-d3	468.24	256.2	70	35

Camptothecin-11 Assay

LC gradient program

Acquity UPLC® HSS T3 C18 column (2.1 × 100 mm, 1.8 μm)

Time (min)	Flow rate (ml/min)	Water with 0.1% formic acid, %	Acetonitrile with 0.1% formic acid, %
0	0.3	95	5
0.6	0.3	95	5
5	0.3	5	95
6	0.3	90	10
6.1	0.3	90	10

MS Parameters

Compound# or Internal Standard*	Parent ion (*m/z*)	Product ion (*m/z*)	DP (V)	CE (eV)
Camptothecin-11 (CPT-11)	587.27	124.2	80	43
Camptothecin-11 (CPT-11)	587.27	166.9	80	49
Camptothecin-11 (CPT-11)	587.27	331.1	80	57
Camptothecin-11 (CPT-11)	587.27	245.2	80	95
SN38	393.21	348.8	156	37
SN38	393.21	248.6	156	63
SN38 Glucuronide (SN38-G)	569.2	393.3	140	41
SN38 Glucuronide (SN38-G)	569.2	349.3	140	57
Testosterone-d3	292.2	109.1	80	30
Testosterone-d3	292.2	97.1	80	30
Testosterone Glucuronide-d3	468.24	292.2	70	25
Testosterone Glucuronide-d3	468.24	274.2	70	30
Testosterone Glucuronide-d3	468.24	256.2	70	35

All MRMs listed were used for relative quantification.

* Testosterone-d3 was used as an internal standard for CPG and CPT-11

* Testosterone glucuronide-d3 was an internal standard for CCA, SN38, TG, CAG, and SN38-G

Table 4.4. Enterocyte marker normalized relative abundance values

	Duodenum	Jejunum	Ileum	A	B	C	D	E	F	G	H	I	J
CES1	**0.014**	**0.003**	**0.002**	**0.014**	**0.005**	**0.006**	**0.004**	**0.004**	**0.002**	**0.002**	**0.001**	**0.001**	**0.001**
	0.01	0.003	0.001	0.012	0.005	n/a	0.004	0.004	0.004	0.003	0.002	0.001	0.002
CES2	**3.2**	**1.4**	**1.4**	**2.2**	**1.8**	**2.1**	**1.7**	**1.6**	**1.1**	**1.2**	**1.2**	**1.2**	**1.2**
	1.9	0.4	0.2	1.1	1.1	n/a	1	0.7	0.9	1.1	1.1	0.6	0.9
UGT1A1	**0.44**	**0.23**	**0.16**	**0.37**	**0.32**	**0.35**	**0.3**	**0.25**	**0.24**	**0.29**	**0.26**	**0.21**	**0.21**
	0.26	0.09	0.09	0.11	0.13	n/a	0.1	0.03	0.06	0.07	0.06	0.09	0.12
UGT1A3	**0.10**	**0.08**	**0.06**	**0.09**	**0.08**	**0.12**	**0.07**	**0.08**	**0.10**	**0.11**	**0.10**	**0.10**	**0.10**
	0.06	0.05	0.06	0.01	0.02	n/a	0.02	0.01	0.03	0.04	0.04	0.02	0.04
UGT1A10	**1.62**	**0.91**	**1.01**	**1.51**	**1.04**	**1.51**	**1.22**	**1.04**	**0.54**	**0.89**	**0.71**	**0.63**	**0.65**
	0.76	0.21	0.39	0.79	0.42	n/a	0.71	0.38	0.5	0.45	0.37	0.24	0.52
UGT2B7	**0.15**	**0.09**	**0.08**	**0.11**	**0.11**	**0.14**	**0.13**	**0.11**	**0.13**	**0.16**	**0.15**	**0.15**	**0.14**
	0.08	0.02	0.04	0.01	0.04	n/a	0.03	0.02	0.02	0.03	0.03	0.02	0.04
UGT2B17	**4.1**	**1.3**	**2.3**	**2.5**	**1.6**	**1.7**	**1.5**	**1.2**	**2.2**	**2.7**	**2.8**	**2.6**	**2.9**
	3.7	0.5	1.3	2.4	1.8	n/a	1.4	1.1	1.3	1.6	1.6	1.5	1.8
SULT1A1	**0.67**	**0.29**	**0.34**	**0.47**	**0.41**	**0.48**	**0.31**	**0.33**	**0.34**	**0.23**	**0.28**	**0.39**	**0.3**
	0.38	0.22	0.24	0.29	0.22	n/a	0.2	0.22	0.16	n/a	n/a	n/a	0.2
SULT1A3	**2.1**	**1**	**1**	**2**	**1.7**	**1.5**	**1.3**	**1.4**	**1.4**	**1**	**1.1**	**1.2**	**0.9**
	0.7	0.2	0.2	0.9	0.5	n/a	0.8	0.6	0.3	n/a	n/a	n/a	0.2
SULT1B1	**1.5**	**0.9**	**0.8**	**1.7**	**1.6**	**1.5**	**1.2**	**1.3**	**1.3**	**0.8**	**1.1**	**1.5**	**1.1**
	0.3	0.1	0.1	1	0.8	n/a	0.7	0.8	0.5	n/a	n/a	n/a	0.2
SULT2A1	**0.24**	**0.16**	**0.13**	**0.22**	**0.24**	**0.22**	**0.21**	**0.22**	**0.23**	**0.19**	**0.21**	**0.23**	**0.2**
	0.05	0.04	0.05	0.01	0.03	n/a	0.06	0.03	0.03	n/a	n/a	n/a	0.02

Means are in bold and standard deviations are below means
CES and UGT values are from membrane proteins, SULTs from cytosolic proteins.
* Normalization was performed using the average of area ratios for villin-1 and sucrase isomaltase for membrane proteins and intestinal fatty acid binding protein for cytosolic proteins
A-J indicate ten different intestinal sections from duodenum to ileum

Table 4.5. Absolute protein abundance values of non-CYP enzymes in the human intestine

Protein	Duodenum	Jejunum	Ileum	A	B	C	D	E	F	G	H	I	J	LLOQ*
CES1	**9.1**	**4.1**	**2.8**	**14.9**	**7.2**	**6.6**	**4.2**	**4.4**	**4.7**	**3.4**	**3.5**	**3.3**	**3.5**	1.9
	4.7	2.9	0.7	11.5	5.8	n/a	2.4	3	2.8	1.7	1.9	1.6	2.1	
CES2	**693**	**646**	**682**	**718**	**756**	**756**	**626**	**604**	**664**	**631**	**753**	**784**	**753**	54.9
	168	139	215	271	366	n/a	157	85	141	225	348	177	265	
UGT1A1	**1.8**	**1.8**	**1.3**	**2.1**	**2.3**	**2.2**	**2**	**1.8**	**1.9**	**2**	**2.1**	**1.9**	**1.7**	0.32
	1	0.6	0.8	0.8	0.8	n/a	0.5	0.7	1.2	1.3	1	0.8	0.9	
UGT1A3	**0.09**	**0.12**	**0.1**	**0.1**	**0.11**	**0.15**	**0.1**	**0.11**	**0.15**	**0.14**	**0.16**	**0.17**	**0.15**	0.03
	0.06	0.06	0.1	0.02	0.02	n/a	0.03	0.04	0.11	0.13	0.11	0.04	0.06	
UGT1A10	**23.3**	**26.9**	**29.7**	**30.5**	**27.5**	**35.3**	**28.1**	**25.6**	**20.2**	**26.1**	**24.7**	**24.9**	**26.8**	10.2
	6.3	6.5	10.8	12	7.2	2.3	8.6	2.3	2.2	15.3	8	3.9	10.4	
UGT2B7	**2.7**	**3**	**2.9**	**2.6**	**3.4**	**3.8**	**3.6**	**3.3**	**4.3**	**4.7**	**5.2**	**5.6**	**4.6**	0.17
	1.2	0.9	1.8	0.6	0.9	n/a	0.8	1.2	2.4	2.8	2.3	0.9	1.4	
UGT2B17	**6.9**	**4.9**	**7.8**	**7.3**	**5.5**	**5.1**	**5.4**	**4.9**	**7.3**	**7.3**	**7.8**	**8.3**	**8.1**	0.17
	3.5	1.7	3	7.1	5.8	n/a	4.7	4.5	6.8	7.2	7.4	7.2	7.1	
SULT1A1	**9.5**	**9.9**	**6.9**	**7.5**	**15.3**	**6.8**	**4.6**	**11.3**	**12.5**	**7.4**	**5.1**	**28.4**	**13**	0.73
	7.4	7.1	5.1	7.8	12.5	n/a	2.8	n/a	10.5	n/a	n/a	n/a	16.3	
SULT2A1	**7.9**	**13.5**	**5.6**	**9.5**	**22.7**	**7.3**	**8.7**	**23.1**	**21.9**	**13.8**	**28.2**	**36.9**	**16.2**	0.3
	3.7	7.4	3.4	7.2	12.1	n/a	5.5	n/a	14.8	n/a	n/a	n/a	15.1	

Mean are in bold and standard deviations are below means
CES and UGT values are from membrane proteins, SULTs from cytosolic proteins.
*Lower limit of quantification (pmol/mg protein)
A-J indicate ten different intestinal sections from duodenum to ileum

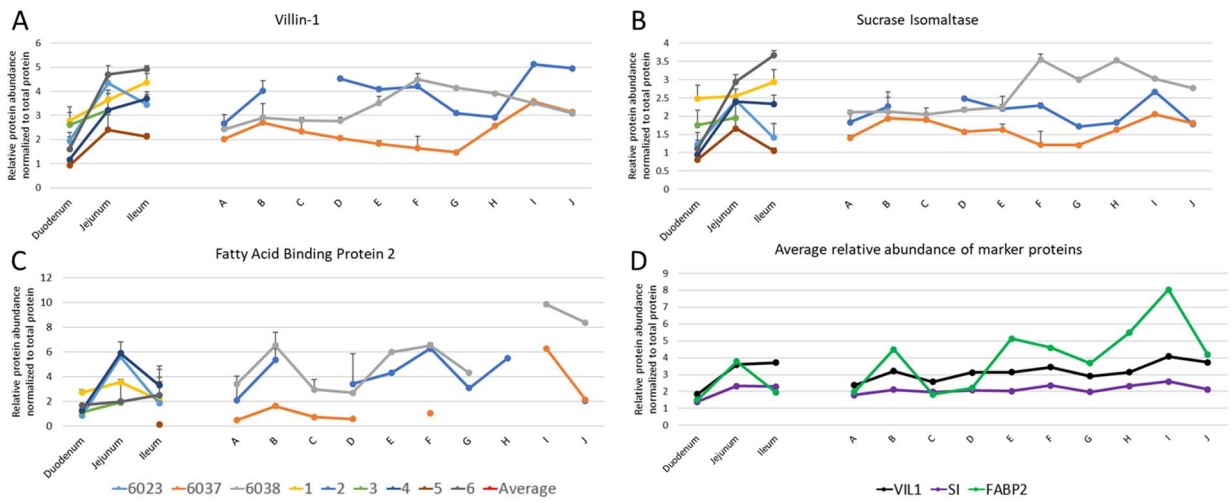

Figure 4.1. Relative abundance of enterocyte marker proteins along the intestine.

Relative area ratios for villin-1 (VIL1), sucrase isomaltase (SI), fatty acid binding protein 2 (FABP2) are normalized by total protein concentrations and shown in A-C. Average values for all marker proteins are shown in Figure 4.1D. Left panel in each figure shows CHIMs from duodenum, jejunum, and ileum in 6 donors. Right panel shows 10 segments down the intestinal tract (A through J) in 3 donors. Blank points indicate missing or excluded samples, and error bars show standard deviation.

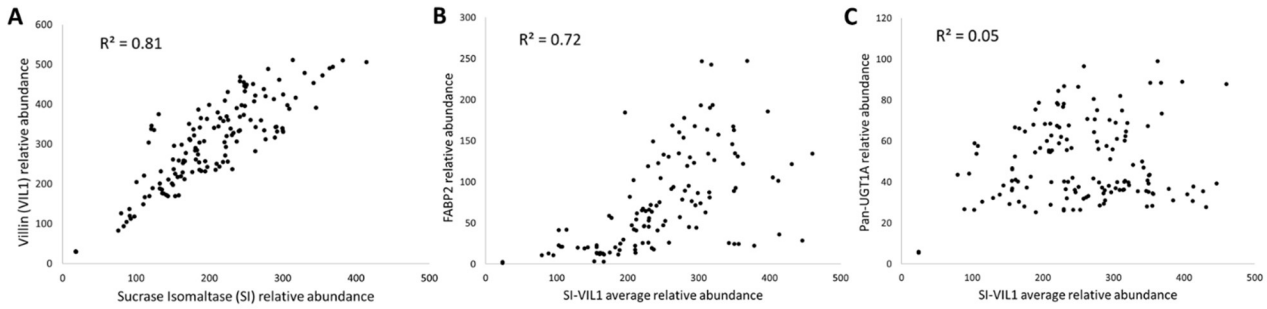

Figure 4.2. Enterocyte marker peptide correlation.

Peptide correlation between sucrase isomaltase (SI) and villin-1 (VIL1) in membrane protein fraction is shown in A ($p < 0.001$). Average of SI and VIL1 was used for relative normalization,

and shows correlation with cytosolic intestinal fatty acid binding protein (FABP2) as another enterocyte marker (B) ($p < 0.001$) while showing no correlation with pan-UGT1A (C).

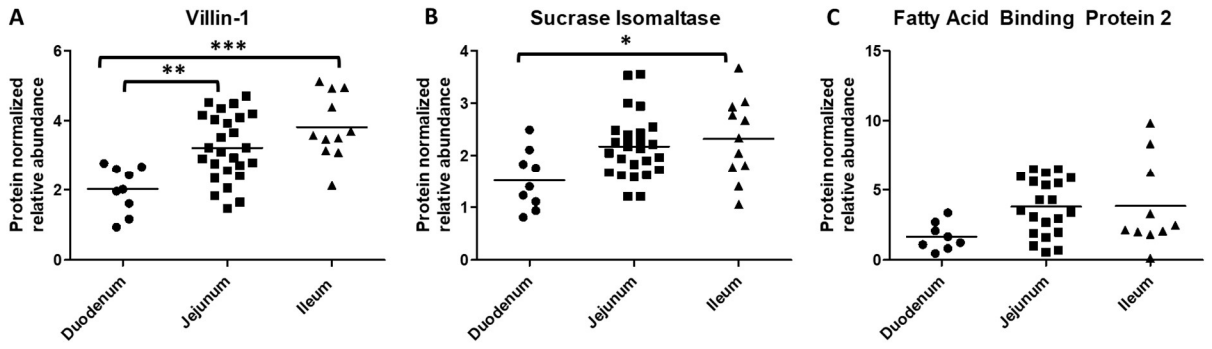

Figure 4.3. Sectional comparison of protein-normalized relative abundance of enterocyte marker proteins.

Sectional comparisons (duodenum, jejunum, and ileum) for villin-1 (VIL1), sucrase isomaltase (SI), and fatty acid binding protein 2 (FABP2) were evaluated using nonparametric Kruskal-Wallis test, followed by Dunn's multiple comparison test (A-C). Segmented CHIM lots (A-J) (6023, 6037, and 6038) were grouped into duodenum (A), jejunum (B-H), and ileum (I and J). * indicates $p < 0.05$, ** indicates $p < 0.01$, and *** indicates $p < 0.001$.

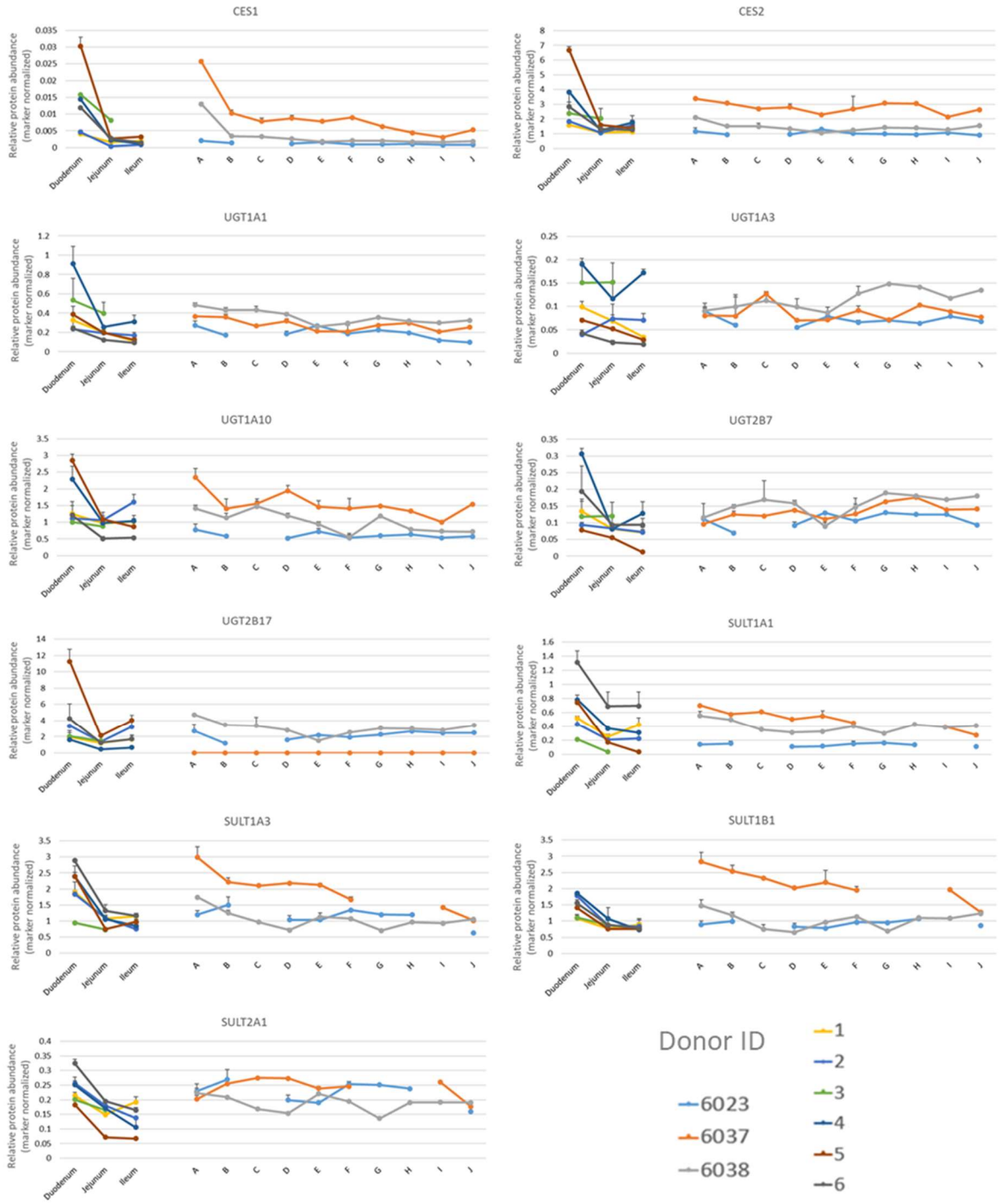

Figure 4.4. Relative protein abundance of non-CYP enzymes along the intestine in CHIMs. Relative protein abundance was calculated by normalizing relative area ratios of each enzyme with average area ratios of villin-1 (VIL1) and sucrase isomaltase (SI) for CESs and UGTs, and

intestinal fatty acid binding protein 2 (FABP2) for SULTs. Left panel in each graph shows CHIMs from duodenum, jejunum, and ileum in 6 donors. Right panel shows 10 segments down the intestinal tract (A through J) in 3 donors. Blank points indicate missing or excluded samples, and error bars show standard deviation.

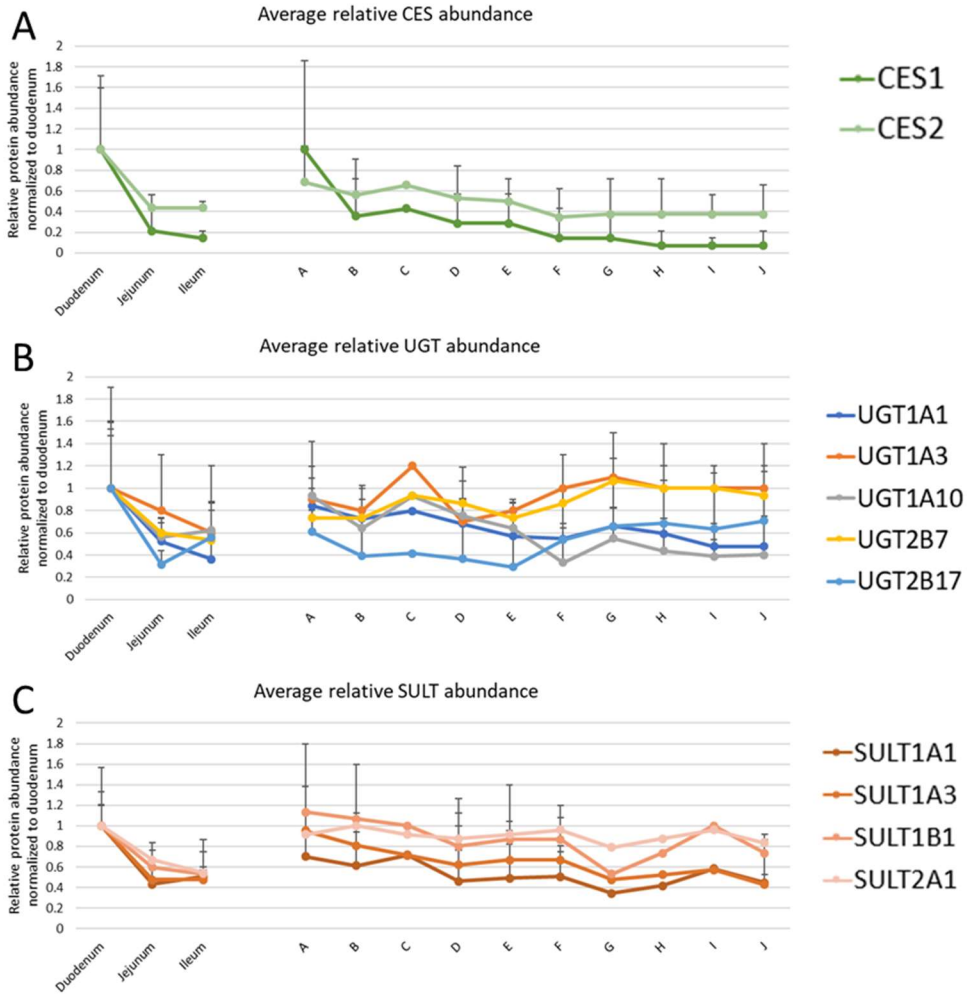

Figure 4.5. Average relative abundance of non-CYP enzymes along the intestine. Compiled average relative abundance values for CESs (A), UGTs (B), and SULTs (C). Relative values have been standardized to duodenum values as 1. Left panel in each graph shows CHIMs from duodenum, jejunum, and ileum in 6 donors. Right panel shows 10 segments down the intestinal tract (A through J) in 3 donors. Error bars show standard deviation.

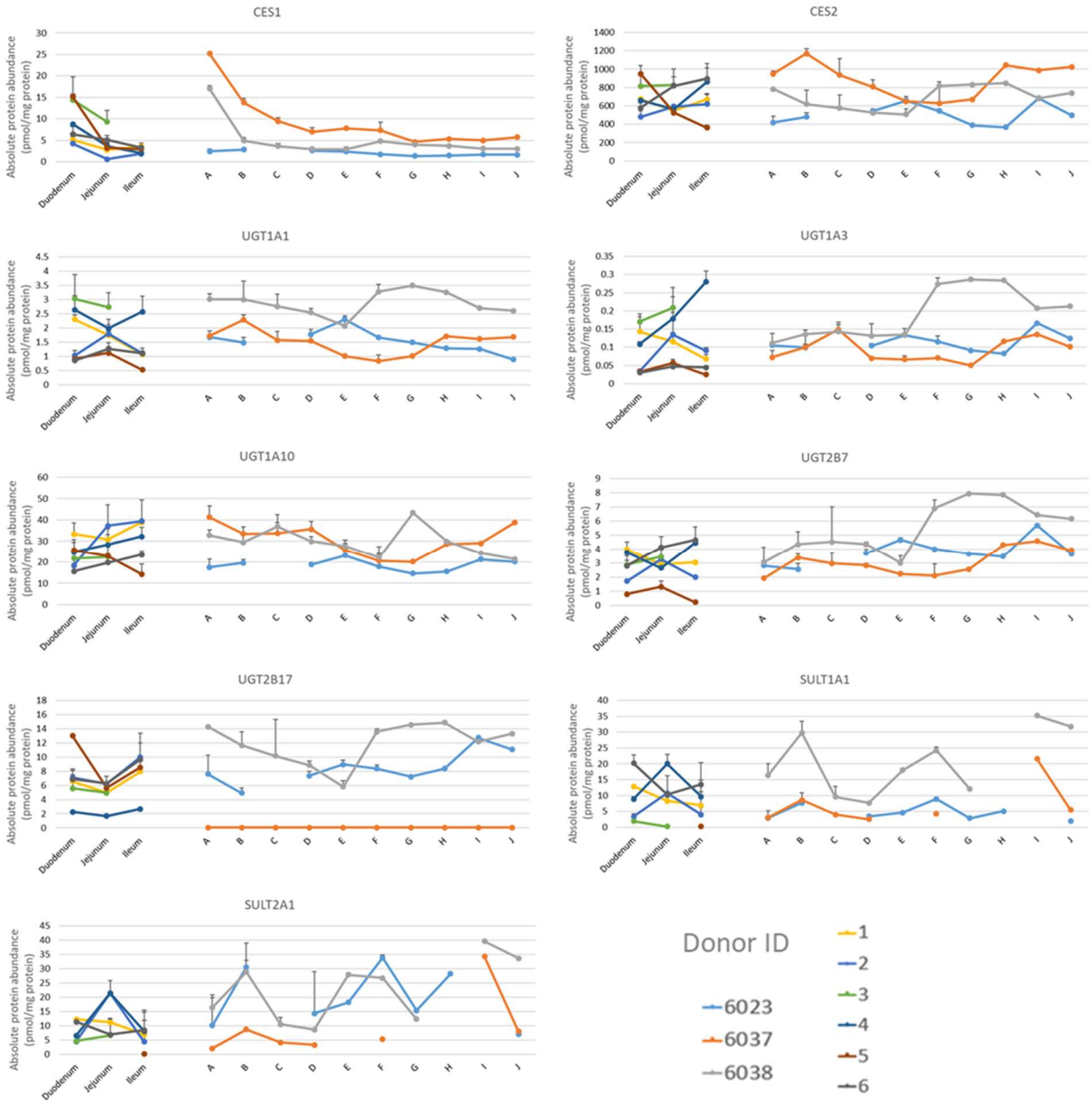

Figure 4.6. Absolute protein abundance of non-CYP enzymes along the intestine in CHIMs. Absolute protein abundance (pmol/mg protein) is shown for membrane proteins (CESs and UGTs) and cytosolic proteins (SULTs) extracted from CHIMs. Left panel in each graph shows CHIMs from duodenum, jejunum, and ileum in 6 donors. Right panel shows 10 segments down the intestinal tract (A through J) in 3 donors. Blank points indicate missing or excluded samples, and error bars show standard deviation.

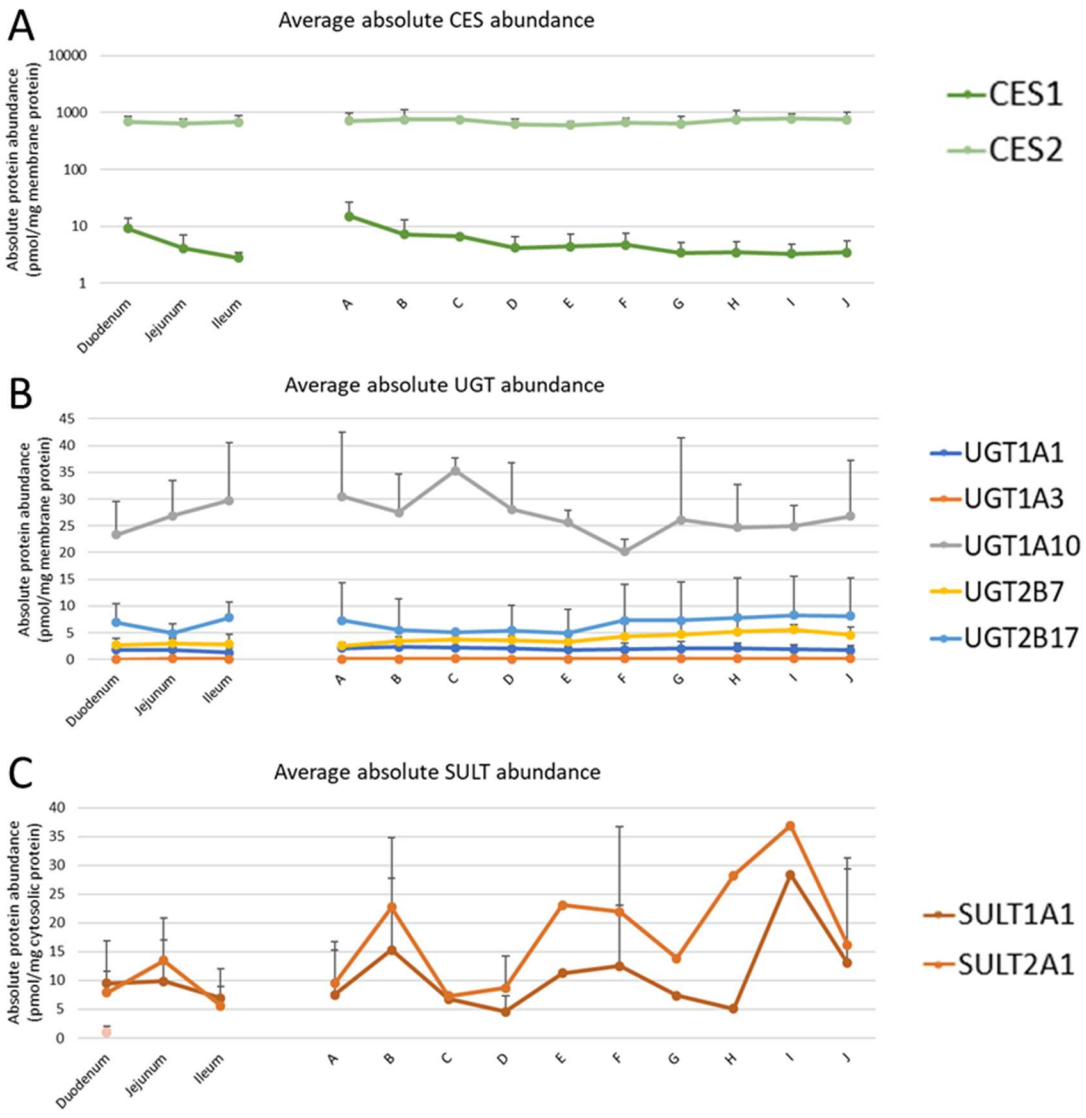

Figure 4.7. Average absolute abundance of non-CYP DMEs along the intestine.

Absolute abundance (pmol/mg protein) average values for CES, UGT, and SULT isoforms (A-C). Left panel in each graph shows CHIMs from duodenum, jejunum, and ileum in 6 donors. Right panel shows 10 segments down the intestinal tract (A through J) in 3 donors. Error bars show standard deviation.

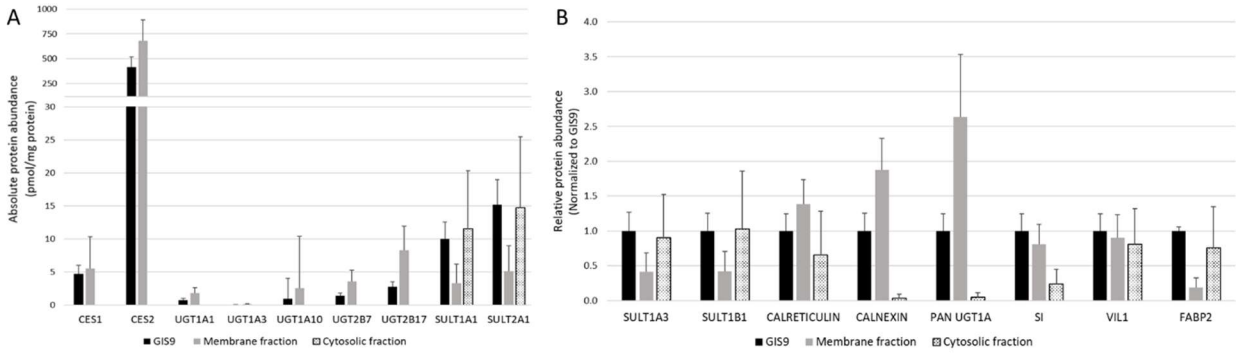

Figure 4.8. Comparison of protein abundance between pooled GIS9 and CHIM protein extraction.

Protein abundance for non-CYP enzymes and enterocyte marker proteins are compared between an independent pooled GIS9 (black) to CHIM membrane fractions (gray) and cytosolic fractions (patterned) in absolute abundance (A, pmol/mg protein) and relative abundance (B, normalized to GIS9), with error bars showing standard deviation. CESs and UGTs were undetectable in cytosolic fractions, while SULTs were detected in both fractions.

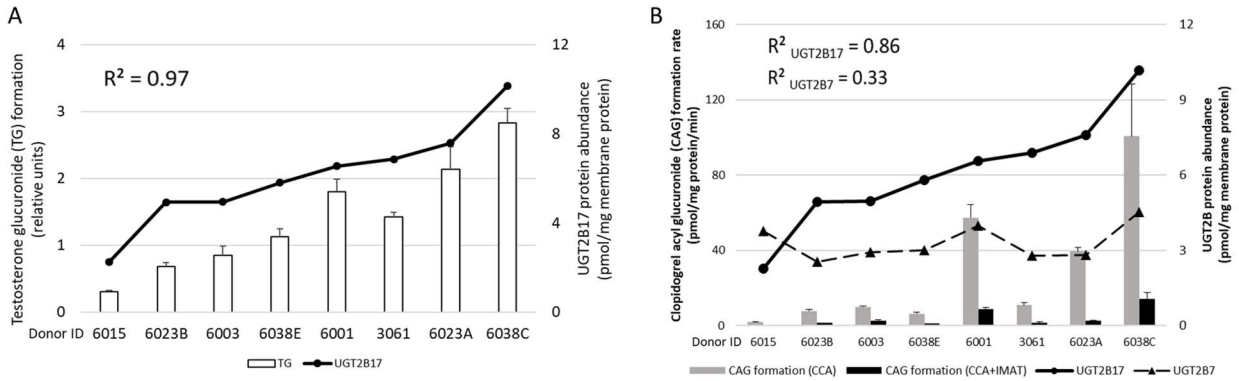

Figure 4.9. CHIM activity in glucuronide formation and UGT2B protein abundance.

Testosterone glucuronide (TG) formation (open bars), UGT2B17 protein abundance (solid line), and activity-expression correlation (p =0.004) are shown in A. Clopidogrel acyl glucuronide (CAG) formation rate, UGT2B protein abundance (UGT2B17 in solid line and UGT2B7 in truncated line), and correlation coefficients (nonsignificant for UGT2B7, p =0.011 for UGT2B17) are shown in B. CAG formation from clopidogrel carboxylic acid (CCA) without or

with imatinib as a UGT2B17-specific inhibitor is shown in grey and black bars, respectively. Error bars show standard deviation. Intestinal TG formation is solely UGT2B17 mediated, while CAG formation is mainly mediated by both UGT2B7 and UGT2B17.

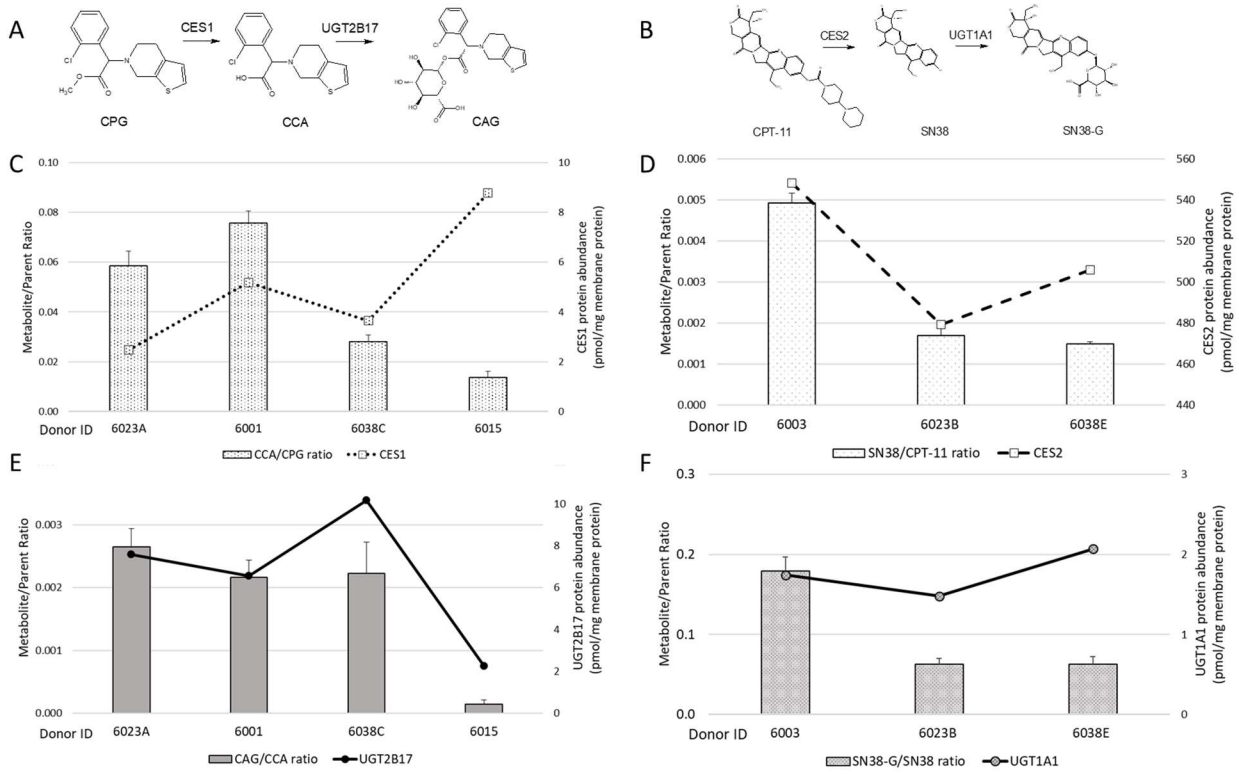

Figure 4.10. Sequential metabolism of clopidogrel (CPG) and camptothecin-11 (CPT-11) in CHIMs.

Sequential metabolism of CPG to clopidogrel carboxylic acid (CCA) by CES1 and glucuronidation to clopidogrel acyl glucuronide (CAG) by UGT2B17 and UGT2B7 (A) is shown in C and E, respectively. Hydrolysis of CPT-11 to SN38 by CES2 and subsequent glucuronidation to SN38-Gluc by UGT1A1 (B) is shown in D and F, respectively. Metabolite/parent ratios are shown in bars, enzyme abundances are shown in lines, and error bars show standard deviation.

Chapter 5. CONCLUSIONS AND FUTURE DIRECTIONS

UGT2B17 is an androgen- and drug-conjugating enzyme whose main endogenous substrates are C_{19} androgens, notably testosterone [10]. UGT2B17 has a remarkably high interindividual variability in its hepatic protein expression [1], and mRNA analysis predicts protein expression in intestine, prostate, lung, kidney, uterus, placenta, and adrenal glands [2]. Multiple factors contribute to this variability, including a common CNV, sex, age, and SNPs. UGT2B17 harbors one of the most common gene deletions [11], and males have a 2.6-fold higher hepatic abundance compared to females. UGT2B17 also exhibits a unique ontogeny curve, with a dramatic increase in abundance around the age of puberty, with the increase more prominent in males compared to females; this brings up the potential for differential variabilities in drug disposition and DDI magnitude that are dependent on sex as well as age. However, only a small portion (26%) can be explained by CNV, sex, age, and certain SNPs combined [10].

Unexplained protein abundance variability highlights the potential limitations in current research strategies when studying UGT2B17 associations with various disease outcomes, where stratification by genotype alone may be confounded by other, as yet unknown, sources of UGT2B17 variability. Nonetheless, significant associations have been demonstrated with testosterone-related outcomes, such as prostate cancer [26,27], antidoping-tests [20,25], body mass index [30], and osteoporosis [33,34], as well as other diseases such as lung cancer and pancreatic cancer [36,39]. These associations may arise from UGT2B17's potential role in testosterone homeostasis and as a detoxifying enzyme involved in carcinogen conjugation and elimination. UGT2B17 variability has also impacted drug development, leading to discontinued development of an investigational asthma medication (MK-7246) and impacting the disposition

of the anticancer agents, vorinostat and 17-hydroxyexemestane, compound (or active metabolites) that are substrates for UGT2B17.

Despite its proven involvement in drug disposition, UGT2B17 is an understudied enzyme in part due to its low hepatic content as well as relatively few known drug substrates [1,19]. While UGT2B17's presence in the liver is minor, representing only 4% of all UGT isoforms, it is the major UGT isoform in the intestine, constituting 30% of intestinal UGTs, when the gene is present [1]. High intestinal expression brings in further consideration of UGT2B17's role in first pass metabolism. Variable first pass metabolism not only affects systemic drug exposure following oral administration, but can also affect the potential magnitude of drug-drug interactions (DDIs), such as that caused by clopidogrel acyl glucuronide (CAG)-mediated CYP2C8 inactivation. Currently utilized intestinal *in vitro* models are limited by low reproducibility for quantitative assessment, and the absence of quantitative enzyme abundance data [66], which pose difficulties for accurate quantitative evaluations of intestinal drug metabolism. Physiologically-based pharmacokinetic (PBPK) modeling has been proposed as a useful tool to address the difficulties stemming from the complex histology and physiology of the intestine [135], and quantitative proteomics has shown to be invaluable for filling in the knowledge gaps required for PBPK modeling [74]. Much of the research presented in this dissertation involved application of quantitative proteomic analysis.

The overarching hypothesis for this dissertation was that **high variability and uniquely high intestinal abundance of UGT2B17 can result in inherently unpredictable drug pharmacokinetics and drug-drug interactions, but that can be prospectively predicted using a phenotypic biomarker and quantitative proteomics applied to physiologically-based pharmacokinetic (PBPK) modeling**.

The first aim was to examine the role of UGT2B17 in testosterone first-pass metabolism. Testosterone levels in men decline steadily after thirty years of age, and up to 50% of men in their 80s are considered hypogonadal [82]. Testosterone replacement therapy (TRT) alleviates symptoms of hypogonadism, which includes fatigue, depression, and decreased BMI, through exogenous administration of testosterone [51]. Despite the growing use and popularity of TRT, no oral formulation is approved in the United States, and TRT is administered as intramuscular injections or transdermal applications. Oral formulations used in Canada and Europe have raised concerns for hepatotoxicity and other adverse events [52,83]. Development of a safe, viable oral testosterone formulation requires characterization of testosterone's reported low and variable oral bioavailability [155]. In Chapter 2, we examined UGT2B17 abundance in paired intestinal microsomes and testosterone glucuronidation activity in HLMs to study individual fractional contribution (f_m) for UGT2B17, compared to UGT2B15, and performed quantitative metabolite profiling in cryopreserved human hepatocytes and enterocytes after testosterone incubation. We confirmed a 4.4-fold higher UGT2B17 abundance in HIMs compared to HIMs, and that UGT2B17 drives TG formation in HLMs (r^2= 0.77, p<0.001) with a wide range of f_m values observed (0 to 91%). We also found significant correlation between UGT2B17 abundance in enterocytes and TG formation (r^2=0.69, p=0.003), and TG was the second most abundant metabolite formed after androstenedione (AED) in both hepatocytes and enterocytes. That AED was the dominant metabolite formed was unexpected, but also unsurprising, as it is an intermediary metabolite connecting multiple androgen metabolic pathways and is found in high circulating concentrations. AED formation from testosterone is mediated by 17β-hydroxysteroid dehydrogenase 2 (17βHSD2), one of a multitude of enzymes that are involved in androgen disposition [58].

Given highly variable UGT2B17 tissue abundance, any first pass metabolic process or systemic clearance pathway dependent on UGT2B17 activity should also be highly variable. Considering that 76% of the enzyme abundance variability is unexplained, a phenotypic biomarker would be beneficial for identifying novel sources of enzyme variability, predicting *in vivo* UGT2B17 activity with PBPK modeling, and predicting individual risk of androgen-dependent diseases. Although significant associations between UGT2B17 and various clinical outcomes have been shown, reports of conflicting results can be found [31,40], which may partially be due to UGT2B17's high variability masking its gene-dose effect, making the differences less prominent and detectable. An ideal biomarker possesses selectivity, sensitivity, and minimal external factors that would change its endogenous levels [156]. Testosterone glucuronide (TG) is an excellent starting point as a candidate, as its formation is driven mainly by UGT2B17 and to a lesser extent by UGT2B15, and due to the clearly established associations between urinary excretion of TG and UGT2B17. However, homeostatic regulation and interindividual variability in the endogenous production of testosterone need to be addressed [58]. We thus proposed androsterone glucuronide (AG) as a normalizer to control for a variable testosterone synthesis rate. AG is a reasonable normalizer for multiple reasons. Androsterone is in the same metabolic pathway but it is a biologically inactive androgen. It is considered a marker for androgen activity in women [157], and shows no significant fluctuations with menstrual periods, pregnancy, or oral contraceptives [117,158]. AG is abundantly found in urine and blood [58], so instrumental sensitivity for quantitative analysis is not as concerning as for low abundance androgen metabolites. Also, of practical importance, normalized urinary TG (TG/AG) is a noninvasive method to phenotype UGT2B17 activity in developing children.

As described in Chapter 3, we completed targeted urinary metabolomics of androgen conjugates in urine samples of 63 pediatric subjects who were 7 to 18 years of age and followed over a period of 3 years in 7 visits (n=441). We quantified both glucuronides and sulfates for six androgens: testosterone, epitestosterone, androsterone, epiandrosterone, dihydrotestosterone, dehydroepiandrosterone (DHEA), and etiocholanolone, and examined the associations between urinary TG/AG and sex, age, and UGT2B17 CNV, which were all statistically significant. TG/AG has been shown to be promising phenotypic biomarker for UGT2B17, although further clinical validation studies using exogenous probe substrate are warranted. However, the lack of a safe, specific UGT2B17-specific probe substrate is a major obstacle in achieving this goal. Similarly, a larger sample size in pediatrics as well as adults would be necessary to confirm association of TG/AG and UGT2B17 genetic polymorphisms. If validated, use of the urinary TG/AG ratio can potentially extend beyond safety assessment in drug development and DDI studies, to investigating disease states as a prognostic or susceptibility biomarker.

The urinary TG/AG biomarker shows promising applications, but is likely more representative of hepatic UGT2B17 over intestinal UGT2B17, considering the relative systemic blood flow to each organ. Aforementioned shortcomings in investigating intestinal metabolism include limitations in current *in vitro* tools and knowledge deficits in intestinal enzyme abundances. Cryopreserved human intestinal mucosa (CHIM) is a novel *in vitro* model for studying intestinal metabolism, and is prepared with gentle tissue homogenization rather than individual enterocyte isolation in an effort to retain more functionality and some the heterogeneity in cell and tissue composition [72]. In Chapter 4, we used CHIM as a surrogate for intestinal tissue utilizing LC-MS/MS-based targeted quantitative proteomics for quantification of non-CYP enzymes including UGT2B17, after protein extraction of cytosolic and membrane

proteins. We also validated our proteomic findings using activity assays including testosterone and clopidogrel carboxylic acid (CCA) as substrates and imatinib as a UGT2B17-specific inhibitor. Two types of quantifications were performed: absolute quantifications in pmol per mg membrane or cytosolic proteins, and relative quantifications using mature enterocyte-specific marker proteins, i.e. average of villin-1 (VIL1) and sucrase isomaltase (SI) area ratios for membrane proteins, and intestinal fatty acid binding protein (FABP2) for cytosolic proteins. Absolute protein quantification showed larger intra-subject variability between intestinal regions and lots, possibly also indicating technical variability. Relative quantification revealed a comparatively smoother trend with less inter-subject overlap, suggesting intestinal regional variability may be less than interindividual variability in enzyme abundance. UGT2B17 abundance showed significant correlation with both TG formation (r^2= 0.97, p <0.001) and CAG formation from CCA (r^2= 0.86, p =0.01), and correlation with CAG formation was abolished with the addition of imatinib, a UGT inhibitor. CHIM lots are reported in protein concentrations (mg protein/mL), which are standardized for activity assays. Due to its multicellular preparation process, it may be valuable to further characterize CHIM in its proteomic content and composition, to generate a more accurate scaling factor. In particular, characterization of mature enterocyte marker proteins or possibly specific markers for other cell types may be beneficial for better understanding of the intestinal proteome and further translatability. Quantitative CHIM activity experiments coupled to proteomic assays and successful application to PBPK modeling would be a promising approach for intestinal drug metabolism prediction.

In summary, the highly variable UGT2B17 is an understudied enzyme with unknown epigenetic regulators that govern its variability. The UGT2B17 CNV has significant clinical implications, including androgen-dependent disease risk, as well as cancer-associated diseases.

TG/AG as a phenotypic biomarker shows promise, based on strong associations with sex, age, and UGT2B17 CNV, with numerous potential applications in medicine and drug development, once validated. The high abundance of intestinal UGT2B17 will be a significant factor in first pass metabolism and drug interactions for UGT2B17-specific substrates, which can be predicted using functional *in vitro* tools such as CHIM, quantitative proteomics, and PBPK modeling.

BIBLIOGRAPHY

[1] S. Oda, T. Fukami, T. Yokoi, M. Nakajima, A comprehensive review of UDP-glucuronosyltransferase and esterases for drug development, Drug Metab. Pharmacokinet. 30 (2015) 30–51. doi:10.1016/j.dmpk.2014.12.001.

[2] M. Beaulieu, E. Lévesque, D.W. Hum, A. Bélanger, Isolation and characterization of a novel cDNA encoding a human UDP-glucuronosyltransferase active on C19 steroids, J Biol Chem. 271 (1996) 22855–22862. https://www.ncbi.nlm.nih.gov/pubmed/8798464.

[3] A. Bélanger, G. Pelletier, F. Labrie, O. Barbier, S. Chouinard, Inactivation of androgens by UDP-glucuronosyltransferase enzymes in humans., Trends Endocrinol. Metab. 14 (2003) 473–9. http://www.ncbi.nlm.nih.gov/pubmed/14643063 (accessed October 2, 2018).

[4] S.G. Dubois, M. Beaulieu, E. Lévesque, D.W. Hum, A. Bélanger, Alteration of human UDP-glucuronosyltransferase UGT2B17 regio-specificity by a single amino acid substitution, J Mol Biol. 289 (1999) 29–39. doi:10.1006/jmbi.1999.2735.

[5] D. Turgeon, J.S. Carrier, S. Chouinard, A. Bélanger, Glucuronidation activity of the UGT2B17 enzyme toward xenobiotics, Drug Metab Dispos. 31 (2003) 670–676. https://www.ncbi.nlm.nih.gov/pubmed/12695357.

[6] S. Kozlovich, G. Chen, P. Lazarus, Stereospecific Metabolism of the Tobacco-Specific Nitrosamine, NNAL, Chem Res Toxicol. 28 (2015) 2112–2119. doi:10.1021/acs.chemrestox.5b00278.

[7] R.M. Balliet, G. Chen, C.J. Gallagher, R.W. Dellinger, D. Sun, P. Lazarus, Characterization of UGTs active against SAHA and association between SAHA glucuronidation activity phenotype with UGT genotype., Cancer Res. 69 (2009) 2981–9. doi:10.1158/0008-5472.CAN-08-4143.

[8] D. Sun, G. Chen, R.W. Dellinger, A.K. Sharma, P. Lazarus, Characterization of 17-dihydroexemestane glucuronidation: potential role of the UGT2B17 deletion in exemestane pharmacogenetics, Pharmacogenet Genomics. 20 (2010) 575–585. doi:10.1097/FPC.0b013e32833b04af.

[9] H. Kahma, A.M. Filppula, M. Neuvonen, E.K. Tarkiainen, A. Tornio, M.T. Holmberg, M.K. Itkonen, M. Finel, P.J. Neuvonen, M. Niemi, J.T. Backman, Clopidogrel Carboxylic Acid Glucuronidation is Mediated Mainly by UGT2B7, UGT2B4, and UGT2B17: Implications for Pharmacogenetics and Drug-Drug Interactions ., Drug Metab. Dispos. 46 (2018) 141–150. doi:10.1124/dmd.117.078162.

[10] D.K. Bhatt, A. Basit, H. Zhang, A. Gaedigk, S. Lee, K.G. Claw, A. Mehrotra, A.S. Chaudhry, R.E. Pearce, R. Gaedigk, U. Broeckel, T.A. Thornton, D.A. Nickerson, E.G. Schuetz, J. Amory, J.S. Leeder, B. Prasad, Hepatic Abundance and Activity of Androgen and Drug Metabolizing Enzyme, UGT2B17, are Associated with Genotype, Age, and Sex, Drug Metab. Dispos. (2018) dmd.118.080952. doi:10.1124/dmd.118.080952.

[11] S.A. McCarroll, T.N. Hadnott, G.H. Perry, P.C. Sabeti, M.C. Zody, J.C. Barrett, S. Dallaire, S.B. Gabriel, C. Lee, M.J. Daly, D.M. Altshuler, The International HapMap Consortium, Common deletion polymorphisms in the human genome, Nat. Genet. 38 (2006) 86–92. doi:10.1038/ng1696.

[12] Y. Xue, D. Sun, A. Daly, F. Yang, X. Zhou, M. Zhao, N. Huang, T. Zerjal, C. Lee, N.P. Carter, M.E. Hurles, C. Tyler-Smith, Adaptive evolution of UGT2B17 copy-number variation, Am. J. Hum. Genet. 83 (2008) 337–346. doi:10.1016/j.ajhg.2008.08.004.

[13] J.-P. Emond, A. Labriet, S. Desjardins, M. Rouleau, L. Villeneuve, H. Hovington, H. Brisson, L. Lacombe, D. Simonyan, P. Caron, M. Perigny, B. Tetu, J.K. Fallon, K. Klein, P.C. Smith, U. Zanger, C. Guillemette, E. Levesque, Factors Affecting Interindividual Variability of Hepatic UGT2B17 Protein Expression Examined Using a Novel Specific Monoclonal Antibody., Drug Metab. Dispos. (2019) dmd.119.086330. doi:10.1124/dmd.119.086330.

[14] S. Chouinard, M.-F.F. Yueh, R.H. Tukey, F. Giton, J. Fiet, G. Pelletier, O. Barbier, A. Bélanger, Inactivation by UDP-glucuronosyltransferase enzymes: the end of androgen signaling, J Steroid Biochem Mol Biol. 109 (2008) 247–253. doi:10.1016/j.jsbmb.2008.03.016.

[15] O. Barbier, A. Bélanger, Inactivation of androgens by UDP-glucuronosyltransferases in the human prostate, Best Pr. Res Clin Endocrinol Metab. 22 (2008) 259–270. doi:10.1016/j.beem.2008.01.001.

[16] O. Barbier, H. Lapointe, M. El Alfy, D.W. Hum, A. Bélanger, Cellular localization of uridine diphosphoglucuronosyltransferase 2B enzymes in the human prostate by in situ hybridization and immunohistochemistry, J Clin Endocrinol Metab. 85 (2000) 4819–4826. doi:10.1210/jcem.85.12.7019.

[17] N.R. Jones, P. Lazarus, UGT2B gene expression analysis in multiple tobacco carcinogen-targeted tissues, Drug Metab Dispos. 42 (2014) 529–536. doi:10.1124/dmd.113.054718.

[18] Y. Sato, M. Nagata, K. Tetsuka, K. Tamura, A. Miyashita, A. Kawamura, T. Usui, Optimized methods for targeted peptide-based quantification of human uridine 5'-diphosphate-glucuronosyltransferases in biological specimens using liquid chromatography-tandem mass spectrometry., Drug Metab. Dispos. 42 (2014) 885–9. doi:10.1124/dmd.113.056291.

[19] J.C.C. Stingl, H. Bartels, R. Viviani, M.L.L. Lehmann, J. Brockmöller, Relevance of UDP-glucuronosyltransferase polymorphisms for drug dosing: A quantitative systematic review, 2014. doi:10.1016/j.pharmthera.2013.09.002.

[20] T. Kuuranne, M. Saugy, N. Baume, Confounding factors and genetic polymorphism in the evaluation of individual steroid profiling., Br. J. Sports Med. 48 (2014) 848–55. doi:10.1136/bjsports-2014-093510.

[21] U. Mareck, H. Geyer, G. Fusshöller, A. Schwenke, N. Haenelt, T. Piper, M. Thevis, W. Schänzer, Reporting and managing elevated testosterone/epitestosterone ratios--novel aspects after five years' experience, Drug Test Anal. 2 (2010) 637–642. doi:10.1002/dta.234.

[22] J. Jakobsson, L. Ekström, N. Inotsume, M. Garle, M. Lorentzon, C. Ohlsson, H.K. Roh, K. Carlström, A. Rane, Large differences in testosterone excretion in Korean and Swedish men are strongly associated with a UDP-glucuronosyl transferase 2B17 polymorphism, J Clin Endocrinol Metab. 91 (2006) 687–693. doi:10.1210/jc.2005-1643.

[23] P. Martín-Escudero, J. Muñoz-Guerra, N. Del Prado, M. Galindo Canales, M. Fuentes Ferrer, S. Vargas, A.B. Soldevilla, E. Serrano-Garde, F. Miguel-Tobal, M. de Las Casas, C. Fernandez-Pérez, Impact of UGT2B17 gene deletion on the steroid profile of an athlete, Physiol Rep. 3 (2015). doi:10.14814/phy2.12645.

[24] J.J. Schulze, J. Lundmark, M. Garle, I. Skilving, L. Ekström, A. Rane, Doping test results dependent on genotype of uridine diphospho-glucuronosyl transferase 2B17, the major enzyme for testosterone glucuronidation, J Clin Endocrinol Metab. 93 (2008) 2500–2506. doi:10.1210/jc.2008-0218.

[25] E. Strahm, J.E. Mullen, N. Gårevik, M. Ericsson, J.J. Schulze, A. Rane, L. Ekström, Dose-dependent testosterone sensitivity of the steroidal passport and GC-C-IRMS analysis in relation to the UGT2B17 deletion polymorphism, Drug Test. Anal. 7 (2015) 1063–1070. doi:10.1002/dta.1841.

[26] L. Cai, W. Huang, K.C. Chou, Prostate cancer with variants in CYP17 and UGT2B17 genes: a meta-analysis, Protein Pept Lett. 19 (2012) 62–69. https://www.ncbi.nlm.nih.gov/pubmed/21919858.

[27] M.A. Kpoghomou, J.E. Soatiana, F.W. Kalembo, G. Bishwajit, W. Sheng, UGT2B17 Polymorphism and Risk of Prostate Cancer: A Meta-Analysis, ISRN Oncol. 2013 (2013) 465916. doi:10.1155/2013/465916.

[28] L. Gauthier-Landry, A. Bélanger, O. Barbier, Multiple roles for UDP-glucuronosyltransferase (UGT)2B15 and UGT2B17 enzymes in androgen metabolism and prostate cancer evolution, J Steroid Biochem Mol Biol. 145 (2015) 187–192. doi:10.1016/j.jsbmb.2014.05.009.

[29] C. Swanson, D. Mellström, M. Lorentzon, L. Vandenput, J. Jakobsson, A. Rane, M. Karlsson, O. Ljunggren, U. Smith, A.L. Eriksson, A. Bélanger, F. Labrie, C. Ohlsson, The uridine diphosphate glucuronosyltransferase 2B15 D85Y and 2B17 deletion polymorphisms predict the glucuronidation pattern of androgens and fat mass in men, J Clin Endocrinol Metab. 92 (2007) 4878–4882. doi:10.1210/jc.2007-0359.

[30] A.Z. Zhu, L.S. Cox, J.S. Ahluwalia, C.C. Renner, D.K. Hatsukami, N.L. Benowitz, R.F. Tyndale, Genetic and phenotypic variation in UGT2B17, a testosterone-metabolizing enzyme, is associated with BMI in males, Pharmacogenet Genomics. 25 (2015) 263–269. doi:10.1097/FPC.0000000000000135.

[31] S. Chew, B.H. Mullin, J.R. Lewis, T.D. Spector, R.L. Prince, S.G. Wilson, Homozygous deletion of the UGT2B17 gene is not associated with osteoporosis risk in elderly Caucasian women, Osteoporos Int. 22 (2011) 1981–1986. doi:10.1007/s00198-010-1405-0.

[32] M. Yokota, A. Hirasawa, K. Makita, T. Akahane, K. Sakai, T. Makabe, Y. Horiba, W. Yamagami, M. Ogawa, T. Iwata, S. Yanamoto, R. Deshimaru, K. Banno, N. Susumu, D. Aoki, Polymorphisms of estrogen metabolism-related genes ESR1, UGT2B17, and UGT1A1 are not associated with osteoporosis in surgically menopausal Japanese women, Prz Menopauzalny. 14 (2015) 161–167. doi:10.5114/pm.2015.54339.

[33] S. Giroux, J. Bussières, A. Bureau, F. Rousseau, UGT2B17 gene deletion associated with an increase in bone mineral density similar to the effect of hormone replacement in postmenopausal women, Osteoporos Int. 23 (2012) 1163–1170. doi:10.1007/s00198-011-1662-6.

[34] T.L. Yang, X.D. Chen, Y. Guo, S.F. Lei, J.T. Wang, Q. Zhou, F. Pan, Y. Chen, Z.X. Zhang, S.S. Dong, X.H. Xu, H. Yan, X. Liu, C. Qiu, X.Z. Zhu, T. Chen, M. Li, H. Zhang, L. Zhang, B.M. Drees, J.J. Hamilton, C.J. Papasian, R.R. Recker, X.P. Song, J. Cheng, H.W. Deng, Genome-wide copy-number-variation study identified a susceptibility gene, UGT2B17, for osteoporosis, Am J Hum Genet. 83 (2008) 663–674. doi:10.1016/j.ajhg.2008.10.006.

[35] R.C. Petering, N.A. Brooks, Testosterone Therapy: Review of Clinical Applications., Am. Fam. Physician. 96 (2017) 441–449.

http://www.ncbi.nlm.nih.gov/pubmed/29094914 (accessed December 17, 2019).

[36] X. Che, D. Yu, Z. Wu, J. Zhang, Y. Chen, Y. Han, C. Wang, J. Qi, Association of Genetic Polymorphisms in UDP-Glucuronosyltransferases 2B17 with the Risk of Pancreatic Cancer in Chinese Han Population, Clin Lab. 61 (2015) 1905–1910. http://www.ncbi.nlm.nih.gov/pubmed/26882814 (accessed May 22, 2018).

[37] E. Eskandari-Nasab, M. Hashemi, H. Rezaei, A. Fazaeli, M.A. Mashhadi, S.S. Moghaddam, F. Arbabi, M. Jahantigh, M. Taheri, Evaluation of UDP-glucuronosyltransferase 2B17 (UGT2B17) and dihydrofolate reductase (DHFR) genes deletion and the expression level of NGX6 mRNA in breast cancer, Mol Biol Rep. 39 (2012) 10531–10539. doi:10.1007/s11033-012-1938-8.

[38] A.Y. Angstadt, A. Berg, J. Zhu, P. Miller, T.J. Hartman, S.M. Lesko, J.E. Muscat, P. Lazarus, C.J. Gallagher, The effect of copy number variation in the phase II detoxification genes UGT2B17 and UGT2B28 on colorectal cancer risk, Cancer. 119 (2013) 2477–2485. doi:10.1002/cncr.28009.

[39] C.J. Gallagher, J.E. Muscat, A.N. Hicks, Y. Zheng, A.-M.M. Dyer, G.A. Chase, J. Richie, P. Lazarus, The UDP-glucuronosyltransferase 2B17 gene deletion polymorphism: sex-specific association with urinary 4-(methylnitrosamino)-1-(3-pyridyl)-1-butanol glucuronidation phenotype and risk for lung cancer, Cancer Epidemiol Biomarkers Prev. 16 (2007) 823–828. doi:10.1158/1055-9965.EPI-06-0823.

[40] M. Gruber, T. Le, M. Filipits, A. Gsur, C. Mannhalter, U. Jäger, K. Vanura, UDP-glucuronosyltransferase 2B17 genotype and the risk of lung cancer among Austrian Caucasians, Cancer Epidemiol. 37 (2013) 625–628. doi:10.1016/j.canep.2013.06.004.

[41] S. Ishimaru, Y. Yuza, T. Kaneko, M. Urashima, Effect of UGT2B17 deletion polymorphism on prognosis in pediatric cancer, Pediatr Int. 59 (2017) 427–431. doi:10.1111/ped.13198.

[42] M. Gruber, J. Bellemare, G. Hoermann, A. Gleiss, E. Porpaczy, M. Bilban, T. Le, S. Zehetmayer, C. Mannhalter, A. Gaiger, M. Shehata, K. Fleiss, C. Skrabs, É. Lévesque, K. Vanura, C. Guillemette, U. Jaeger, Overexpression of uridine diphospho glucuronosyltransferase 2B17 in high-risk chronic lymphocytic leukemia, Blood. 121 (2013) 1175–1183. doi:10.1182/blood-2012-08-447359.

[43] E.P. Allain, K. Venzl, P. Caron, V. Turcotte, D. Simonyan, M. Gruber, T. Le, E. Lévesque, C. Guillemette, K. Vanura, Sex-dependent association of circulating sex steroids and pituitary hormones with treatment-free survival in chronic lymphocytic leukemia patients, Ann. Hematol. (2018). doi:10.1007/s00277-018-3356-z.

[44] M. Murata, E.H. Warren, S.R. Riddell, A human minor histocompatibility antigen resulting from differential expression due to a gene deletion, J Exp Med. 197 (2003) 1279–1289. doi:10.1084/jem.20030044.

[45] S. Jervis, P. Collins, D. Tate, L. Foster, V. Bowman, C. Adhern, A. Bloor, J. Yin, R. Wynn, K. Poulton, Increased severity of acute graft versus host disease as a result of differential expression following a homozygous gene deletion, Int J Immunogenet. 40 (2013) 116–119. doi:10.1111/j.1744-313X.2012.01138.x.

[46] N. Santos, R. Rodríguez-Romanos, J.B. Nieto, I. Buño, C. Vallejo, A. Jiménez-Velasco, S. Brunet, E. Buces, J. López-Jiménez, M. González, C. Ferrá, A. Sampol, R. de la Cámara, C. Martínez, D. Gallardo, G.W.P. of the S.G. of H.T. (GETH), UGT2B17 minor histocompatibility mismatch and clinical outcome after HLA-identical sibling donor stem cell transplantation, Bone Marrow Transpl. 51 (2016) 79–82. doi:10.1038/bmt.2015.207.

[47] M.J. Martínez-Bravo, C. Calderón-Cabrera, F.J. Márquez-Malaver, N. Rodríguez, M. Guijarro, I. Espigado, A. Núñez-Roldán, J.A. Pérez-Simón, I. Aguilera, Mismatch on glutathione S-transferase T1 increases the risk of graft-versus-host disease and mortality after allogeneic stem cell transplantation, Biol Blood Marrow Transpl. 20 (2014) 1356–1362. doi:10.1016/j.bbmt.2014.05.008.

[48] Shen, Kunze, Thummel, Enzyme-catalyzed processes of first-pass hepatic and intestinal drug extraction., Adv. Drug Deliv. Rev. 27 (1997) 99–127. doi:10.1016/s0169-409x(97)00039-2.

[49] C.R. Jones, O.J.D. Hatley, A.-L. Ungell, C. Hilgendorf, S.A. Peters, A. Rostami-Hodjegan, Gut Wall Metabolism. Application of Pre-Clinical Models for the Prediction of Human Drug Absorption and First-Pass Elimination, AAPS J. 18 (2016) 589–604. doi:10.1208/s12248-016-9889-y.

[50] Y.H. Wang, M. Trucksis, J.J. McElwee, P.H. Wong, C. Maciolek, C.D. Thompson, T. Prueksaritanont, G.C. Garrett, R. Declercq, E. Vets, K.J. Willson, R.C. Smith, J.A. Klappenbach, G.J. Opiteck, J.A. Tsou, C. Gibson, T. Laethem, P. Panorchan, M. Iwamoto, P.M. Shaw, J.A. Wagner, J.C. Harrelson, UGT2B17 genetic polymorphisms dramatically affect the pharmacokinetics of MK-7246 in healthy subjects in a first-in-human study, Clin Pharmacol Ther. 92 (2012) 96–102. doi:10.1038/clpt.2012.20.

[51] J.J. Shoskes, M.K. Wilson, M.L. Spinner, Pharmacology of testosterone replacement therapy preparations, Transl. Androl. Urol. 5 (2016) 834–843. doi:10.21037/tau.2016.07.10.

[52] E. Nieschlag, J. Mauss, A. Coert, P. Kićović, Plasma androgen levels in men after oral administration of testosterone or testosterone undecanoate., Acta Endocrinol. (Copenh). 79 (1975) 366–74. http://www.ncbi.nlm.nih.gov/pubmed/1173495 (accessed June 5, 2018).

[53] P.R. Daggett, M.J. Wheeler, J.D. Nabarro, Oral testosterone, a reappraisal., Horm. Res. 9 (1978) 121–9. doi:10.1159/000178904.

[54] Y. Ma, Y. Fu, S.C. Khojasteh, D. Dalvie, D. Zhang, Glucuronides as Potential Anionic Substrates of Human Cytochrome P450 2C8 (CYP2C8), J. Med. Chem. 60 (2017) 8691–8705. doi:10.1021/acs.jmedchem.7b00510.

[55] S.-J. Kim, T. Yoshikado, I. Ieiri, K. Maeda, M. Kimura, S. Irie, H. Kusuhara, Y. Sugiyama, Clarification of the Mechanism of Clopidogrel-Mediated Drug-Drug Interaction in a Clinical Cassette Small-dose Study and Its Prediction Based on In Vitro Information., Drug Metab. Dispos. 44 (2016) 1622–32. doi:10.1124/dmd.116.070276.

[56] A. Tornio, A.M. Filppula, O. Kailari, M. Neuvonen, T.H. Nyrönen, T. Tapaninen, P.J. Neuvonen, M. Niemi, J.T. Backman, Glucuronidation converts clopidogrel to a strong time-dependent inhibitor of CYP2C8: a phase II metabolite as a perpetrator of drug-drug interactions., Clin. Pharmacol. Ther. 96 (2014) 498–507. doi:10.1038/clpt.2014.141.

[57] S.N. Savu, L. Silvestro, M. Surmeian, L. Remis, Y. Rasit, S.R. Savu, C. Mircioiu, Evaluation of Clopidogrel Conjugation Metabolism: PK Studies in Man and Mice of Clopidogrel Acyl Glucuronide., Drug Metab. Dispos. 44 (2016) 1490–7. doi:10.1124/dmd.116.071092.

[58] L. Schiffer, W. Arlt, K.H. Storbeck, Intracrine androgen biosynthesis, metabolism and action revisited, Mol. Cell. Endocrinol. (2017). doi:10.1016/j.mce.2017.08.016.

[59] W. Wilson, F. de Villena, B.D. Lyn-Cook, P.K. Chatterjee, T.A. Bell, D.A. Detwiler, R.C. Gilmore, I.C. Valladeras, C.C. Wright, D.W. Threadgill, D.J. Grant, Characterization of a common deletion polymorphism of the UGT2B17 gene linked to UGT2B15, Genomics. 84 (2004) 707–714. doi:10.1016/j.ygeno.2004.06.011.

[60] A. Basit, J.K. Amory, B. Prasad, Effect of Dose and 5α-Reductase Inhibition on the Circulating Testosterone Metabolite Profile of Men Administered Oral Testosterone, Clin. Transl. Sci. (2018). doi:10.1111/cts.12569.

[61] D.B. Goldstein, G.L. Cavalleri, Genomics: understanding human diversity., Nature. 437 (2005) 1241–2. doi:10.1038/4371241a.

[62] C.-X. Xue, X.-M. He, D.-H. Zou, Glutathione S-transferase M1 Polymorphism and Breast Cancer Risk: a Meta-Analysis in the Chinese Population., Clin. Lab. 62 (2016) 2277–2284. doi:10.7754/Clin.Lab.2016.160333.

[63] C. Ramos Hernández, C. Mouronte-Roibás, J.M. Barros-Dios, A. Fernández-Villar, A. Ruano-Ravina, Deletion of GSTM1 and GSTT1 genes and lung cancer survival: a systematic review., Tumori. 103 (2017) 338–344. doi:10.5301/tj.5000621.

[64] A. Gaedigk, K. Sangkuhl, M. Whirl-Carrillo, T. Klein, J.S. Leeder, Prediction of CYP2D6 phenotype from genotype across world populations, Genet. Med. 19 (2017) 69–76. doi:10.1038/gim.2016.80.

[65] F.-N.B.W. Group, BEST (Biomarkers, EndpointS, and other Tools) Resource, Food and Drug Administration (US), 2016. http://www.ncbi.nlm.nih.gov/pubmed/27010052 (accessed May 13, 2019).

[66] O.J.D. Hatley, C.R. Jones, A. Galetin, A. Rostami-Hodjegan, Quantifying gut wall metabolism: methodology matters., Biopharm. Drug Dispos. 38 (2017) 155–160. doi:10.1002/bdd.2062.

[67] B.T. Gufford, G. Chen, P. Lazarus, T.N. Graf, N.H. Oberlies, M.F. Paine, Identification of diet-derived constituents as potent inhibitors of intestinal glucuronidation., Drug Metab. Dispos. 42 (2014) 1675–83. doi:10.1124/dmd.114.059451.

[68] G. Yang, S. Ge, R. Singh, S. Basu, K. Shatzer, M. Zen, J. Liu, Y. Tu, C. Zhang, J. Wei, J. Shi, L. Zhu, Z. Liu, Y. Wang, S. Gao, M. Hu, Glucuronidation: driving factors and their impact on glucuronide disposition., Drug Metab. Rev. 49 (2017) 105–138. doi:10.1080/03602532.2017.1293682.

[69] J.A. Williams, R. Hyland, B.C. Jones, D.A. Smith, S. Hurst, T.C. Goosen, V. Peterkin, J.R. Koup, S.E. Ball, Drug-drug interactions for UDP-glucuronosyltransferase substrates: a pharmacokinetic explanation for typically observed low exposure (AUCi/AUC) ratios., Drug Metab. Dispos. 32 (2004) 1201–8. doi:10.1124/dmd.104.000794.

[70] M. Li, I.A.M. de Graaf, G.M.M. Groothuis, Precision-cut intestinal slices: alternative model for drug transport, metabolism, and toxicology research, Expert Opin. Drug Metab. Toxicol. 12 (2016) 175–190. doi:10.1517/17425255.2016.1125882.

[71] M.-C.D. Ho, N. Ring, K. Amaral, U. Doshi, A.P. Li, Human Enterocytes as an In Vitro Model for the Evaluation of Intestinal Drug Metabolism: Characterization of Drug-Metabolizing Enzyme Activities of Cryopreserved Human Enterocytes from Twenty-Four Donors, Drug Metab. Dispos. 45 (2017) 686–691. doi:10.1124/dmd.116.074377.

[72] A.P. Li, N. Alam, kirsten Amaral, M.-C.D. Ho, C. Loretz, W. Mitchell, Q. Yang, Cryopreserved human intestinal mucosal epithelium: a novel in vitro experimental system for the evaluation of enteric drug metabolism, P450 induction, and enterotoxicity, Drug Metab. Dispos. (2018) dmd.118.082875. doi:10.1124/dmd.118.082875.

[73] D.K. Bhatt, A. Mehrotra, A. Gaedigk, R. Chapa, A. Basit, H. Zhang, P. Choudhari, M. Boberg, R.E. Pearce, R. Gaedigk, U. Broeckel, J.S. Leeder, B. Prasad, Age- and Genotype-Dependent Variability in the Protein Abundance and Activity of Six Major Uridine Diphosphate-Glucuronosyltransferases in Human Liver., Clin. Pharmacol. Ther. (2018). doi:10.1002/cpt.1109.

[74] B. Prasad, M. Vrana, A. Mehrotra, K. Johnson, D.K. Bhatt, The Promises of Quantitative Proteomics in Precision Medicine, J. Pharm. Sci. 106 (2017) 738–744. doi:10.1016/j.xphs.2016.11.017.

[75] D.K. Bhatt, B. Prasad, Critical Issues and Optimized Practices in Quantification of Protein Abundance Level to Determine Interindividual Variability in DMET Proteins by LC-MS/MS Proteomics, Clin Pharmacol Ther. (2017). doi:10.1002/cpt.819.

[76] P.M. Escudero, J.A. Muñoz-Guerra, S.V. García-Tenorio, E.S. Garde, A.B.S. Navarro, M.G. Canales, N. Prado, M.E.F. Ferrer, C.F. Pérez, Impact of the UGT2B17 polymorphism on the steroid profile. Results of a crossover clinical trial in athletes submitted to testosterone administration, Steroids. (2018). doi:10.1016/J.STEROIDS.2018.11.009.

[77] A. Mouritsen, A.S. Busch, L. Aksglaede, E. Rajpert-De Meyts, A. Juul, Deletion in the uridine diphosphate glucuronyltransferase 2B17 gene is associated with delayed pubarche in healthy boys., Endocr. Connect. 7 (2018) 460–465. doi:10.1530/EC-18-0080.

[78] N.S. Wong, E.Z.. Seah, L.Z. Wang, W.L. Yeo, H.L. Yap, B. Chuah, Y.W. Lim, P.C. Ang, B.C. Tai, R. Lim, B.C. Goh, S.C. Lee, Impact of UDP-gluconoryltransferase 2B17 genotype on vorinostat metabolism and clinical outcomes in Asian women with breast cancer, Pharmacogenet Genomics. 21 (2011) 760–768. doi:10.1097/FPC.0b013e32834a8639.

[79] H. Johansson, V. Aristarco, S. Gandini, J. Gjerde, D. Macis, A. Guerrieri-Gonzaga, D. Serrano, M. Lazzeroni, A. Rajasekaran, C. V Williard, G. Mellgren, A. DeCensi, B. Bonanni, Prognostic impact of genetic variants of CYP19A1 and UGT2B17 in a randomized trial for endocrine-responsive postmenopausal breast cancer, Pharmacogenomics J. (2019). doi:10.1038/s41397-019-0087-z.

[80] S. Luo, G. Chen, C. Truica, C.C. Baird, K. Leitzel, P. Lazarus, Role of the UGT2B17 deletion in exemestane pharmacogenetics, Pharmacogenomics J. (2017). doi:10.1038/tpj.2017.18.

[81] G. Chen, S. Luo, S. Kozlovich, P. Lazarus, Association between Glucuronidation Genotypes and Urinary NNAL Metabolic Phenotypes in Smokers, Cancer Epidemiol Biomarkers Prev. 25 (2016) 1175–1184. doi:10.1158/1055-9965.EPI-15-1245.

[82] T.C. Cheetham, J. An, S.J. Jacobsen, F. Niu, S. Sidney, C.P. Quesenberry, S.K. VanDenEeden, Association of Testosterone Replacement With Cardiovascular Outcomes Among Men With Androgen Deficiency, JAMA Intern. Med. 177 (2017) 491. doi:10.1001/jamainternmed.2016.9546.

[83] A.M. Pavlatos, O. Fultz, M.J. Monberg, A. Vootkur, Pharmd, Review of oxymetholone: a 17alpha-alkylated anabolic-androgenic steroid., Clin. Ther. 23 (2001) 789–801; discussion 771. http://www.ncbi.nlm.nih.gov/pubmed/11440282 (accessed June 5, 2018).

[84] D. Westaby, S.J. Ogle, F.J. Paradinas, J.B. Randell, I.M. Murray-Lyon, Liver damage from long-term methyltestosterone., Lancet (London, England). 2 (1977) 262–3. http://www.ncbi.nlm.nih.gov/pubmed/69876 (accessed June 5, 2018).

[85] A. Morales, A.J. Bella, S. Chun, J. Lee, P. Assimakopoulos, R. Bebb, I. Gottesman, P. Alarie, H. Dugré, S. Elliott, A practical guide to diagnosis, management and treatment of testosterone deficiency for Canadian physicians., Can. Urol. Assoc. J. 4 (2010) 269–75. http://www.ncbi.nlm.nih.gov/pubmed/20694106 (accessed June 7, 2018).

[86] L.J. Gooren, A ten-year safety study of the oral androgen testosterone undecanoate., J. Androl. 15 (n.d.) 212–5. http://www.ncbi.nlm.nih.gov/pubmed/7928661 (accessed June 5, 2018).

[87] P. Franchimont, P.M. Kicovic, A. Mattei, R. Roulier, Effects of oral testosterone undecanoate in hypogonadal male patients., Clin. Endocrinol. (Oxf). 9 (1978) 313–20. http://www.ncbi.nlm.nih.gov/pubmed/102469 (accessed June 5, 2018).

[88] U. Täuber, K. Schröder, B. Düsterberg, H. Matthes, Absolute bioavailability of testosterone after oral administration of testosterone-undecanoate and testosterone., Eur. J. Drug Metab. Pharmacokinet. 11 (n.d.) 145–9. http://www.ncbi.nlm.nih.gov/pubmed/3770015 (accessed May 16, 2018).

[89] A.A. SANDBERG, W.R. SLAUNWHITE, Metabolism of 4-C14-testosterone in human subjects. I. Distribution in bile, blood, feces and urine., J. Clin. Invest. 35 (1956) 1331–9. doi:10.1172/JCI103389.

[90] K.E. Thummel, Gut instincts: CYP3A4 and intestinal drug metabolism., J. Clin. Invest. 117 (2007) 3173–6. doi:10.1172/JCI34007.

[91] T. Sano, G. Hirasawa, J. Takeyama, A.D. Darnel, T. Suzuki, T. Moriya, K. Kato, H. Sekine, S. Ohara, T. Shimosegawa, J. Nakamura, M. Yoshihama, N. Harada, H. Sasano, 17 beta-Hydroxysteroid dehydrogenase type 2 expression and enzyme activity in the human gastrointestinal tract., Clin. Sci. (Lond). 101 (2001) 485–91. http://www.ncbi.nlm.nih.gov/pubmed/11672453 (accessed January 18, 2018).

[92] Z. Riches, E.L. Stanley, J.C. Bloomer, M.W.H. Coughtrie, Quantitative Evaluation of the Expression and Activity of Five Major Sulfotransferases (SULTs) in Human Tissues: The SULT "Pie", Drug Metab. Dispos. 37 (2009) 2255–2261. doi:10.1124/dmd.109.028399.

[93] H.-C.C. Shin, H.-R.R. Kim, H.-J.J. Cho, H. Yi, S.-M.M. Cho, D.-G.G. Lee, A.M. Abd El-Aty, J.-S.S. Kim, D. Sun, G.L. Amidon, Comparative gene expression of intestinal metabolizing enzymes, Biopharm Drug Dispos. 30 (2009) 411–421. doi:10.1002/bdd.675.

[94] M. Xu, D.K. Bhatt, C.K. Yeung, K.G. Claw, A.S. Chaudhry, A. Gaedigk, R.E. Pearce, U. Broeckel, R. Gaedigk, D.A. Nickerson, E. Schuetz, A.E. Rettie, S. Leeder, K.E. Thummel, B. Prasad, J.S. Leeder, K.E. Thummel, B. Prasad, Genetic and Non-genetic Factors Associated with Protein Abundance of Flavin-containing Monooxygenase 3 in Human Liver, J Pharmacol Exp Ther. 363 (2017) 265–274. doi:10.1124/jpet.117.243113.

[95] D. Busch, A. Fritz, L.I. Partecke, C.-D. Heidecke, S. Oswald, LC–MS/MS method for the simultaneous quantification of intestinal CYP and UGT activity, J. Pharm. Biomed. Anal. 155 (2018) 194–201. doi:10.1016/J.JPBA.2018.04.003.

[96] M. Drozdzik, D. Busch, J. Lapczuk, J. Müller, M. Ostrowski, M. Kurzawski, S. Oswald, Protein Abundance of Clinically Relevant Drug-Metabolizing Enzymes in the Human Liver and Intestine: A Comparative Analysis in Paired Tissue Specimens., Clin. Pharmacol. Ther. (2017). doi:10.1002/cpt.967.

[97] C. Gröer, D. Busch, M. Patrzyk, K. Beyer, A. Busemann, C.D. Heidecke, M. Drozdzik, W. Siegmund, S. Oswald, Absolute protein quantification of clinically relevant cytochrome P450 enzymes and UDP-glucuronosyltransferases by mass spectrometry-based targeted proteomics, J. Pharm. Biomed. Anal. 100 (2014) 393–401. https://www.sciencedirect.com/science/article/pii/S0731708514004002 (accessed January 26, 2018).

[98] N. Zhang, Y. Liu, H. Jeong, Drug-Drug Interaction Potentials of Tyrosine Kinase Inhibitors via Inhibition of UDP-Glucuronosyltransferases, Sci Rep. 5 (2015) 17778. doi:10.1038/srep17778.

[99] E. Miyauchi, M. Tachikawa, X. Declèves, Y. Uchida, J.-L.L. Bouillot, C. Poitou, J.-M.M. Oppert, S. Mouly, J.-F.F. Bergmann, T. Terasaki, J.-M.M. Scherrmann, C. Lloret-Linares, Quantitative Atlas of Cytochrome P450, UDP-Glucuronosyltransferase, and Transporter Proteins in Jejunum of Morbidly Obese Subjects, Mol Pharm. 13 (2016) 2631–2640. doi:10.1021/acs.molpharmaceut.6b00085.

[100] Z. Yan, S. Wong, J. Kelly, H. Le, N. Liu, M. Kosaka, S. Tey, P. Vuong, A. Li, Utility of Pooled Cryopreserved Human Enterocytes as An In Vitro Model for Assessing Intestinal Clearance and Drug-Drug Interactions, Drug Metab. Lett. 12 (2017). doi:10.2174/1872312812666171213114422.

[101] M.M. Miettinen, M. V Mustonen, M.H. Poutanen, V. V Isomaa, R.K. Vihko, Human 17 beta-hydroxysteroid dehydrogenase type 1 and type 2 isoenzymes have opposite activities in cultured cells and characteristic cell- and tissue-specific expression., Biochem. J. 314 (Pt 3) (1996) 839–45. http://www.ncbi.nlm.nih.gov/pubmed/8615778 (accessed April 3, 2018).

[102] J. Takeyama, T. Suzuki, G. Hirasawa, Y. Muramatsu, H. Nagura, K. Iinuma, J. Nakamura, K. Kimura, M. Yoshihama, N. Harada, S. Andersson, H. Sasano, 17β-Hydroxysteroid Dehydrogenase Type 1 and 2 Expression in the Human Fetus [1], J. Clin. Endocrinol. Metab. 85 (2000) 410–416. doi:10.1210/jcem.85.1.6323.

[103] T. Sten, I. Bichlmaier, T. Kuuranne, A. Leinonen, J. Yli-Kauhaluoma, M. Finel, UDP-glucuronosyltransferases (UGTs) 2B7 and UGT2B17 display converse specificity in testosterone and epitestosterone glucuronidation, whereas UGT2A1 conjugates both androgens similarly, Drug Metab Dispos. 37 (2009) 417–423. doi:10.1124/dmd.108.024844.

[104] B.C. Lewis, P.I. Mackenzie, D.J. Elliot, B. Burchell, C.R. Bhasker, J.O. Miners, Amino terminal domains of human UDP-glucuronosyltransferases (UGT) 2B7 and 2B15 associated with substrate selectivity and autoactivation., Biochem. Pharmacol. 73 (2007) 1463–73. doi:10.1016/j.bcp.2006.12.021.

[105] J.-Z. Ji, B.-B. Huang, T.-T. Gu, T. Tai, H. Zhou, Y.-M. Jia, Q.-Y. Mi, M.-R. Zhang, H.-G. Xie, Human UGT2B7 is the major isoform responsible for the glucuronidation of clopidogrel carboxylate, Biopharm. Drug Dispos. (2018). doi:10.1002/bdd.2117.

[106] J. Clavell-Hernández, R. Wang, Emerging Evidences in the Long Standing Controversy Regarding Testosterone Replacement Therapy and Cardiovascular Events, World J. Mens. Health. 36 (2018) 92. doi:10.5534/wjmh.17050.

[107] O.J. Ponce, G. Spencer-Bonilla, N. Alvarez-Villalobos, V. Serrano, N. Singh-Ospina, R. Rodriguez-Gutierrez, A. Salcido-Montenegro, R. Benkhadra, L.J. Prokop, S. Bhasin, J.P. Brito, The Efficacy and Adverse Events of Testosterone Replacement Therapy in

Hypogonadal Men: A Systematic Review and Meta-Analysis of Randomized, Placebo-Controlled Trials, J. Clin. Endocrinol. Metab. 103 (2018) 1745–1754. doi:10.1210/jc.2018-00404.

[108] R. Vigen, C.I. O'Donnell, A.E. Barón, G.K. Grunwald, T.M. Maddox, S.M. Bradley, A. Barqawi, G. Woning, M.E. Wierman, M.E. Plomondon, J.S. Rumsfeld, P.M. Ho, Association of testosterone therapy with mortality, myocardial infarction, and stroke in men with low testosterone levels., JAMA. 310 (2013) 1829–36. doi:10.1001/jama.2013.280386.

[109] H. Zhang, A. Basit, D. Busch, K. Yabut, D.K. Bhatt, M. Drozdzik, M. Ostrowski, A. Li, C. Collins, S. Oswald, B. Prasad, Quantitative characterization of UDP-glucuronosyltransferase 2B17 in human liver and intestine and its role in testosterone first-pass metabolism, Biochem. Pharmacol. 156 (2018) 32–42. doi:10.1016/j.bcp.2018.08.003.

[110] D.K. Bhatt, A. Basit, H. Zhang, A. Gaedigk, S.-B. Lee, K.G. Claw, A. Mehrotra, A.S. Chaudhry, R.E. Pearce, R. Gaedigk, U. Broeckel, T.A. Thornton, D.A. Nickerson, E.G. Schuetz, J.K. Amory, J.S. Leeder, B. Prasad, Hepatic Abundance and Activity of Androgen- and Drug-Metabolizing Enzyme UGT2B17 Are Associated with Genotype, Age, and Sex., Drug Metab. Dispos. 46 (2018) 888–896. doi:10.1124/dmd.118.080952.

[111] D.W. Hum, A. Bélanger, E. Lévesque, O. Barbier, M. Beaulieu, C. Albert, M. Vallée, C. Guillemette, A. Tchernof, D. Turgeon, S. Dubois, Characterization of UDP-glucuronosyltransferases active on steroid hormones, J Steroid Biochem Mol Biol. 69 (1999) 413–423. https://www.ncbi.nlm.nih.gov/pubmed/10419020.

[112] D. Turgeon, J.S. Carrier, E. Lévesque, D.W. Hum, A. Bélanger, Relative enzymatic activity, protein stability, and tissue distribution of human steroid-metabolizing UGT2B subfamily members, Endocrinology. 142 (2001) 778–787. doi:10.1210/endo.142.2.7958.

[113] C. Xie, X. Gao, D. Sun, Y. Zhang, K.W. Krausz, X. Qin, F. Gonzalez, Metabolic profiling of the novel HIF2α inhibitor PT2385 in vivo and in vitro, Drug Metab. Dispos. (2018) dmd.117.079723. doi:10.1124/dmd.117.079723.

[114] S.M. Chen, D.H. Atchley, M.A. Murphy, B.J. Gurley, L.K. Kamdem, Impact of UGT2B17 Gene Deletion on the Pharmacokinetics of 17-Hydroexemestane in Healthy Volunteers, J Clin Pharmacol. 56 (2016) 875–884. doi:10.1002/jcph.673.

[115] Y. Lai, S. Mandlekar, H. Shen, V.K. Holenarsipur, R. Langish, P. Rajanna, S. Murugesan, N. Gaud, S. Selvam, O. Date, Y. Cheng, P. Shipkova, J. Dai, W.G. Humphreys, P. Marathe, Coproporphyrins in Plasma and Urine Can Be Appropriate Clinical Biomarkers to Recapitulate Drug-Drug Interactions Mediated by Organic Anion Transporting Polypeptide Inhibition, J. Pharmacol. Exp. Ther. 358 (2016) 397–404. doi:10.1124/JPET.116.234914.

[116] A. Juul, K. Sørensen, L. Aksglaede, I. Garn, E. Rajpert-De Meyts, I. Hullstein, P. Hemmersbach, A.M. Ottesen, A common deletion in the uridine diphosphate glucuronyltransferase (UGT) 2B17 gene is a strong determinant of androgen excretion in healthy pubertal boys, J Clin Endocrinol Metab. 94 (2009) 1005–1011. doi:10.1210/jc.2008-1984.

[117] J.E. Mullen, J.-O. Thörngren, J.J. Schulze, M. Ericsson, N. Gårevik, M. Lehtihet, L. Ekström, Urinary steroid profile in females - the impact of menstrual cycle and emergency contraceptives., Drug Test. Anal. 9 (2017) 1034–1042. doi:10.1002/dta.2121.

[118] A. Rane, L. Ekström, Androgens and doping tests: genetic variation and pit-falls., Br. J. Clin. Pharmacol. 74 (2012) 3–15. doi:10.1111/j.1365-2125.2012.04294.x.

[119] J.W. Mueller, L.C. Gilligan, J. Idkowiak, W. Arlt, P.A. Foster, The Regulation of Steroid Action by Sulfation and Desulfation., Endocr. Rev. 36 (2015) 526–63. doi:10.1210/er.2015-1036.

[120] J. Tay-Sontheimer, L.M. Shireman, R.P. Beyer, T. Senn, D. Witten, R.E. Pearce, A. Gaedigk, C.L. Gana Fomban, J.D. Lutz, N. Isoherranen, K.E. Thummel, O. Fiehn, J.S. Leeder, Y.S. Lin, Detection of an endogenous urinary biomarker associated with CYP2D6 activity using global metabolomics., Pharmacogenomics. 15 (2014) 1947–62. doi:10.2217/pgs.14.155.

[121] A. Gaedigk, G.P. Twist, J.S. Leeder, CYP2D6, SULT1A1 and UGT2B17 copy number variation: quantitative detection by multiplex PCR, Pharmacogenomics. 13 (2012) 91–111. doi:10.2217/pgs.11.135.

[122] L. Dehennin, A. Delgado, G. Pérès, Urinary profile of androgen metabolites at different stages of pubertal development in a population of sporting male subjects, Eur. J. Endocrinol. 130 (1994) 53–59. doi:10.1530/eje.0.1300053.

[123] J. Mullen, Y. Gadot, E. Eklund, A. Andersson, J. J Schulze, M. Ericsson, A. Lindén Hirschberg, A. Rane, L. Ekström, Pregnancy greatly affects the steroidal module of the Athlete Biological Passport., Drug Test. Anal. 10 (2018) 1070–1075. doi:10.1002/dta.2361.

[124] J.J. Schulze, J.-O.O. Thörngren, M. Garle, L. Ekström, A. Rane, Androgen sulfation in healthy UDP-glucuronosyl transferase 2B17 enzyme-deficient men, J Clin Endocrinol Metab. 96 (2011) 3440–3447. doi:10.1210/jc.2011-0521.

[125] A. Tornio, P.J. Neuvonen, M. Niemi, J.T. Backman, Role of gemfibrozil as an inhibitor of CYP2C8 and membrane transporters, Expert

Opin. Drug Metab. Toxicol. 13 (2017) 83–95. doi:10.1080/17425255.2016.1227791.

[126] Z. Huang, E.-L. Yong, Ethnic differences: Is there an Asian phenotype for polycystic ovarian syndrome?, Best Pract. Res. Clin. Obstet. Gynaecol. 37 (2016) 46–55. doi:10.1016/j.bpobgyn.2016.04.001.

[127] D.J. Grant, Z. Chen, L.E. Howard, E. Wiggins, A. De Hoedt, A.C. Vidal, S.T. Carney, J. Squires, C.E. Magyar, J. Huang, S.J. Freedland, UDP-glucuronosyltransferases and biochemical recurrence in prostate cancer progression, BMC Cancer. 17 (2017) 463. doi:10.1186/s12885-017-3463-6.

[128] H. Li, N. Xie, R. Chen, M. Verreault, L. Fazli, M.E. Gleave, O. Barbier, X. Dong, UGT2B17 Expedites Progression of Castration-Resistant Prostate Cancers by Promoting Ligand-Independent AR Signaling, Cancer Res. 76 (2016) 6701–6711. doi:10.1158/0008-5472.CAN-16-1518.

[129] E.P. Allain, M. Rouleau, T. Le, K. Vanura, L. Villeneuve, P. Caron, V. Turcotte, E. Lévesque, C. Guillemette, Inactivation of Prostaglandin E2 as a Mechanism for UGT2B17-Mediated Adverse Effects in Chronic Lymphocytic Leukemia, Front. Oncol. 9 (2019) 606. doi:10.3389/fonc.2019.00606.

[130] E.S. Orwoll, C.M. Nielson, F. Labrie, E. Barrett-Connor, J.A. Cauley, S.R. Cummings, K. Ensrud, M. Karlsson, E. Lau, P.C. Leung, O. Lunggren, D. Mellström, A.L. Patrick, M.L. Stefanick, K. Nakamura, N. Yoshimura, J. Zmuda, L. Vandenput, C. Ohlsson, Osteoporotic Fractures in Men (MrOS) Research Group, Evidence for geographical and racial variation in serum sex steroid levels in older men., J. Clin. Endocrinol. Metab. 95 (2010) E151-60. doi:10.1210/jc.2009-2435.

[131] J. Deng, X. Zhu, Z. Chen, C.H. Fan, H.S. Kwan, C.H. Wong, K.Y. Shek, Z. Zuo, T.N. Lam, A Review of Food–Drug Interactions on Oral Drug Absorption, Drugs. 77 (2017) 1833–1855. doi:10.1007/s40265-017-0832-z.

[132] J.. Kolars, P.. Watkins, R.. Merion, W.. Awni, First-pass metabolism of cyclosporin by the gut, Lancet. 338 (1991) 1488–1490. doi:10.1016/0140-6736(91)92302-I.

[133] M.F. Paine, D.D. Shen, K.L. Kunze, J.D. Perkins, C.L. Marsh, J.P. McVicar, D.M. Barr, B.S. Gillies, K.E. Thummel, First-pass metabolism of midazolam by the human intestine*, Clin. Pharmacol. Ther. 60 (1996) 14–24. doi:10.1016/S0009-9236(96)90162-9.

[134] D.G. Bailey, G. Dresser, J.M.O. Arnold, Grapefruit-medication interactions: Forbidden fruit or avoidable consequences?, Can. Med. Assoc. J. 185 (2013) 309–316. doi:10.1503/cmaj.120951.

[135] S.A. Peters, C.R. Jones, A.-L. Ungell, O.J.D. Hatley, Predicting Drug Extraction in the Human Gut Wall: Assessing Contributions from Drug Metabolizing Enzymes and Transporter Proteins using Preclinical Models, Clin. Pharmacokinet. 55 (2016) 673–696. doi:10.1007/s40262-015-0351-6.

[136] A. Rostami-Hodjegan, I. Tamai, K.S. Pang, Revisiting the role of gut wall in the fate of orally administered drugs: Why now and to what effect?, Biopharm. Drug Dispos. 38 (2017) 87–93. doi:10.1002/bdd.2071.

[137] O.J.D. Hatley, C.R. Jones, A. Galetin, A. Rostami-Hodjegan, Optimization of intestinal microsomal preparation in the rat: A systematic approach to assess the influence of various methodologies on metabolic activity and scaling factors, Biopharm. Drug Dispos. 38 (2017) 187–208. doi:10.1002/bdd.2070.

[138] J. Küblbeck, J.J. Hakkarainen, A. Petsalo, K.-S. Vellonen, A. Tolonen, P. Reponen, M.M. Forsberg, P. Honkakoski, Genetically Modified Caco-2 Cells With Improved Cytochrome P450 Metabolic Capacity, J. Pharm. Sci. 105 (2016) 941–949. doi:10.1016/S0022-3549(15)00187-2.

[139] Y. Yamaura, B.D. Chapron, Z. Wang, J. Himmelfarb, K.E. Thummel, Functional Comparison of Human Colonic Carcinoma Cell Lines and Primary Small Intestinal Epithelial Cells for Investigations of Intestinal Drug Permeability and First-Pass Metabolism, Drug Metab. Dispos. 44 (2016) 329–335. doi:10.1124/dmd.115.068429.

[140] K.R. Yeo, M. Jamei, A. Rostami-Hodjegan, Predicting drug–drug interactions: application of physiologically based pharmacokinetic models under a systems biology approach, Expert Rev. Clin. Pharmacol. 6 (2013) 143–157. doi:10.1586/ecp.13.4.

[141] M. Jamei, Recent Advances in Development and Application of Physiologically-Based Pharmacokinetic (PBPK) Models: a Transition from Academic Curiosity to Regulatory Acceptance., Curr. Pharmacol. Reports. 2 (2016) 161–169. doi:10.1007/s40495-016-0059-9.

[142] A. Margolskee, A.S. Darwich, X. Pepin, S.M. Pathak, M.B. Bolger, L. Aarons, A. Rostami-Hodjegan, J. Angstenberger, F. Graf, L. Laplanche, T. Müller, S. Carlert, P. Daga, D. Murphy, C. Tannergren, M. Yasin, S. Greschat-Schade, W. Mück, U. Muenster, D. van der Mey, K.J. Frank, R. Lloyd, L. Adriaenssen, J. Bevernage, L. De Zwart, D. Swerts, C. Tistaert, A. Van Den Bergh, A. Van Peer, S. Beato, A.-T. Nguyen-Trung, J. Bennett, M. McAllister, M. Wong, P. Zane, C. Ollier, P. Vicat, M. Kolhmann, A. Marker, P. Brun, F. Mazuir, S. Beilles, M. Venczel, X. Boulenc, P. Loos, H. Lennernäs, B. Abrahamsson, IMI – oral biopharmaceutics tools project – evaluation of bottom-up PBPK prediction success part 1: Characterisation of the OrBiTo database of compounds, Eur. J. Pharm. Sci. 96

(2017) 598–609. doi:10.1016/j.ejps.2016.09.027.

[143] A.S. Darwich, A. Margolskee, X. Pepin, L. Aarons, A. Galetin, A. Rostami-Hodjegan, S. Carlert, M. Hammarberg, C. Hilgendorf, P. Johansson, E. Karlsson, D. Murphy, C. Tannergren, H. Thörn, M. Yasin, F. Mazuir, O. Nicolas, S. Ramusovic, C. Xu, S.M. Pathak, T. Korjamo, J. Laru, J. Malkki, S. Pappinen, J. Tuunainen, J. Dressman, S. Hansmann, E. Kostewicz, H. He, T. Heimbach, F. Wu, C. Hoft, Y. Pang, M.B. Bolger, E. Huehn, V. Lukacova, J.M. Mullin, K.X. Szeto, C. Costales, J. Lin, M. McAllister, S. Modi, C. Rotter, M. Varma, M. Wong, A. Mitra, J. Bevernage, J. Biewenga, A. Van Peer, R. Lloyd, C. Shardlow, P. Langguth, I. Mishenzon, M.A. Nguyen, J. Brown, H. Lennernäs, B. Abrahamsson, IMI – Oral biopharmaceutics tools project – Evaluation of bottom-up PBPK prediction success part 3: Identifying gaps in system parameters by analysing In Silico performance across different compound classes, Eur. J. Pharm. Sci. 96 (2017) 626–642. doi:10.1016/j.ejps.2016.09.037.

[144] A. Margolskee, A.S. Darwich, X. Pepin, L. Aarons, A. Galetin, A. Rostami-Hodjegan, S. Carlert, M. Hammarberg, C. Hilgendorf, P. Johansson, E. Karlsson, D. Murphy, C. Tannergren, H. Thörn, M. Yasin, F. Mazuir, O. Nicolas, S. Ramusovic, C. Xu, S.M. Pathak, T. Korjamo, J. Laru, J. Malkki, S. Pappinen, J. Tuunainen, J. Dressman, S. Hansmann, E. Kostewicz, H. He, T. Heimbach, F. Wu, C. Hoft, L. Laplanche, Y. Pang, M.B. Bolger, E. Huehn, V. Lukacova, J.M. Mullin, K.X. Szeto, C. Costales, J. Lin, M. McAllister, S. Modi, C. Rotter, M. Varma, M. Wong, A. Mitra, J. Bevernage, J. Biewenga, A. Van Peer, R. Lloyd, C. Shardlow, P. Langguth, I. Mishenzon, M.A. Nguyen, J. Brown, H. Lennernäs, B. Abrahamsson, IMI – Oral biopharmaceutics tools project – Evaluation of bottom-up PBPK prediction success part 2: An introduction to the simulation exercise and overview of results, Eur. J. Pharm. Sci. 96 (2017) 610–625. doi:10.1016/j.ejps.2016.10.036.

[145] A. Rostami-Hodjegan, Physiologically Based Pharmacokinetics Joined With In Vitro–In Vivo Extrapolation of ADME: A Marriage Under the Arch of Systems Pharmacology, Clin. Pharmacol. Ther. 92 (2012) 50–61. doi:10.1038/clpt.2012.65.

[146] R. Hodin, Transcriptional activation of the human villin gene during enterocyte differentiation, J. Gastrointest. Surg. 1 (1997) 433–438. doi:10.1016/S1091-255X(97)80130-8.

[147] T. Iwao, M. Toyota, Y. Miyagawa, H. Okita, N. Kiyokawa, H. Akutsu, A. Umezawa, K. Nagata, T. Matsunaga, Differentiation of human induced pluripotent stem cells into functional enterocyte-like cells using a simple method., Drug Metab. Pharmacokinet. 29 (2014) 44–51. doi:10.2133/dmpk.dmpk-13-rg-005.

[148] G. Piton, G. Capellier, Biomarkers of gut barrier failure in the ICU, Curr. Opin. Crit. Care. 22 (2016) 1. doi:10.1097/MCC.0000000000000283.

[149] H. Gehart, H. Clevers, Tales from the crypt: new insights into intestinal stem cells, Nat. Rev. Gastroenterol. Hepatol. 16 (2019) 19–34. doi:10.1038/s41575-018-0081-y.

[150] A. Sawant-Basak, A.D. Rodrigues, M. Lech, R. Doyonnas, M. Kasaian, B. Prasad, N. Tsamandouras, Physiologically Relevant, Humanized Intestinal Systems to Study Metabolism and Transport of Small Molecule Therapeutics, Drug Metab. Dispos. 46 (2018) 1581–1587. doi:10.1124/dmd.118.082784.

[151] K. Nakamura, M. Hirayama-Kurogi, S. Ito, T. Kuno, T. Yoneyama, W. Obuchi, T. Terasaki, S. Ohtsuki, Large-scale multiplex absolute protein quantification of drug-metabolizing enzymes and transporters in human intestine, liver, and kidney microsomes by SWATH-MS: Comparison with MRM/SRM and HR-MRM/PRM., Proteomics. 16 (2016) 2106–17. doi:10.1002/pmic.201500433.

[152] T. Akazawa, Y. Uchida, E. Miyauchi, M. Tachikawa, S. Ohtsuki, T. Terasaki, High Expression of UGT1A1/1A6 in Monkey Small Intestine: Comparison of Protein Expression Levels of Cytochromes P450, UDP-Glucuronosyltransferases, and Transporters in Small Intestine of Cynomolgus Monkey and Human, Mol. Pharm. 15 (2018) 127–140. doi:10.1021/acs.molpharmaceut.7b00772.

[153] D.E. Harbourt, J.K. Fallon, S. Ito, T. Baba, J.K. Ritter, G.L. Glish, P.C. Smith, Quantification of Human Uridine-Diphosphate Glucuronosyl Transferase 1A Isoforms in Liver, Intestine, and Kidney Using Nanobore Liquid Chromatography–Tandem Mass Spectrometry, Anal. Chem. 84 (2012) 98–105. doi:10.1021/ac201704a.

[154] D. Taubert, N. von Beckerath, G. Grimberg, A. Lazar, N. Jung, T. Goeser, A. Kastrati, A. Schömig, E. Schömig, Impact of P-glycoprotein on clopidogrel absorption, Clin. Pharmacol. Ther. 80 (2006) 486–501. doi:10.1016/j.clpt.2006.07.007.

[155] U. Täuber, K. Schröder, B. Düsterberg, H. Matthes, Absolute bioavailability of testosterone after oral administration of testosterone-undecanoate and testosterone, Eur. J. Drug Metab. Pharmacokinet. 11 (1986) 145–149. doi:10.1007/BF03189840.

[156] X. Chu, G.H. Chan, R. Evers, Identification of Endogenous Biomarkers to Predict the Propensity of Drug Candidates to Cause Hepatic or Renal Transporter-Mediated Drug-Drug Interactions, J. Pharm. Sci. 106 (2017) 2357–2367. doi:10.1016/J.XPHS.2017.04.007.

[157] F. Labrie, A. Bélanger, P. Bélanger, R. Bérubé, C. Martel, L. Cusan, J. Gomez, B. Candas, I. Castiel, V. Chaussade, C. Deloche, J. Leclaire, Androgen glucuronides, instead of testosterone, as the new markers of androgenic activity in women, J. Steroid Biochem. Mol. Biol. 99 (2006) 182–188. doi:10.1016/j.jsbmb.2006.02.004.

[158] Y. Gadot, J.-O. Thörngren, E. Eklund, L. Ekström, A. Rane, Pregnancy-Induced Perturbation of Urinary Androgenic Steroid Disposition., J. Endocr. Soc. 2 (2018) 597–608. doi:10.1210/js.2018-00064.

VITA

Hae Young Zhang was born in South Korea. She received a Doctor of Pharmacy degree from University of Washington School of Pharmacy in 2008.